

MECHANISTIC-EMPIRICAL PAVEMENT
DESIGN GUIDE FLEXIBLE PAVEMENT
PERFORMANCE PREDICTION MODELS
FOR MONTANA: *VOLUME I EXECUTIVE
RESEARCH SUMMARY*

FHWA/MT-07-008/8158-1

Final Report

prepared for
THE STATE OF MONTANA
DEPARTMENT OF TRANSPORTATION

in cooperation with
THE U.S. DEPARTMENT OF TRANSPORTATION
FEDERAL HIGHWAY ADMINISTRATION

August 2007

prepared by
Harold L. VonQuintus, PE
Applied Research Associates, Inc.

James S. Moulthrop, PE
Fugro Consultants, Inc.



RESEARCH PROGRAMS

Montana Department of Transportation



You are free to copy, distribute, display, and perform the work; make derivative works; make commercial use of the work under the condition that you give the original author and sponsor credit. For any reuse or distribution, you must make clear to others the license terms of this work. Any of these conditions can be waived if you get permission from the sponsor. Your fair use and other rights are in no way affected by the above.

**Mechanistic-Empirical Pavement Design Guide
Flexible Pavement Performance Prediction Models
for Montana**

**Volume I
Executive Research Summary**

**Prepared for:
Research Programs
Montana Department of Transportation
2701 Prospect Avenue
Helena, Montana 59620**

**Prepared by:
Harold L. Von Quintus, PE, Applied Research Associates, Inc.
James S. Moulthrop, PE, Fugro Consultants, Inc.
Fugro Consultants, Inc.
8613 Cross Park Drive
Austin, Texas 78754
Project 1101-3074**

August 2007

Technical Report Documentation Page

1. Report No. FHWA/MT-07-008/8158-1		2. Government Accession No.	3. Recipient's Catalog No.
4. Title and Subtitle Mechanistic-Empirical Pavement Design Guide Flexible Pavement Performance Prediction Models Volume I Executive Research Summary		5. Report Date August 2007	
		6. Performing Organization Code	
7. Author(s) Harold L. Von Quintus, PE, Applied Research Assoc. Inc. James S. Moulthrop, PE, Fugro Consultants, Inc.		8. Performing Organization Report No.	
9. Performing Organization Name and Address Fugro Consultants, Inc. 8613 Cross Park Drive Austin TX 78754		10. Work Unit No. (TR AIS)	
		11. Contract or Grant No. Montana Department of Transportation Contract HWY-30604-DT, Project #8158	
12. Sponsoring Agency Name and Address Research Programs Montana Department of Transportation 2701 Prospect Avenue PO Box 201001 Helena MT 59620-1001		13. Type of Report and Period Covered Final Report 2001 - 2007	
		14. Sponsoring Agency Code 5401	
15. Supplementary Notes Research performed in cooperation with the Montana Department of Transportation and the United States Department of Transportation, Federal Highway Administration. This report can be found at http://www.mdt.mt.gov/research/projects/pave/pave_model.shtml .			
16. Abstract The objective of this research study was to develop performance characteristics or variables (e.g., ride quality, rutting, fatigue cracking, transverse cracking) of flexible pavements in Montana, and to use these characteristics in the implementation of the distress prediction models or transfer functions included in the Mechanistic-Empirical Pavement Design Guide (MEPDG) software that was developed under NCHRP Project 1-37A. Reliable distress prediction models will enable the Montana Department of Transportation (MDT) to use Mechanistic-Empirical (ME) based principles for flexible pavement design and in managing their highway network. The work conducted within this study included using the MEPDG software to develop local calibration factors in the use of that software for Montana climate, structures, and materials for flexible pavements. The report is comprised of three volumes: Volume I – Executive Research Summary; Volume II – Reference Manual (which includes Selection of Distress Prediction Models, Traffic Characterization and Analyses, and Database for Calibration of ME Distress Prediction Models); and Volume III – Field Guide – Calibration and User's Guide for the Mechanistic-Empirical Pavement Design Guide.			
17. Key Words Flexible Pavements, Pavement Design, Mechanistic-Empirical, Fatigue Cracking, Rutting, Thermal Cracking, IRI, Smoothness, Surface Initiated Cracks, Bottom Initiated Cracks, Calibration, Transfer Functions, Distress Prediction Models.		18. Distribution Statement Unrestricted. This document is available through the National Technical Information Service, Springfield, VA 21161.	
19. Security Classif. (of this report) Unclassified.	20. Security Classif. (of this page) Unclassified.	21. No. of Pages 129	22. Price

DISCLAIMER STATEMENT (MDT)

This document is disseminated under the sponsorship of the Montana Department of Transportation and the United States Department of Transportation in the interest of information exchange. The State of Montana and the United States Government assume no liability of its contents or use thereof.

The contents of this report reflect the views of the authors, who are responsible for the facts and accuracy of the data presented herein. The contents do not necessarily reflect the official policies of the Montana Department of Transportation or the United States Department of Transportation.

The State of Montana and the United States Government do not endorse products of manufacturers. Trademarks or manufacturers' names appear herein only because they are considered essential to the object of this document.

This report does not constitute a standard, specification, or regulation.

ALTERNATIVE FORMAT STATEMENT (MDT)

MDT attempts to provide accommodations for any known disability that may interfere with a person participating in any service, program, or activity of the Department. Alternative accessible formats of this information will be provided upon request. For further information, call (406) 444-7693, TTY (800) 335-7592, or Montana Relay at 711.

ACKNOWLEDGEMENTS

This report was prepared under sponsorship of the Montana Department of Transportation. The project team recognizes and appreciates the services provided by the Montana Department of Transportation. These services included profile and deflection basins measurements, materials sampling, traffic control, and assistance with project activities to recover construction properties from selected project segments. Other individuals and organizations involved in the work and in preparation and review of the report are listed below.

Dragos Andrei, PhD, PE
Brian Killingsworth, PE
Matthew Witczak, PhD

Weng-On Tam, PhD, PE
Amy Simpson, PhD, PE
Mark Hallenbeck, PhD

SI* (MODERN METRIC) CONVERSION FACTORS				
APPROXIMATE CONVERSIONS TO SI UNITS				
Symbol	When You Know	Multiply By	To Find	Symbol
LENGTH				
in	inches	25.4	millimeters	mm
ft	feet	0.305	meters	m
yd	yards	0.914	meters	m
mi	miles	1.61	kilometers	km
AREA				
in ²	square inches	645.2	square millimeters	mm ²
ft ²	square feet	0.093	square meters	m ²
yd ²	square yard	0.836	square meters	m ²
ac	acres	0.405	hectares	ha
mi ²	square miles	2.59	square kilometers	km ²
VOLUME				
fl oz	fluid ounces	29.57	milliliters	mL
gal	gallons	3.785	liters	L
ft ³	cubic feet	0.028	cubic meters	m ³
yd ³	cubic yards	0.765	cubic meters	m ³
[NOTE: volumes greater than 1,000 shall be shown in m ³]				
MASS				
oz	ounces	28.35	grams	g
lb	pounds	0.454	kilograms	kg
T	short tons (2000 lb)	0.907	megagrams (metric tons)	Mg (or t)
TEMPERATURE (exact degrees)				
°F	Fahrenheit or (F-32)/1.8	5 (F-32)/9	Celsius	°C
ILLUMINATION				
fc	foot-candles	10.76	lux	lx
fl	foot-Lamberts	3.426	candela/m ²	cd/m ²
FORCE and PRESSURE or STRESS				
lbf	pounds	4.45	Newtons	N
lbf/in ² (psi)	pounds per square inch	6.89	kiloPascals	kPa
k/in ² (ksi)	kips per square inch	6.89	megaPascals	MPa
DENSITY				
lb/ft ³ (pcf)	pounds per cubic foot	16.02	kilograms per cubic meter	kg/m ³
APPROXIMATE CONVERSIONS FROM SI UNITS				
Symbol	When You Know	Multiply By	To Find	Symbol
LENGTH				
mm	millimeters	0.039	inches	in
m	meters	3.28	feet	ft
m	meters	1.090	yards	yd
km	kilometers	0.621	miles	mi
AREA				
mm ²	square millimeters	0.0016	square inches	in ²
m ²	square meters	10.764	square feet	ft ²
m ²	square meters	1.195	square yards	yd ²
ha	hectares	2.47	acres	ac
km ²	square kilometers	0.386	square miles	mi ²
VOLUME				
mL	Milliliters	0.034	fluid ounces	fl oz
L	liters	0.264	gallons	gal
m ³	cubic meters	35.314	cubic feet	ft ³
m ³	cubic meters	1.307	cubic yards	yd ³
MASS				
g	grams	0.035	ounces	oz
kg	kilograms	2.202	pounds	lb
Mg (or t)	megagrams (metric tons)	1.103	short tons (2000 lb)	T
TEMPERATURE (exact degrees)				
°C	Celsius	1.8C+32	Fahrenheit	°F
ILLUMINATION				
lx	lux	0.0929	foot-candles	fc
cd/m ²	candela/m ²	0.2919	foot-Lamberts	fl
FORCE and PRESSURE or STRESS				
N	Newtons	0.225	pounds	lbf
kPa	kiloPascals	0.145	pounds per square inch	lbf/in ² (psi)
MPa	megaPascals	0.145	kips per square inch	k/in ² (ksi)
DENSITY				
kg/m ³	pounds per cubic foot	0.062	kilograms per cubic meter	lb/ft ³ (pcf)

*SI is the symbol for the International System of Units. Appropriate rounding should be made to comply with Section 4 of ASTM E 380. (Revised March 2003)

TABLE OF CONTENTS

CHAPTER I-1 INTRODUCTION.....	1
I-1.1 BACKGROUND.....	1
I-1.2 PROJECT OBJECTIVE.....	2
I-1.3 ME BASED DESIGN PRINCIPLES.....	2
I-1.4 SCOPE OF WORK AND APPROACH.....	6
I-1.5 ORGANIZATION OF PROJECT DOCUMENTATION.....	7
CHAPTER I-2 EXPERIMENTAL PLAN.....	9
I-2.1 EXPERIMENTAL FACTORIAL.....	9
I-2.2 TEST SECTIONS.....	10
I-2.2.1 Test Sections in Montana.....	11
I-2.2.2 Test Sections In Adjacent States.....	11
I-2.3 FIELD TESTING PLAN AND INVESTIGATIONS.....	14
I-2.4 LABORATORY TESTING PLAN.....	15
I-2.5 TEST SECTION MONITORING PROGRAM.....	15
I-2.5.1 Falling Weight Deflectometer Tests.....	15
I-2.5.2 Longitudinal and Transverse Profiles.....	15
I-2.5.3 Distress Surveys.....	16
CHAPTER I-3 PERFORMANCE INDICATOR PREDICTION MODELS.....	17
I-3.1 PERFORMANCE DATA FOR CALIBRATION.....	17
I-3.2 LOAD RELATED CRACKING.....	22
I-3.2.1 Area Fatigue Cracking – Bottom-Up Cracking.....	22
I-3.2.2 Longitudinal Cracking Within Wheel Path – Surface-Down Cracking.....	24
I-3.3 NON-LOAD RELATED CRACKING – TRANSVERSE CRACKING.....	25
I-3.4 SURFACE DISTORTION – RUTTING.....	26
I-3.4.1 Permanent Deformation in HMA Layers.....	26
I-3.4.2 Permanent Deformation in Unbound Layers.....	27
I-3.5 HMA MIXTURE DISINTEGRATION DISTRESSES.....	28
I-3.5.1 Raveling.....	28
I-3.5.2 Block Cracking.....	29
I-3.6 SMOOTHNESS – LONGITUDINAL PROFILES.....	29
I-3.7 SUMMARY – HMA MIXTURE PROPERTIES FOR DISTRESS TRANSFER FUNCTIONS.....	29
CHAPTER I-4 CLIMATE CHARACTERIZATION.....	32
CHAPTER I-5 TRUCK TRAFFIC CHARACTERIZATION.....	35
I-5.1 TRUCK CATEGORIES.....	35
I-5.2 WHEEL AND AXLE LOAD CONFIGURATIONS.....	35
I-5.3 TRUCK VOLUME DISTRIBUTIONS AND PATTERNS.....	37
I-5.3.1 Truck Classification Volume Distribution Factors.....	37
I-5.3.2 Seasonal Distribution Factors.....	38
I-5.4 AXLE LOAD DISTRIBUTIONS AND PATTERNS.....	39
CHAPTER I-6 MATERIALS CHARACTERIZATION.....	41
I-6.1 FIELD INVESTIGATIONS.....	41
I-6.1.1 Material Recovery – Cores and Borings.....	42

I-6.1.2 Deflection Basin Tests	42
I-6.1.3 Backcalculation of Elastic Layer Modulus Values	43
I-6.1.4 Comparison of FWD Equipment	43
I-6.1.5 Profile Measurements	51
I-6.1.6 Dynamic Cone Penetrometer Tests	52
I-6.2 LABORATORY TESTS	52
I-6.2.1 Unbound Materials and Soils	52
I-6.2.2 Cement Treated Base Materials	66
I-6.2.3 HMA Mixtures	66
I-6.3 MATERIAL CHARACTERIZATION SUMMARY – LAYER PROPERTIES FOR CALIBRATION AND VALIDATION	80
I-6.3.1 Unbound Materials and Soils	80
I-6.3.2 Cement Aggregate Mixtures	85
I-6.3.3 HMA Mixtures	86
CHAPTER I-7 CALIBRATION REFINEMENT OF ME PAVEMENT DESIGN PROCEDURES FOR MONTANA	89
I-7.1 CALIBRATION APPROACH – STATISTICAL MODELING AND RATIONALITY ASSESSMENT	89
I-7.2 CALIBRATION DATABASE	90
I-7.3 PRELIMINARY OBSERVATIONS FROM THE PERFORMANCE DATA	91
I-7.4 RUT DEPTH PREDICTION MODEL	93
I-7.4.1 Calibration Refinement Process for Predicted Rutting	93
I-7.4.2 Comparison of Predicted to Measured Total Rut Depths	96
I-7.5 LOAD RELATED CRACKING, ALLIGATOR CRACKING & LONGITUDINAL CRACKING IN WHEEL PATHS	98
I-7.5.1 Calibration Refinement Process for Load Related Fatigue Cracking	99
I-7.5.2 Comparison of Predicted to Measured Load Related Cracking	102
I-7.6 NON-LOAD RELATED TRANSVERSE CRACKING	107
I-7.7 HMA MIXTURE DISINTEGRATION	107
I-7.8 SMOOTHNESS	108
CHAPTER I-8 CONCLUSIONS AND RECOMMENDATIONS	110
I-8.1 FINDINGS AND CONCLUSIONS	110
I-8.1.1 Rut Depth Prediction Model	110
I-8.1.2 Fatigue Cracking Prediction Model for Flexible Pavements and HMA Overlays – Alligator Cracking or Bottom-Up Fatigue Cracking	111
I-8.1.3 Fatigue Cracking Prediction Model for Semi-Rigid Pavements	111
I-8.1.4 Fatigue Cracking Prediction Model – Longitudinal Cracking or Top-Down Fatigue Cracking	112
I-8.1.5 Transverse Cracking Prediction Model	112
I-8.1.6 Smoothness Prediction Models	113
I-8.2 RECOMMENDATIONS FOR FUTURE CALIBRATION STUDIES	113
I-8.2.1 MEPDG Distress Prediction Models Requiring Future Updates	113
I-8.2.2 Activities and Schedule for Future Calibration Updates	114
CHAPTER I-9 REFERENCES	116

LIST OF TABLES

Table I-1	Hierarchical Input Levels Included in the MEPDG	6
Table I-2	Cell Identification for the Experimental Factorial.....	9
Table I-3	Number of Test Sections Included within Each Cell of the Experimental Factorial....	10
Table I-4	LTPP and Non-LTPP Test Sections Located in Montana	12
Table I-5	LTPP Test Sections Located in States and Canadian Provinces Adjacent to Montana	14
Table I-6	Laboratory Tests to be Completed on the Materials Recovered from the Non-LTPP Test Sections Located in Montana.....	16
Table I-7	Summary of Distress Surveys for the Test Sections Located in Montana.....	18
Table I-8	Summary of Distress Surveys for the Test Sections Located in States and Canadian Provinces Adjacent to Montana	20
Table I-9	Performance Indicator Prediction Models Considered for Use in Montana	30
Table I-10	Material Properties Needed for Performance Indicator Prediction Models.....	30
Table I-11	Climatic Parameters and Information Needed for Performance Indicator Prediction Models.....	31
Table I-12	Weather Stations that are Available in the MEPDG Software for Montana	32
Table I-13	Latitude, Longitude, and Elevation of the Test Sections Located in Montana for Selecting Weather Stations.....	33
Table I-14	Latitude, Longitude, and Elevation of the Test Sections Located in States and Canadian Provinces Adjacent to Montana for Selecting Weather Stations.....	34
Table I-15	Summary of Truck Traffic Input Parameters and Values Used in Verification and Calibration of the Distress Transfer Functions for Montana.....	37
Table I-16	Primary Truck Type Normalized Volume Distribution Factors Recommended for Use in Montana.....	38
Table I-17	Recommended Monthly Distribution Factors for Use in Montana	39
Table I-18	Summary of Backcalculated Elastic Layer Modulus Values for Each of the Test Sections Located in Montana.....	44
Table I-19	Summary of Results from the Classification Tests Performed on the Base Materials Recovered from the LTPP Test Sections in Montana.....	54
Table I-20	Summary of Results from the Classification Tests Performed on the Subgrade Soils Recovered from the LTPP and Non-LTPP Test Sections in Montana	55
Table I-21	Summary of Moisture-Density and Resilient Modulus Test Results for the Unbound Aggregate Base Materials Recovered from the LTPP and Non-LTPP Test Sections in Montana	56
Table I-22	Summary of Moisture-Density and Resilient Modulus Test Results for the Subgrade Soils Recovered from the LTPP and Non-LTPP Test Sections in Montana.....	57
Table I-23	Summary of the Regression Constants from the Constitutive Equation for the Repeated Load Resilient Modulus Test Results for the Non-LTPP Sites	64
Table I-24	Summary of CAM Properties Measured in the Laboratory on Cores or Portion of Cores Recovered from the Non-LTPP Sites in Montana	67
Table I-25	Summary of Laboratory Measured IDT Resilient Modulus for the HMA Mixtures Sampled from the Non-LTPP Test Sections in Montana	71
Table I-26	Summary of Laboratory Measured Tensile Strengths and Tensile Strain at Failure for the HMA Mixtures Sampled from the Non-LTPP Test Sections in Montana	72
Table I-27	Summary of the Laboratory Creep Compliance Tests for HMA Mixtures Recovered from the Non-LTPP Test Sections Located in Montana.....	73

Table I-28	IDT Resilient Modulus Model Parameters for the Non-LTPP HMA Mixtures Sampled from the Montana Test Sections	78
Table I-29	Tensile Strain at Failure Model Parameters for the Non-LTPP HMA Mixtures Sampled from the Montana Test Sections	79
Table I-30	Summary of the Adjustment Factors Recommended for Use in Montana to Convert Backcalculated Layer Modulus Values to Laboratory Equivalent Resilient Modulus Values	82
Table I-31	Summary of the DCP Adjustment Factors Recommended for Use in Montana to Convert the Elastic Layer Modulus Values to Laboratory Equivalent Modulus Values ..	85
Table I-32	Fine Aggregate Angularity Index Used to Adjust Permanent Deformation Parameters, F_{Index}	95
Table I-33	Coarse Aggregate Angularity Index Used to Adjust Permanent Deformation Parameters, C_{Index}	95
Table I-34	Summary of the Bias and Standard Error for the Rutting Prediction Model Using the Montana Calibration Factors for Unbound and HMA Rutting.....	98
Table I-35	Summary of the Bias and Standard Error for the Alligator Cracking Prediction Model Using the Montana Calibration Factors	107

LIST OF FIGURES

Figure I-1	Conceptual schematic of the three-stage design process for the ME Design Guide.	3
Figure I-2	Simplified flowchart of the minimum steps needed to integrate a structural and HMA mixture design procedure.	4
Figure I-3	Typical steps involved in the design-construction process and the differences between an empirical design process to that of an integrated ME design system in terms of HMA mixture characterization.	5
Figure I-4	LTPP test sections in Montana.	13
Figure I-5	Non-LTPP test sections in Montana.	13
Figure I-6	WIM sites in Montana.	36
Figure I-7	Comparison of the deflections measured by the LTPP Dynatest and MDT JILS FWDs at Sensors 1, 2, and 3 for the 16 kip test load.	46
Figure I-8	Comparison of the deflections measured by the LTPP Dynatest and MDT JILs FWDs at Sensors 4, 5, and 6 for the 16 kip test load.	47
Figure I-9	Comparison of the deflections measured by the LTPP Dynatest and MDT JILs FWDs at Sensors 7, 8 and 9 for the 16 kip test load.	48
Figure I-10	Graphical comparison of the backcalculated HMA layer modulus values for the JILS and Dynatest FWDs that were used to measure deflection basins within this study.	49
Figure I-11	Graphical comparison of the backcalculated crushed aggregate base modulus values for the JILs and Dynatest FWDs that were used to measure deflection basins within this study.	49
Figure I-12	Backcalculated subgrade modulus.	50
Figure I-13	Comparison of backcalculated subgrade modulus from the deflection basins measured with the Dynatest and JILs FWDs (reduced data).	52
Figure I-14	Summary of repeated load resilient modulus test for the crushed gravel recovered from the Beckhill / Deerlodge test section.	58
Figure I-15	Summary of repeated load resilient modulus test for the soil-aggregate base mixture recovered from the Fort Belknap test section.	59
Figure I-16	Summary of repeated load resilient modulus test for the clayey gravel with sand soil recovered from the Beckhill / Deerlodge test section.	59
Figure I-17	Summary of repeated load resilient modulus test for the silty sand with gravel soil recovered from the Fort Belknap test section.	60
Figure I-18	Summary of repeated load resilient modulus test for the silty clay with gravel soil recovered from the Roundup test section.	60
Figure I-19	Graphical presentation of the results from the resilient modulus test performed on the crushed gravel base material recovered from the Condon test section.	62
Figure I-20	Example Excel spreadsheet for completing the resilient modulus regression analysis to determine the coefficients and exponents of the universal constitutive equation (refer to Equation I-17a).	63
Figure I-21	Resilient Modulus at Typical State of Stress for All MDT Base Materials	65
Figure I-22	Resilient Modulus at Typical State of Stress for All MDT Subgrades.	65
Figure I-23	Comparison of the elastic modulus values measured with the seismic and indirect tensile tests.	68
Figure I-24	Relationship between the elastic modulus and tensile strain at failure as measured from the indirect tensile strength test for the HMA mixtures recovered from the non-LTPP test sections in Montana (data taken from Tables I-25 and I-26).	76

Figure I-25 Relationship between the elastic modulus and the tensile strength of the HMA mixtures recovered from the non-LTPP test sections in Montana (data taken from Tables I-25 and I-26).....	76
Figure I-26 Relationship between the IDT elastic modulus measured at 32°F and the tensile creep compliance measured at 4°F for different loading times of the HMA mixtures recovered from the non-LTPP test sections in Montana.....	77
Figure I-27 Relationship between the IDT elastic modulus measured at 68°F and the tensile creep compliance measured at 14°F for different loading times of the HMA mixtures recovered from the non-LTPP test sections in Montana.....	77
Figure I-28 Comparison of the laboratory measured resilient modulus values to those backcalculated from deflection basins.....	81
Figure I-29 Comparison of the laboratory measured resilient modulus values to the adjusted backcalculated modulus values from deflection basins using the Montana adjustment factors.....	82
Figure I-30 Comparison of the resilient modulus values measured in the laboratory to the in place values estimated with the DCP.....	84
Figure I-31 Comparison of the laboratory measured and backcalculated elastic modulus of the CAM mixtures.....	86
Figure I-32 Comparison of the laboratory measured and adjusted backcalculated elastic modulus of the CAM mixtures.....	87
Figure I-33 Comparison of the laboratory measured and backcalculated elastic modulus of the HMA mixtures.....	88
Figure I-34 Comparison of the laboratory measured and adjusted backcalculated elastic modulus of the HMA mixtures.....	88
Figure I-35 Estimate of the K_{r1} intercept parameter from Voids Filled with Asphalt (VFA) and gradation.....	94
Figure I-36 Comparison of the predicted and measured total rut depths for the sites located in Montana.....	96
Figure I-37 Comparison of the predicted and measured total rut depths for the sites located in States and Canadian provinces adjacent to Montana.....	97
Figure I-38 Residual error (predicted minus measured total rut depths) as a function of the predicted rut depth for all sites combined.....	97
Figure I-39 Determination of the k_{r1} parameter from the VFA of the lower dense graded HMA layer.....	100
Figure I-40 Determination of the k_{r3} parameter from the k_{r1} parameter of the lower dense graded HMA layer.....	101
Figure I-41 Determination of the C_2 parameter from the VFA of the lower dense graded HMA layers.....	101
Figure I-42 Comparison of the predicted and measured alligator cracking for the sites, with the exception of the semi-rigid pavements.....	103
Figure I-43 Residual error (predicted minus measured total alligator cracking) as a function of the predicted alligator cracking with the exception of the semi-rigid pavements.....	104
Figure I-44 Comparison of the predicted and measured longitudinal cracking for the Montana sites, excluding the semi-rigid pavements.....	105
Figure I-45 Comparison of the predicted and measured alligator cracking for the semi-rigid pavement sites.....	106
Figure I-46 Residual error (predicted minus measured total alligator cracking) as a function of the predicted alligator cracking.....	106

Figure I-47 Comparison of the predicted and measured transverse cracking for the Montana sites.....108
Figure I-48 Comparison of the predicted and measured IRI for the Montana test sections.....109

CHAPTER I-1 INTRODUCTION

I-1.1 BACKGROUND

A Mechanistic-Empirical (ME) based pavement design method is a rational engineering approach that has been used by some agencies to replace the empirical American Association of State Highway and Transportation Officials (AASHTO) Design Guide (*AASHTO 1993*). Illinois, Kentucky, Texas, and Washington Departments of Transportation (DOTs) are all agencies that use an ME based approach for pavement design. The main advantage of an ME based design system is that it is based on pavement fatigue and deformation characteristics of all layers, rather than solely on the pavement's surface condition (ride quality). Such a rational engineering design approach provides a more accurate and cost effective method of diagnosing pavement problems, and forecasting maintenance, repair, and rehabilitation needs.

AASHTO, Federal Highway Administration (FHWA), and other agencies recognized this benefit and the need for an ME based design procedure, because of changing truck loading configurations, the use of superior materials, and other design features. As a result, the National Cooperative Highway Research Program (NCHRP) Project 1-37A (*ARA 2004a,b,c,d*) to develop an ME pavement analysis procedure using state-of-the-art distress prediction models. This project has now been completed, and resulted in the Mechanistic-Empirical Pavement Design Guide (MEPDG) (*ARA 2004a,b,c,d*). Version 0.9 Software of the MEPDG was released for distribution to State highway agencies in July 2006 (*NCHRP 2006*).

In adopting an ME based design method, each agency needs to assess their own implementation costs and increased level of effort for using this type of design method in two key areas. These two areas include, determining the design inputs and accuracy of the ME based distress prediction models. The verification and calibration, if needed, of the performance models to local conditions is an essential step in implementing a successful and credible ME based design process.

The Montana Department of Transportation (MDT) recognized the benefits and advantages of using an ME based design method, and began the process of identifying the modeling tools (e.g., pavement response model, climatic model, distress prediction models) and developing a pavement performance database for storing standard inputs. The distress prediction models (transfer function) will provide a benefit for optimizing rehabilitation strategies and the predictions inherent in a pavement management system involving the forecasting of maintenance, repair, rehabilitation, and reconstruction costs. The pavement performance database can be used to determine the robustness and accuracy of the transfer functions to Montana's materials and local conditions.

Montana currently has a variety of different design strategies (flexible and composite pavements) that have been and are being used. The Hot Mix Asphalt (HMA) mixtures vary from the older Grade B and Grade D mixtures to the more recent Grade S, Superpave mixture. Some of the newer modified mixtures may have different performance characteristics than included in the global models developed and calibrated under NCHRP Projects 1-37A (*ARA 2004a,b,c,d*) and 1-40D (*NCHRP 2006*). The performance of Montana's flexible pavements and HMA overlays should be documented to determine if and how they might fit into the global models being proposed for use. It is probable that revisions will be needed to the existing global

calibration factors to ensure Montana will have reliable, locally calibrated models for use in day to day designs and to access the appropriateness of new design features and materials.

The purpose of this report is to document the field and laboratory investigations, the calibration coefficients of the distress transfer functions, and the implementation recommendations of the ME based design process to Montana materials and environment – specifically the MEPDG developed under NCHRP Project 1-37A (*ARA 2004a,b,c,d*).

I-1.2 PROJECT OBJECTIVE

The objective of this project is to develop performance characteristics for variables (e.g., ride quality, rutting, fatigue cracking, transverse cracking) of flexible pavements in Montana, and to use these characteristics in the verification and calibration of the distress prediction models (transfer functions) included in the MEPDG software. Reliable distress prediction models will enable MDT to use ME principles for flexible pavement design and in managing their highway network.

I-1.3 ME BASED DESIGN PRINCIPLES

Unlike empirical design procedures, the concepts of ME based methods allow the pavement design engineer to quantify the effect of changes in materials, load, climate, age, pavement geometry, and construction practices on pavement performance. Although the advantages of ME based procedures were enumerated in the 1986 AASHTO Design Guide (*AASHTO 1986*), availability and computational speed of desktop computers were major hurdles to implementation. This is no longer the case. The MEPDG process includes a uniform and comprehensive set of procedures for the design of new and rehabilitated flexible pavements.

Figure I-1 shows a flow chart for the design process of the MEPDG for flexible pavements and HMA overlays of flexible pavements. ME based methods allow the designer to consider multiple failure criteria to optimize a design strategy in a specific climate and for unique truck loadings. The MEPDG predicts load and non-load related fracture, distortion, and smoothness to evaluate each trial design. Furthermore, concepts pertaining to reliability and rehabilitation have been integrated into the ME based approach.

ME based methods allow the capability for integrating the HMA mixture and structural design process. Figure I-2 is an example flow chart that shows the integration of mixture and structural design. Empirical-based design methods exclude this integration capability. As an example, Figure I-3 shows a comparison of the HMA inputs needed for the AASHTO empirical design to that for the new MEPDG.

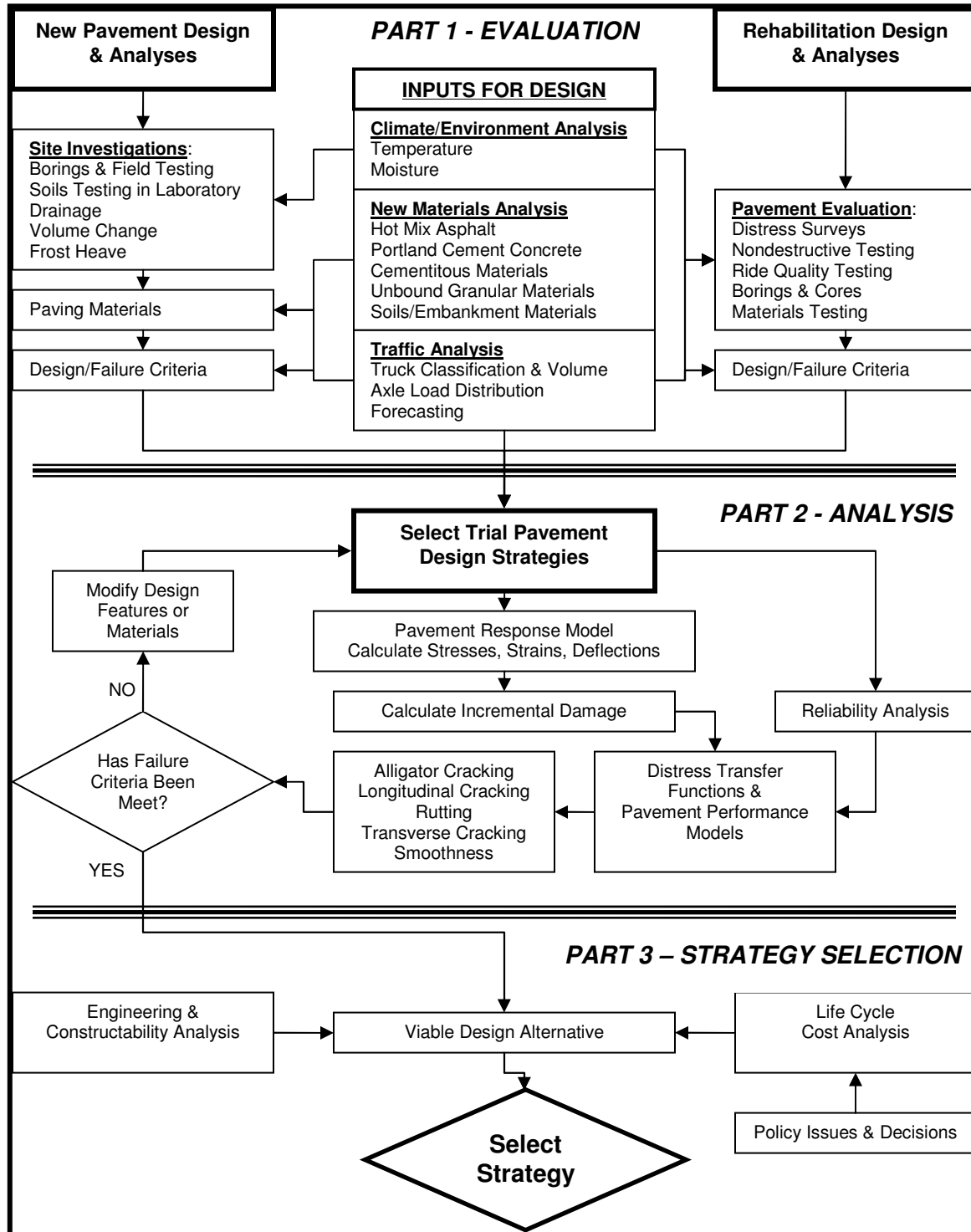


Figure I-1 Conceptual schematic of the three-stage design process for the ME Design Guide.

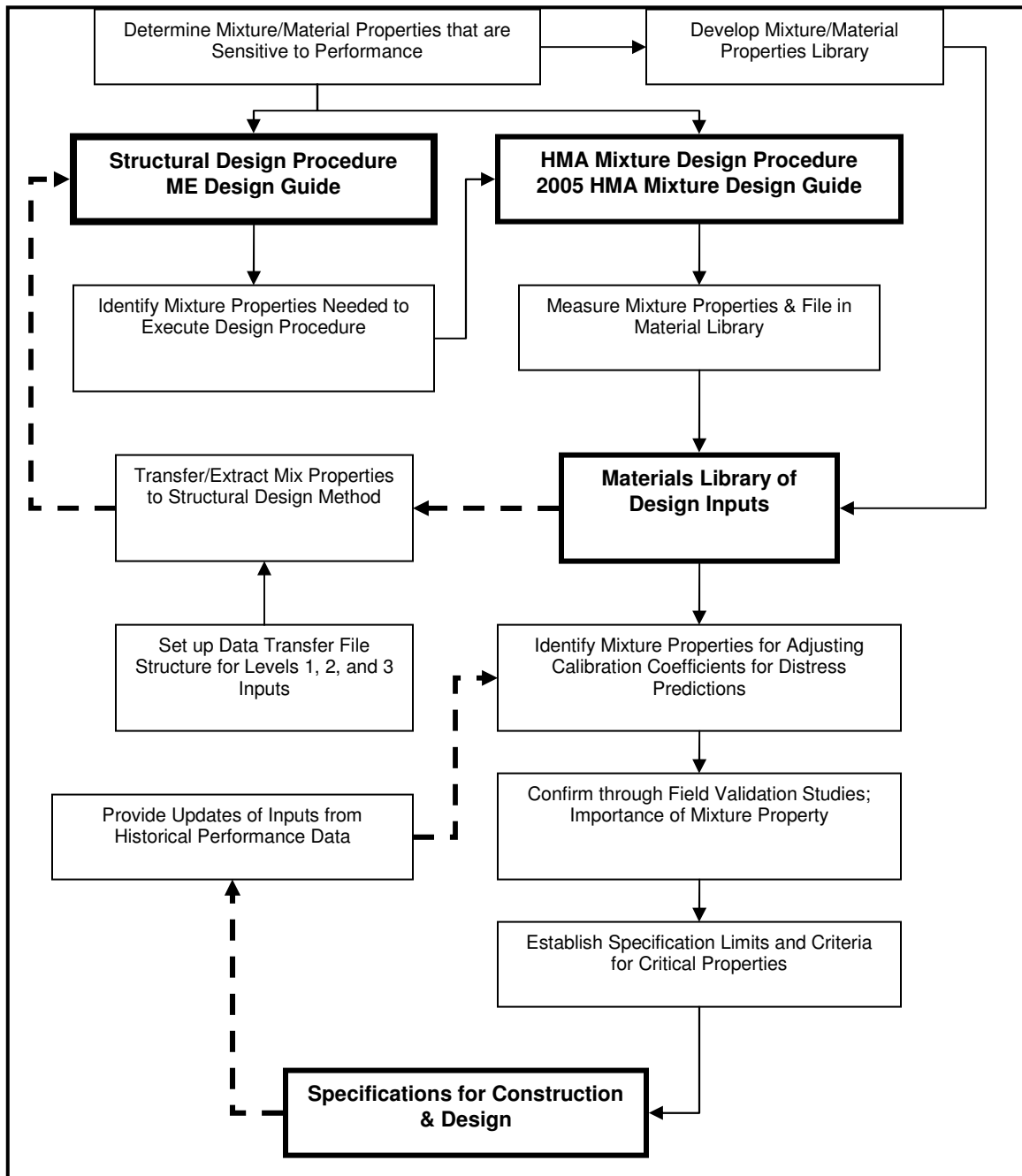


Figure I-2 Simplified flowchart of the minimum steps needed to integrate a structural and HMA mixture design procedure.

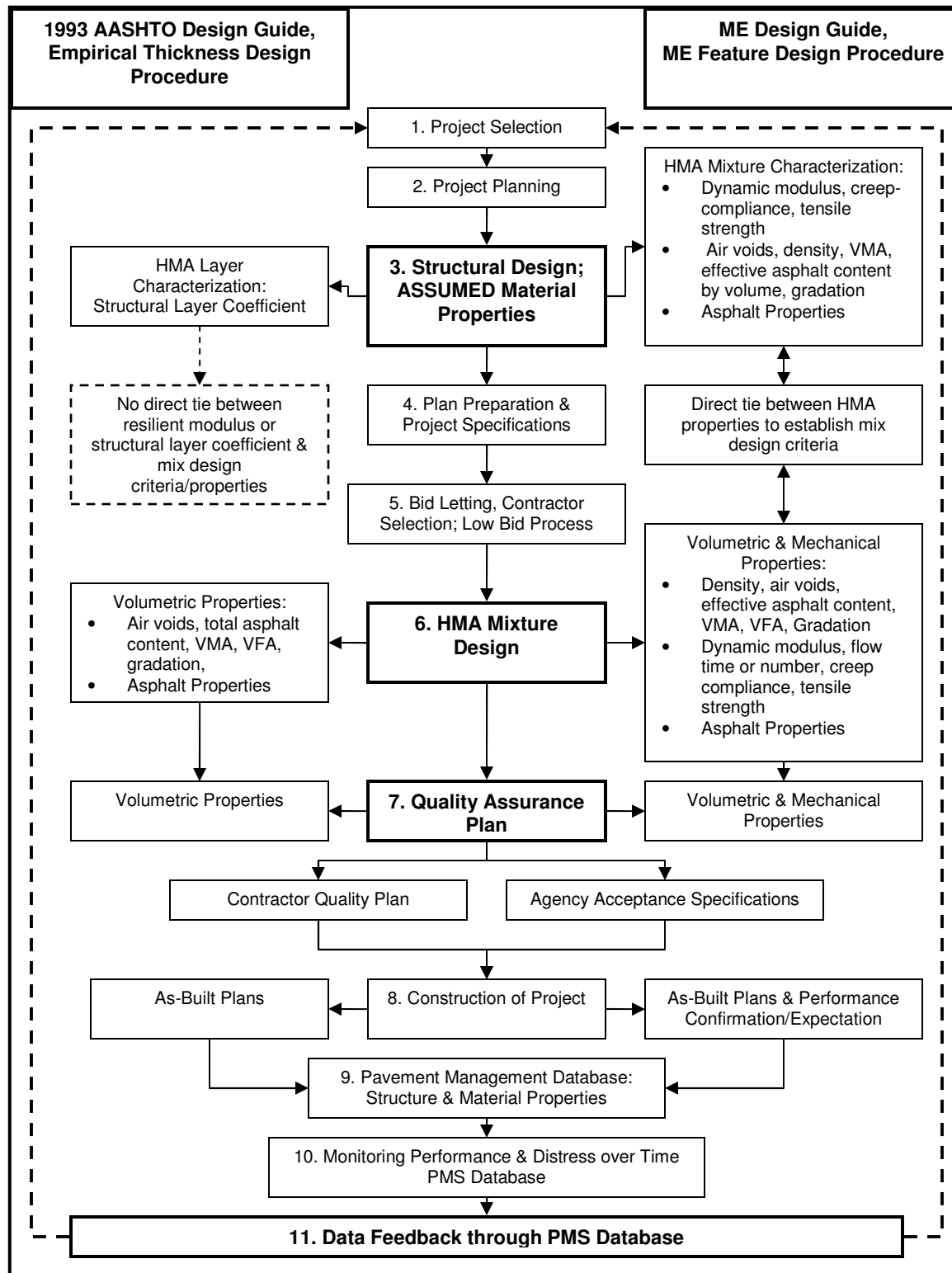


Figure I-3 Typical steps involved in the design-construction process and the differences between an empirical design process to that of an integrated ME design system in terms of HMA mixture characterization.

A unique feature of the MEPDG excluded from earlier versions of the AASHTO design guide and other ME based design methods is a means by which the engineer can choose the complexity of the design that is compatible with the nature of the project (i.e., high volume roadways utilizing a more robust, although more complex procedure versus the procedure that may be used to design a lower volume road). The MEPDG uses a hierarchical approach that allows the user to choose a philosophy for determining the inputs that is consistent with the project importance and that is compatible with the agency’s resources and technical expertise. This approach allows the designer much greater flexibility in selecting the quality of inputs (traffic, materials, and environment). Logically, the quality or reliability of the output is directly related to the quality of the input. Table I-1 shows the general features of each input level.

Table I-1 Hierarchical Input Levels Included in the MEPDG

Input Level	Definition of the Level
1	Input parameter based on site specific data and testing. Level 1 represents the greatest knowledge about the input parameter for the specific project. This input level is limited to designs having unusual site features, materials, or traffic conditions and it has the highest testing costs for determining the input.
2	Regression equations are used to determine the input parameter. The data collection and testing for this input level is much simpler and less costly. This level is expected to be used for the more routine pavement designs.
3	Level 3 inputs are based on “best-guessed” values or default values. The Level 3 inputs can be based on national or regional default values. This input level has the least knowledge about the input parameter for the specific project. Initially, it is expected that this level will be the one more commonly used until agencies become familiar with the MEPDG and its multiple inputs.

I-1.4 SCOPE OF WORK AND APPROACH

The project was divided into two phases, each with a series of tasks to achieve the above objective. The specific tasks for each Phase are listed below.

- PHASE I provided the initial identification of the test sections, established the data collection policies and procedures, and included the preparation of a draft document defining the data collection procedures to be implemented in Phase II. Phase I was divided into four tasks, which included:
 - Task 1 – Literature Review of Distress Prediction Models.
 - Task 2 – Review of MDT Pavement-Related Data.
 - Task 3 – Develop the Experimental Plan and Factorial.
 - Task 4 – Develop Work Plan for Monitoring and Testing.

- PHASE II included the data collection and analysis efforts required for the local calibration of the distress prediction models to Montana’s climate, materials, and design strategies. Phase II was divided into four tasks, which included:
 - Task 5 – Presentation of Work Plan to MDT.
 - Task 6 – Implement Work Plan – Conduct Field Investigations and Collect Data.

- Task 7 – Data Analyses and Calibration of Performance Prediction Models.
- Task 8 – Final Report and Presentation of Results to MDT.

A third phase of this research project was envisioned by the MDT, but was outside the scope of work for the initial effort. Phase III is identified as a mechanism for the MDT to use in obtaining future assistance from an outside agency to continue with the data collection efforts and for updating the calibration factors for each distress prediction model.

I-1.5 ORGANIZATION OF PROJECT DOCUMENTATION

Results from this research project are contained in a three-volume report. Following is a list that describes each report volume from this project:

- **Volume I** (included herein) is the Executive Research Summary for the overall project and summarizes all work completed under this project, Phases I and II. Volume I is divided into eight chapters.
 - Chapter I-1 is the introduction to the project report.
 - Chapter I-2 presents the experimental plan and matrix that was used to ensure that a sufficient number of test sections were selected to cover the range of conditions encountered in Montana.
 - Chapter I-3 presents the performance indicators and the prediction models selected for pavement design and management purposes.
 - Chapter I-4 establishes the climatic and environmental inputs and default values needed for predicting all distresses.
 - Chapter I-5 summarizes the traffic analyses to determine the inputs for the load related distress prediction models.
 - Chapter I-6 summarizes the materials testing and characterization to determine the inputs for each prediction model.
 - Chapter I-7 summarizes the verification and calibration procedure for each distress prediction model.
 - Chapter I-8 provides the conclusions and recommendations from this research project.
 - Chapter I-9 is the reference section for Volume I.
- **Volume II** is a Reference Manual that documents some of the Supplemental Research Studies and Products that resulted from this project (*Von Quintus and Moulthrop 2007a*). Volume II is divided into five parts – each part summarizing a specific product from this study.
 - Part I of Volume II is an introduction to Volume II.
 - Part II of Volume II summarizes the literature review (Task 1 of Phase I) of ME based distress prediction models and recommends specific equations to be used for each distress.
 - Part III of Volume II was prepared by the University of Washington, Washington State Transportation Center (TRAC), and discusses the analyses completed on the traffic data provided by the MDT and summarizes the input values recommended for use in pavement design in Montana.

- Part IV of Volume II discusses the ME database created for Montana. This part provides an overview of the database and defines the format for each data field and category. Part IV also lists the tests sections, both within and outside of Montana, that were used to populate the database with data used in the local calibration process.
- Part V of Volume II is the reference section for Volume II.
- **Volume III** is the Field Guide (Calibration and User Guide) presenting standard practices for updating and enhancing the distress prediction models that were calibrated under this research project (*Von Quintus and Moulthrop 2007b*). This volume is divided into five chapters.
 - Chapter III-1 is the introduction to Volume III.
 - Chapter III-2 provides an overview of the MEPDG.
 - Chapter III-3 is a user manual for the MEPDG.
 - Chapter III-4 presents the local calibration factors that were determined from this research project for immediate use by the MDT for designing pavements and managing their highway network.
 - Chapter III-5 is the reference section for Volume III.

CHAPTER I-2 EXPERIMENTAL PLAN

Chapter I-2 presents the experimental plan, summarizes the initial data collection effort, and lists the test sections that were selected for calibrating ME based distress prediction models to Montana site conditions, materials, and design features.

I-2.1 EXPERIMENTAL FACTORIAL

The experimental factorial (matrix) was developed to ensure that the different materials, design and rehabilitation strategies, climates, soils, and other design-related features and site conditions found in Montana were represented in the experimental data. Another goal of the experimental design was to keep it as simple and efficient as possible. The primary tiers of the factorial were defined in cooperation with MDT, and included climate (Western and Eastern Montana), HMA mixture type (mix designations B, D, and SP), and design strategy. Table I-2 identifies the cells used in the experimental factorial.

Table I-2 Cell Identification for the Experimental Factorial

HMA Mixture Type		Climate					
		Western			Eastern		
		B	D	SP	B	DP	SP
New Construction; Design Features & Strategies	Conventional Base-Type A	1.a	2.a	3.a	4.a	5.a	6.a
	Conventional Base-Type B	1.b	2.b	3.b	4.b	5.b	6.b
	Deep Strength & Full-Depth	7	8	9	10	11	12
	Drainage Layer	13	14	15	16	17	18
	Semi-Rigid Pavement	19.a	20.a	21.a	22.a	23.a	24.a
Reconstruction Using In Place Recycling	Pulverized; Semi-Rigid	19.b	20.b	21.b	22.b	23.b	24.b
	Pulverized Pavement	25	26	27	28	29	30
HMA Overlay, Rehabilitation Strategies	Overlay, Semi-Rigid	31	32	33	34	35	36
	Simple Overlay	37.a	38.a	39.a	40.a	41.a	42.a
	Mill & Overlay	37.b	38.b	39.b	40.b	41.b	42.b

The original intent of the experimental design was to have a balanced factorial with the majority of the test sections located in Montana. Too many of these cells included in Table I-2, however, were found to have no test sections located in Montana with historical performance data. Thus, MDT, agreed to include some of the Long Term Pavement Performance (LTPP) test sections located in adjacent States. Test Sections extracted from the LTPP program were from Idaho, North and South Dakota, Wyoming, and two of the Canadian provinces (Alberta and Saskatchewan).

I-2.2 TEST SECTIONS

Table I-3 lists the number of test sections included within each cell. These test sections include both LTPP and non-LTPP projects that were selected for use in cooperation with MDT. The cells with bold borders in Table I-3 designate those experimental factor combinations for which no test section is available. As shown, none of the test sections have a drainage layer, with the exception of the Strategic Highway Research Program (SHRP), LTPP Special Pavement Study-1 (SPS) project (*SHRP 1990*). In addition, very few of the test sections have Superpave or “SP” designated HMA mixtures. Overall, however, there are a sufficient number of test sections in the factorial to complete the project objective.

Table I-3 Number of Test Sections Included within Each Cell of the Experimental Factorial

Mixture Type		Climate						Total
		Western			Eastern			
		B	D	SP	B	DP	SP	
New Construction; Design Features & Strategies	Conventional Base-Type A	2 - 2	0 - 2	2 - 0	4 - 2	1 - 2	0 - 0	9 - 8
	Conventional Base-Type B	0 - 7	5 - 4	0 - 0	3 - 0	1 - 0	0 - 0	9 - 11
	Deep Strength	0 - 2	3 - 3	0 - 0	1 - 4	1 - 3	0 - 0	5 - 12
	Drainage Layer	0 - 0	6 - 0	0 - 0	0 - 0	0 - 0	0 - 0	6 - 0
	Semi-Rigid Pavement	0 - 5	0 - 4	0 - 0	3 - 1	1 - 0	2 - 0	6 - 10
	<i>Total New Construction</i>	<i>2 - 18</i>	<i>14 - 27</i>	<i>2 - 2</i>	<i>11 - 18</i>	<i>4 - 9</i>	<i>2 - 2</i>	<i>35 - 41</i>
Reconstruction Using In Place Recycling	Pulverized; Semi-Rigid	1 - 0	0 - 0	2 - 0	2 - 0	1 - 0	2 - 0	8 - 0
	Pulverized Pavement	2 - 0	1 - 0	2 - 0	0 - 0	1 - 0	2 - 0	8 - 0
	<i>Total In Place Recycling</i>	<i>3 - 0</i>	<i>1 - 0</i>	<i>4 - 0</i>	<i>2 - 0</i>	<i>2 - 0</i>	<i>4 - 0</i>	<i>16 - 0</i>
HMA Overlay; Rehabilitation Strategies	Overlay, Semi-Rigid	0 - 1	0 - 1	0 - 0	0 - 0	0 - 0	0 - 0	0 - 2
	Simple Overlay	0 - 5	6 - 6	0 - 0	0 - 3	3 - 1	0 - 0	9 - 15
	Mill & Overlay	0 - 4	4 - 0	0 - 0	0 - 0	0 - 0	0 - 0	4 - 4
	<i>Total Rehabilitation</i>	<i>0 - 10</i>	<i>10 - 7</i>	<i>0 - 0</i>	<i>0 - 3</i>	<i>3 - 1</i>	<i>0 - 0</i>	<i>13 - 21</i>
Total		5 - 26	25 - 20	6 - 0	13 - 10	9 - 6	6 - 0	64 - 62
NOTE:								
1. The first number in the table defines the number of test sections located in Montana, while the second number lists the test sections located in States adjacent to Montana.								
2. Cells with bold borders designate those experimental factor combinations for which no test section is available.								

In summary, there are 89 LTPP and 13 non-LTPP sites included in the experimental factorial. Of the 89 LTPP sections, 34 are located in Montana and 55 in neighboring States and Canada.

A set of queries was written that can be used at any time in the future to extract the data needed from the LTPP database to update the information in the calibration/validation database; Part IV of Volume II (*Von Quintus and Moulthrop 2007a*).

I-2.2.1 Test Sections in Montana

Table I-4 lists some of the basic structure information on the 34 LTPP (see Figure I-4) and 13 non-LTPP (see Figure I-5) test sections located in Montana. The test sections included in the LTPP SPS-3 experiment were excluded from use in the verification/calibration study, because of the diversities and anomalies reported in the LTPP program with this experiment. Of the 47 sites located in Montana, 34 are LTPP sections and 13 are non-LTPP sections. Ten of the non-LTPP sections were selected for the factorial to include projects with in place recycling, with and without stabilization, while three were selected to include recently placed projects with Superpave HMA mixtures. The three non-LTPP projects placed after 2003 were excluded from the verification and calibration process because none of these projects exhibit any surface distress. These projects, however, will be useful for future calibration updates as they begin to exhibit surface distress.

The 10 non-LTPP sites are defined as: Condon, Deer Lodge/Beckhill, Ft. Belknap, Geyser, Hammond, Lavina, Perma, Roundup, Silver City, and Wolf Point. Field investigations were required for these sites to determine the pavement layer structure and material properties. The three SPS-3 / Superpave sites were included for future performance observations of Superpave mixtures in Montana. These sites are defined as Baum Road, Lothair, and Vaughn N. Samples of material from these projects were collected by MDT during the 2003 construction season for laboratory testing and characterization.

I-2.2.2 Test Sections In Adjacent States

Table I-5 lists the 55 LTPP test sections and basic structure information for those sections located in adjacent States and Canadian provinces that were used within the study. All information and data for these sections were extracted from the LTPP database.

Table I-4 LTPP and Non-LTPP Test Sections Located in Montana

Type of Structure	Conventional Flexible	Deep Strength & Full Depth	Includes Drainage Layer	Semi-Rigid Pavement	Pulverized Pavement	HMA Overlay of Semi-Rigid	HMA Overlay	Total Number Test Sections	Total Less SPS-3 Sites
Non-LTPP Test Sections	Baum Road* Lothair E* Silver City W			Geyser E Hammond NW Lavina W Perma Roundup E Wolf Point S	Condon N Deer Lodge/Beckhill	Fort Belknap	Vaughn N*		
	3			6	2	1	1	13	10
LTPP Test Sections	30-0113 30-0114 30-0805 30-0806 30-0901 30-0902 30-0903 30-1001 30-8129	30-0115 30-0116 30-0117 30-0118	30-0119 30-0120 30-0121 30-0122 30-0123 30-0124				30-0502 30-0503 30-0504 30-0505 30-0506 30-0507 30-0508 30-0509 30-0560 30-0561 30-6004 30-7066 30-7075 30-7076 30-7088		
	9	4	6				15	34	34
Total	12	4	6	6	2	1	16	47	44
*SPS-3 (Superpave) Sites: Baum Road, Lothair E, Vaughn N									

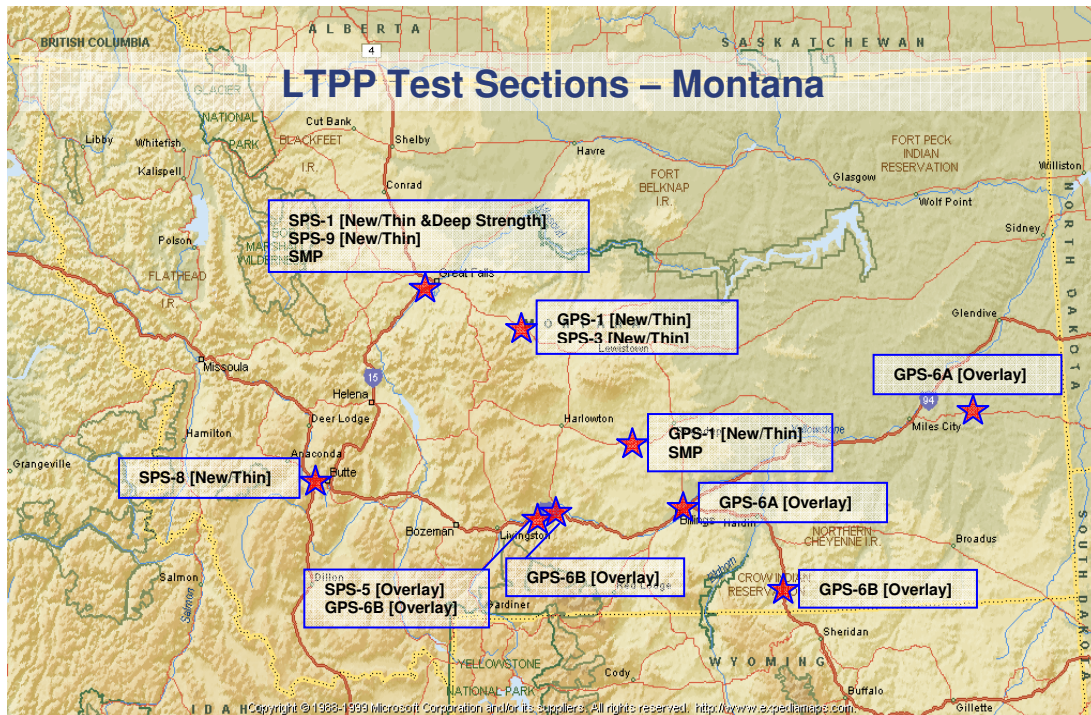


Figure I-4 LTPP test sections in Montana

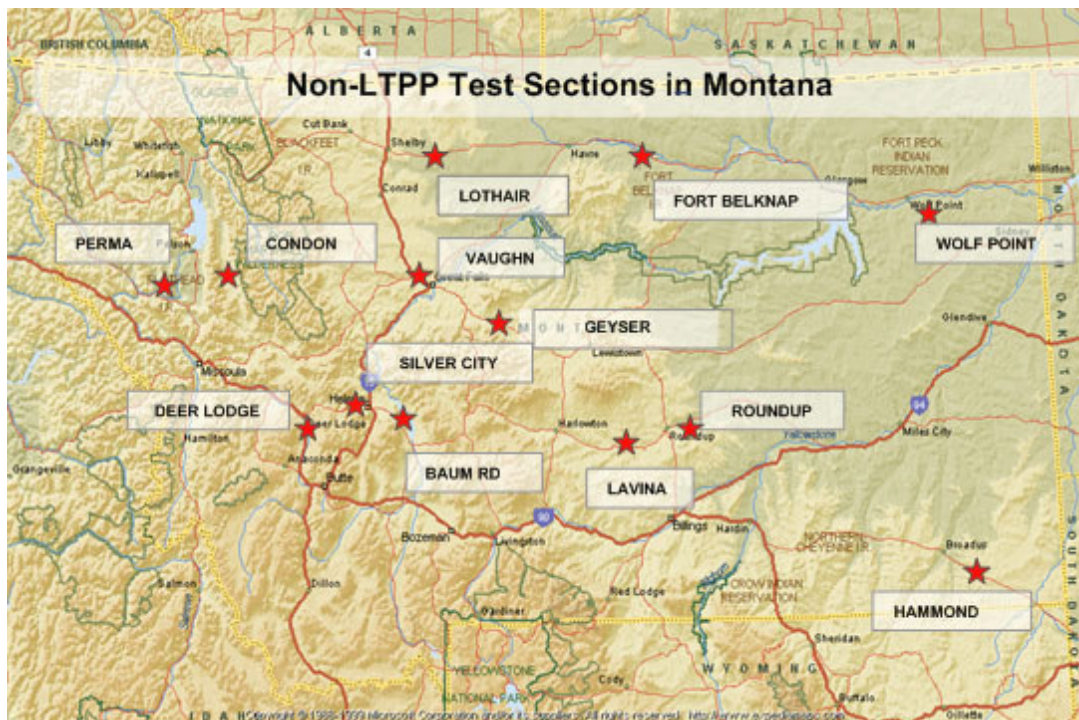


Figure I-5 Non-LTPP test sections in Montana.

Table I-5 LTPP Test Sections Located in States and Canadian Provinces Adjacent to Montana

Type of Structure	Conventional Flexible	Deep Strength & Full Depth	Includes Drainage Layer	Semi-Rigid Pavement	Pulverized Pavement	HMA Overlay of Rigid	HMA Overlay	Total Number Test Sections
	16-1001 16-1020 16-1021 16-9032 46-0803 46-0804 46-9187 56-1007 56-7775 81-0501 81-0901 81-0902 81-0903 81-1803 81-1804 81-1805 90-6405	16-1009 16-1010 16-9034 90-1802		38-2001 56-2015 56-2017 56-2018 56-2019 56-2020 56-2037 56-7772 56-7773 81-2812	81-8529	16-5025 46-7049	16-1005 16-1007 16-6027 46-9106 46-9197 56-6029 56-6031 56-6032 81-0502 81-0503 81-0504 81-0505 81-0506 81-0507 81-0508 81-0509 90-6400 90-6410 90-6412 90-6420 90-6801	
Test Sections By Group	17	4	0	10	1	2	21	55

Note: 16- Idaho, 38- North Dakota, 46- South Dakota, 56- Wyoming, 81- Alberta, 90- Saskatchewan

I-2.3 FIELD TESTING PLAN AND INVESTIGATIONS

The field investigations included coring the HMA and stabilized base layers, drilling bore holes, taking samples of each layer, conducting condition surveys of the pavement surface to identify the types and extent of distress, and field testing. Fourteen cores and two twenty-foot borings were drilled along each non-LTPP test section to measure layer thickness and confirm the materials and soils that were found from a review of the as-built construction plans.

Cores of the HMA layers were used for measuring other mixture properties. Two ten-inch diameter cores were taken to determine the in place volumetric properties of the HMA mixtures. The volumetric properties include air void content, gradation, asphalt content, and asphalt binder viscosity. Twelve six-inch cores were taken to measure the creep compliance, modulus, and strength of the layer for use in distress predictions. All bound layers were cored. Cores of the cement-treated bases were recovered to measure the compressive and Indirect Tensile (IDT) strengths and elastic modulus of that layer.

After core recovery, the unbound pavement layers were augured from the two 10-inch cores for collecting samples to determine the physical properties and resilient modulus of the aggregate materials. Two borings were then drilled to check for the presence of a shallow rigid layer and recover samples of the soil for laboratory testing. Undisturbed samples were taken with a thin-walled Shelby tube, where possible. If undisturbed samples could not be recovered, auger samples were taken. The undisturbed and disturbed samples were taken for measuring the

physical properties of the foundation soils, as well as for measuring the resilient modulus of the soils.

The field testing conducted during the initial investigation included Falling Weight Deflectometer (FWD) deflection basin testing, transverse profile measurements to determine the rut depths, and longitudinal profiles to determine the International Roughness Index (IRI). Details of the field testing program are summarized in Chapter I-2.5 on the monitoring program (this chapter).

I-2.4 LABORATORY TESTING PLAN

Table I-6 summarizes the laboratory materials test program for the materials recovered from each site, and included physical property tests, strength tests, and modulus tests in support of the distress prediction models. A complete listing of the laboratory and field test protocols is included in Volume III (*Von Quintus and Moulthrop 2007b*).

I-2.5 TEST SECTION MONITORING PROGRAM

The annual monitoring program was established to measure the performance of each test section over time, and is consistent with the LTPP program, except that a higher data collection frequency was used for this project. The annual monitoring program includes FWD tests, condition surveys to identify and measure the types and extents of distress at the site, ride quality, and rut depths (determined from the transverse profiles).

I-2.5.1 Falling Weight Deflectometer Tests

The FWD testing was performed in the outside wheel path of the test section in accordance with the LTPP test protocol. Deflection basin tests between the wheel paths were performed at some of the sites. In summary, FWD deflection basin tests using seven sensors were performed at 50-foot intervals along each test section, and within the sampling area both before and after the test section. Two seating drops were used prior to the deflection basin testing program. Four load levels and four drops per load level were used to measure the load-response of the pavement structure and subgrade soil – 6, 9, 12, and 16 kips. Pavement surface temperatures were recorded during the testing sequence.

I-2.5.2 Longitudinal and Transverse Profiles

Both longitudinal and transverse profile measurements were measured along each site in accordance with the LTPP test protocol. A minimum of four runs were made per site visit. The transverse profiles were used for estimating the rut depth along each section, while the longitudinal profiles were used for determining the IRI and other measures of surface smoothness.

Table I-6 Laboratory Tests to be Completed on the Materials Recovered from the Non-LTPP Test Sections Located in Montana

Materials Test	Type of Samples Recovered from Each Site				
	HMA 10 to 12- inch Cores	HMA 4 to 6-inch Cores	Cement Treated Base	Aggregate Base & Soil, Disturbed Samples	Foundation Soil, Undisturbed Samples
Maximum Specific Gravity (Rice)	√(2 cores)				
Bulk Specific Gravity		√ (12 cores)			
Extract Asphalt	√ (2 cores)				
Gradation of HMA	√(1)				
Viscosity	√(2)				
Dynamic or Resilient Modulus		√(3)		√(5) Each Layer	√(5)
Indirect Tensile (IDT) Strength & Failure Strain		√(3)			
IDT Creep Compliance		√(4)			
Compressive & IDT Strength			√ (4 cores)		
Elastic Modulus			√ (4 cores)		
Density				√(5) Each Layer	√ (2 borings)
Moisture Contents				√(5) Each Layer	√ (2 borings)
<p>(1) The gradation of the HMA mixtures is only needed for those projects where the construction files do not have this information. If the gradation is available, gradation tests do not need to be performed.</p> <p>(2) The viscosity is to be performed on the extracted asphalt at three temperatures – 275, 140 and 70 °F, unless this information is already available.</p> <p>(3) The dynamic modulus is to be measured on specific cores and then followed by the indirect tensile strength test. Six cores (3 from the wheel path area and 3 from the between wheel path area) should be tested. Two cores will be tested at 40, two at 60, and two at 80 °F. The LTPP protocols for indirect tensile strength testing should be followed; the dynamic modulus testing on cores should be measured in accordance with the test protocols being developed under NCHRP 9-29 (<i>NCHRP 2007 Active</i>).</p> <p>(4) The creep compliance testing for low temperature characterization will be conducted on 6 cores. Two cores will be tested at a –20, 2 at –10, and 2 at 0 °C, in accordance with the LTPP test protocols. The creep compliance tests will be followed by the indirect tensile strength test at each temperature in accordance with the LTPP protocol.</p> <p>(5) Two test specimens will be compacted and tested from each site for the aggregate base materials and subgrade soils. These repeated load resilient modulus tests will be performed in accordance with the LTPP test protocol (AASHTO T 307) (<i>AASHTO 2006b</i>).</p>					

I-2.5.3 Distress Surveys

Distress surveys were performed along each test section in accordance with the LTPP Distress Identification Manual (*SHRP 1993, FHWA 2003*). The distress surveys were used to measure the type, extent, and severity of each distress. Chip seals had been placed on several of Montana’s test sections and showed relatively little distress.

CHAPTER I-3 PERFORMANCE INDICATOR PREDICTION MODELS

The purpose of this chapter is to summarize the types of distress and performance indicators that were measured along the test sections listed in Chapter I-2. It presents those distress prediction models (transfer functions) recommended for use in pavement design and management. The distress prediction models were reviewed and presented in detail in Part II – Volume II (*Von Quintus and Moulthrop 2007a*).

I-3.1 PERFORMANCE DATA FOR CALIBRATION

As noted in the previous chapter, distress surveys and profile measurements were performed at each site in accordance with the LTPP Distress Identification Manual (*SHRP 1993, FHWA 2003*). Tables I-7 and I-8 summarize the latest measurements of selected distresses exhibited at the test sections located in Montana and in adjacent States, respectively.

As tabulated, about 20 percent of the Montana test sections have exhibited raveling, while less than 10 percent have exhibited block cracking. Most of the sections with raveling were from the SPS-5 experiment. Similarly, less than 10 percent of the sections outside Montana have exhibited block cracking, while over 40 percent have some amount of raveling. Block cracking and raveling are heavily influenced by material and construction quality. As a result, it is expected that there are an insufficient number of sections in Montana with raveling and block cracking for verifying and calibrating ME based transfer functions for these distresses.

Several of the Montana and other agency test sections have chip seals or other surface treatments placed on the surface. The test sections with surface seals generally have lower amounts of distress. The application and use of different pavement preservation policies and materials between the different agencies and test sections will need to be considered in the verification and calibration process of the global transfer function for each distress.

Table I-7 Summary of Distress Surveys for the Test Sections Located in Montana

Test Section ID Number	Alligator Cracking, %	Long. Cracks in Wheel Path, ft./mi.	Surface Seal Placed	Transverse Cracking, ft./mi.	Block Cracking, % Total Area	Raveling, % Wheel Path Area	Rut Depth, in.	IRI, in./mi.
Semi-Rigid or Pulverized Pavements								
Condon N	0	56	Yes	24	0	0		75.5
Deer Lodge/Beckhill	0	0	Yes		0	0		67.0
Geyser	0	0	Yes	828	0	0		72.3
Hammond	0	0	Yes	790	0	0		54.4
Lavina W	0	1476	Yes	3832	0	0		122.6
Perma	0	0	Yes		0	0		73.0
Roundup E	0	0	Yes	1753	0	0		108.4
Wolf Point S	0	0	Yes	1563	0	0		75.0
New Construction or Reconstructed Pavements								
Silver City W	0	0	Yes	28	0	0		76.4
Lothair E	---	---	Yes	---	---	---	---	---
Baum Road	---	---	Yes	---	---	---	---	---
30-0113	6.1	215	None	0	0	0	0.23	48.7
30-0114	8.0	5751	None	0	0	0	0.19	50.6
30-0115	3.7	0	None	0	0	0	0.19	47.4
30-0116	0.6	0	None	0	0	0	0.23	45.8
30-0117	5.2	1067	None	17	0	0	0.19	43.6
30-0118	0.2	10	None	0	0	0	0.15	37.4
30-0805	1.9	2256	None	0	0	0	0.31	62.2
30-0806	0.9	2515	None	0	0	0	0.23	64.3
30-0901	4.3	869	None	76	0	0	0.23	55.1
30-0902	2.3	0	None	0	0	0	0.19	47.6
30-0903	0	0	None	0	0	0	0.23	44.4
30-1001	0	793	Yes	4189	0	0	0.74	79.7
30-8129	0.6	45	Yes	2401	0	0	0.74	89.5
Flexible Pavements with Drainage Layers								
30-0119	7.1	960	None	0	0	0	.23	64.0
30-0120	17.4	9265	None	0	0	0	.35	80.2
30-0121	9.1	5329	None	135	0	0	.35	81.4
30-0122	16.2	4743	None	0	0	0	.27	50.4
30-0123	2.3	76	None	0	0	0	.23	52.2
30-0124	8.1	184	None	0	0	0	.15	49.6

Table I-7 Summary of Distress Surveys for the Test Sections Located in Montana, Continued

Test Section ID Number	Alligator Cracking, %	Long. Cracks in Wheel Path, ft./mi.	Surface Seal Placed	Transverse Cracking, ft./mi.	Block Cracking, % Total Area	Raveling, % Wheel Path Area	Rut Depth, in.	IRI, in./mi.
Rehabilitated Pavements; HMA Overlays								
Vaughn N	---	---	Yes	---	---	---	---	---
Fort Belknap	0	0	Yes	1767	0	0		60.8
30-0502	54.8	319	None	4521	8.7	7.6	0.86	102.7
30-0503	27.7	655	None	4223	0	7.9	0.66	76.1
30-0504	33.8	496	None	3607	0	0	0.66	54.4
30-0505	8.8	1573	None	2210	0	6.4	0.62	89.7
30-0506	21.2	530	None	1937	0	0	0.82	64.3
30-0507	28.6	1458	None	3100	14.7	0	0.82	74.8
30-0508	24.9	2512	None	3177	0	12.0	0.66	61.0
30-0509	100.0	401	None	2696	100.0	4.9	0.66	97.1
30-0560	11.5	2088	None	2193	0	0	0.23	65.0
30-0561	24.6	4034	None	1361	3.8	0	0.23	67.7
30-6004	0.1	4805	Yes	2218	0	18.8	0.51	161.5
30-7066	4.2	59	None	571	0	0	0.55	65.6
30-7075	0	0	Friction	1288	0	2.0	0.66	81.0
30-7076	0.1	32	Yes	2131	0	0	0.82	79.8
30-7088	9.8	127	None	752	3.9	0	0.62	57.3

NOTES:

- The values listed in this table were taken from the LTPP database for the LTPP test sections. These values represent the highest values included within the LTPP database for comparison between the different test sections within Montana and those in adjacent areas. Some of the values also represent the maximum distress value. This may or may not represent the cracking exhibited along the test section. It has been recognized that different distress surveyors have defined the same cracks under different categories. For example, longitudinal cracks being recorded as alligator cracks or block cracking between different surveyors. LTPP has clarified or corrected many of these types of discrepancies. However, variability in the cracking definition still exists to some extent in the LTPP database.

Table I-8 Summary of Distress Surveys for the Test Sections Located in States and Canadian Provinces Adjacent to Montana

Test Section ID Number	Alligator Cracking, %	Long. Cracks in Wheel Path, ft./mi.	Surface Seal Placed	Transverse Cracking, ft./mi.	Block Cracking, % Total Area	Raveling, % Wheel Path Area	Rut Depth, in.	IRI, in./mi.
Semi-Rigid or Pulverized Pavements								
38-2001	0	52	Yes	3808	0	10.3	0.66	127.5
56-2015	1.6	634	None	3954	0	0	0.70	151.1
56-2017	2.3	4202	Yes	3984	100.0	0	0.39	122.7
56-2018	0	5069	Friction	4909	0	0	0.23	66.6
56-2019	3.4	834	Yes	2345	0	0	0.43	69.5
56-2020	0.8	3358	Friction	1126	0	0	0.43	148.5
56-2037	0.4	422	Yes	4833	0	322.2	0.39	90.4
56-7772	0	581	Yes	4514	0	73.2	0.55	118.6
56-7773	0	35	Friction	1333	0	0	0.35	91.7
81-2812	0	1652	Yes	1466	0	0	0.51	88.7
81-8529	2.6	503	None	1756	0	0	0.62	63.5
New Constructed or Reconstructed Pavements								
16-1001	11.1	2101	Yes	1763	0	0	0.51	121.4
16-1020	0.3	24	Yes	1229	0	0	0.55	45.8
16-1021	0	49	Yes	1902	0	0	0.35	78.3
16-9032	0.2	137	Yes	638	0	156.8	0.47	136.1
16-1009	0.4	83	Yes	2297	0	0	0.74	98.6
16-1010	14.5	739	Yes	3863	0	0	0.43	111.6
16-9034	0.5	2292	Yes	942	0	131.6	0.39	121.4
46-0803	0	52	None	1487	0	0	0.23	62.8
46-0804	0	0	None	1026	0	0	0.66	79.4
46-9187	0	79	Yes	1068	0	86.8	0.39	92.9
56-1007	0.3	2608	Yes	3375	0	21.6	0.66	81.4
56-7775	0.2	35	Yes	2646	0	6.8	0.55	124.5
81-0501	0.5	2249	Yes	907	0	1.6	1.10	133.2
81-0901	1.3	0	None	21	0	0	0.27	66.3
81-0902	0	0	None	0	0	0	0.55	88.2
81-0903	0	0	None	0	0	0	0.82	75.6
81-1803	0	296	Yes	1068	0	0	0.43	99.0

Table I-8 Summary of Distress Surveys for the Test Sections Located in States and Canadian Provinces Adjacent to Montana, Continued

Test Section ID Number	Alligator Cracking, %	Long. Cracks in Wheel Path, ft./mi.	Surface Seal Placed	Transverse Cracking, ft./mi.	Block Cracking, % Total Area	Raveling, % Wheel Path Area	Rut Depth, in.	IRI, in./mi.
81-1804	4.7	2017	None	4639	0	0.7	0.78	70.3
81-1805	0	781	None	3714	0	4.7	0.70	105.0
90-6405	13.9	855	None	5659	0	0	0.51	143.9
90-1802	0	623	None	4296	17.0	0	---	183.9
Rehabilitated Pavements; HMA Overlays								
16-1005	0.7	602	Yes	1845	0	0	0.47	157.2
16-1007	5.5	5163	Yes	3192	25.2	0	0.86	89.3
16-6027	0.2	94	Yes	3063	0	0	0.43	87.5
16-5025	0.3	1489	None	0	0	32.4	0.39	155.4
46-9106	0	201	None	2491	0	155.9	0.35	87.0
46-9197	30.2	338	None	10537	100.0	0	0.27	107.5
46-7049	0	35	Yes	4316	100.0	0	1.06	266.8
56-6029	2.7	1880	Yes	6465	0	10.1	0.55	85.3
56-6031	2.4	275	Yes	2186	0	0	0.27	74.1
56-6032	0	0	None	539	0	139.5	0.39	88.5
81-0502	27.7	8353	None	6114	0	2.0	0.70	101.7
81-0503	30.0	10898	None	4594	0	5.3	0.70	85.2
81-0504	13.7	3010	None	2798	0	0.6	0.98	110.4
81-0505	30.7	7339	None	4868	0	0.6	0.78	87.2
81-0506	25.7	6178	None	4372	0	0	0.51	74.0
81-0507	6.3	2196	None	3696	0	0	0.47	92.6
81-0508	8.4	4625	None	2608	0	0.6	0.47	81.4
81-0509	38.8	8511	None	2006	0	1.2	0.43	89.9
90-6400	4.1	4245	None	1721	0	0	0.35	171.5
90-6410	1.0	781	None	1447	0	2.5	0.47	79.1
90-6412	2.1	465	None	1542	0	8.3	0.43	69.7
90-6420	13.2	1457	None	3369	0	32.7	0.98	347.5
90-6801	1.1	1890	None	1900	0	0	0.59	177.7

NOTES:

1. Some of the values listed above exceed 100 percent of the wheel path area. These values include areas outside the wheel path area.
2. Friction as used in this table and the previous one is as defined through and used within the LTPP program. These surface layers represent open-graded friction courses and other thin surface layers to improve the skid resistance.

I-3.2 LOAD RELATED CRACKING

I-3.2.1 Area Fatigue Cracking – Bottom-Up Cracking

The area fatigue (“alligator”) cracking transfer function recommended for use in Montana for pavement design and management is the one included in the MEPDG, which determines the number of allowable strain applications for the incremental damage index approach using Equation I-1.

$$N_f = k_{f1}(C)(C_H)\beta_{f1}(\varepsilon_t)^{k_{f2}\beta_{f2}}(E)^{k_{f3}\beta_{f3}} \quad (I-1a)$$

Where:

N_f = Allowable number of strain repetitions to fatigue cracking failure criteria.

ε_t = Tensile strain at the critical location.

E = Dynamic modulus measured in compression.

k_{f1}, k_{f2}, k_{f3} = Global field calibration parameters:

from the NCHRP Project 1-37A (ARA 2004a,b,c,d) calibration effort:

$$k_{f1}=0.00432, k_{f2}=-3.9492, \text{ and } k_{f3}=-1.281,$$

from the NCHRP Project 1-40D (NCHRP 2006) recalibration effort:

$$k_{f1}=0.007566, k_{f2} \text{ and } k_{f3} \text{ remain the same.}$$

$\beta_{f1}, \beta_{f2}, \beta_{f3}$ = Local or mixture specific field calibration parameters, all parameters were set to 1.0 for the NCHRP Projects 1-37A (ARA 2004a,b,c,d) and 1-40D (NCHRP 2006) calibration efforts.

$$C = 10^M, \text{ and where:} \quad (I-1b)$$

$$M = 4.84 \left(\frac{V_{be}}{V_a + V_{be}} - 0.69 \right) \quad (I-1c)$$

V_a = Air voids at the time the roadway is opened to traffic, percent.

V_{be} = Effective asphalt content by volume of the mix placed on roadway, percent.

C_H = Thickness correction term, dependent on type of cracking.

For bottom-up or alligator cracking:

$$C_H = \frac{1}{0.000398 + \frac{0.003602}{1 + e^{(11.02 - 3.49H_{HMA})}}} \quad (I-1d)$$

For top-down or longitudinal cracking:

$$C_H = \frac{1}{0.01 + \frac{12.00}{1 + e^{(15.676 - 2.8186H_{HMA})}}} \quad (I-1e)$$

H_{HMA} = Total HMA thickness, inches.

The cumulative damage index is determined by summing the incremental damage index over time (see Equation I-2).

$$DI = \sum_{j,m,l,p,T} \left(\frac{n}{N_f} \right) \quad (I-2)$$

Where:

- DI = Damage index.
- n = Actual number of axle load applications within a specific time period
- N_f = Allowable number of strain repetitions to fatigue cracking failure criteria.
- j = Axle load interval.
- m = Axle load type (single, tandem, tridem, quad, or special axle configuration).
- l = Truck type using the truck classification groups included in the MEPDG.
- p = Month.
- T = Median temperature for the five temperature intervals used to subdivide each month.

The MEPDG calculates the amount of alligator area cracking based on the incremental damage index summed with time and different truck loadings (Equation I-2). Equation I-3 is the relationship used to predict area alligator cracking based on total lane area. In accordance with the MEPDG, alligator cracks are assumed to initiate at the bottom of the HMA layers and propagate upward. Many of the test sections included in Table I-7 exhibit alligator cracks.

$$FC_{Bottom} = \left(\frac{1}{60} \right) \left(\frac{C_4}{1 + e^{(C_1 C_1^* + C_2 C_2^* \text{Log}(DI_{Bottom} * 100))}} \right) \quad (I-3)$$

Where:

- FC_{Bottom} = Fatigue cracking at the bottom of the HMA layers.
- C_4, C_1, C_2 = $C_4=6,000, C_1=1.00, C_2=1.00$.
- C_1^* = $-2 C_2^*$.
- C_2^* = $-2.40874 - 39.748(1 + h_{HMA})^{-2.856}$.
- DI_{Bottom} = DI at the bottom of the HMA layers and calculated in accordance with Equation I-2.

For fatigue cracking in cement treated base materials, the allowable number of load applications is determined in accordance with Equation I-4, and the amount of fatigue cracking calculated in accordance with Equation I-5. Few of the semi-rigid pavements have exhibited fatigue cracks, and those with fatigue cracking have only exhibited small amounts of cracking. These transfer functions were never calibrated under NCHRP Projects 1-37A (ARA 2004a,b,c,d) and 1-40D (NCHRP 2006). It is expected that there are too few semi-rigid test sections with higher amounts of fatigue cracking to be confident in the global and regional calibration factors.

$$N_{f-CTB} = 10^{\left[\frac{k_{c1} \beta_{c1} \left(\frac{\sigma_r}{M_r} \right)}{k_{c2} \beta_{c2}} \right]} \quad (I-4)$$

$$FC_{CTB} = C_1 + \frac{C_2}{1 + e^{(C_3 - C_4 \text{Log}(DI_{CTB}))}} \quad (I-5)$$

Where:

- N_{f-CTB} = Allowable number of load applications to fatigue failure in Cement Treated Base (CTB) layer.
- σ_t = Tensile stress at the bottom of the CTB layer.
- M_r = Modulus of rupture for the CTB layer.
- k_{c1}, k_{c2} = Global calibration coefficients to minimize the average residual error.
- β_{c1}, β_{c2} = Local or regional calibration coefficients.
- FC_{CTB} = Fatigue cracking in the CTB.
- C_1, C_2, C_3, C_4 = Regression coefficients relating the predicted and observed amounts of fatigue cracking.
- DI_{CTB} = Damage index for the CTB layer and calculated in accordance with Equation I-2.

I-3.2.2 Longitudinal Cracking Within Wheel Path – Surface-Down Cracking

Longitudinal Cracking Within the Wheel Path (LCWP) distresses are assumed to initiate at the surface and propagate downward in accordance with the MEPDG. Equations I-1(a-e) and I-2 are used to calculate the allowable number of loads and the incremental and cumulative damage indices. The MEPDG calculates the length of LCWP in accordance with Equation I-6. The longitudinal cracking transfer function has a high error term from the calibration work completed under NCHRP Project 1-40D (NCHRP 2006).

Von Quintus, et al., recommended that this model not be used based on work completed under NCHRP Projects 9-30(001) (Von Quintus et al. 2005a) and 1-40B (Von Quintus et al. 2005b), and the standard error reported from the global calibration study under NCHRP Project 1-37A (ARA 2004a,b,c,d). Many of the Montana test sections, however, were found to exhibit this type of fatigue cracking (refer to Table I-7). Thus, this transfer function was evaluated for use in Montana for pavement design.

$$FC_{Top} = 10.56 \left(\frac{C_4}{1 + e^{(C_1 - C_2 \text{Log}(DI_{Top}))}} \right) \quad (I-6)$$

Where:

- FC_{Top} = Fatigue cracking at the pavement surface.
- C_1, C_2, C_4 = Regression coefficients resulting from the global calibration effort under NCHRP Project 1-37A (ARA 2004a,b,c,d) ($C_4=1000$, $C_1=7.00$, and $C_2=3.5$).
- DI_{Top} = Damage index near the top of the HMA layers and calculated in accordance with Equation I-2.

I-3.3 NON-LOAD RELATED CRACKING – TRANSVERSE CRACKING

The MEPDG thermal cracking model is an enhanced version of the approach originally developed under the SHRP A-005 research contract by Drs. Roque and Hiltunen of the Pennsylvania Transportation Institute (*Lytton et al. 1993*). The amount of crack propagation induced by a given thermal cooling cycle is predicted using the Paris law of crack propagation (see Equation I-7).

$$\Delta C = A(\Delta K)^n \quad (I-7)$$

Where:

- ΔC = Change in the crack depth due to a cooling cycle.
- ΔK = Change in the stress intensity factor due to a cooling cycle.
- A, n = Fracture parameters for the HMA mixture.

Experimental results indicate that reasonable estimates of A and n can be obtained from the indirect tensile creep-compliance and strength of the HMA in accordance with Equations I-8a and I-8b.

$$A = 10^{k_t \beta_t (4.389 - 2.52 \text{Log}(E\sigma_m^n))} \quad (I-8a)$$

Where:

- A = Fracture parameter.
- $n = 0.8 \left[1 + \frac{1}{m} \right]$. (I-8b)
- k_t = Coefficient determined through field calibration for each input level (Level 1 = 5.0, Level 2 = 1.5, and Level 3 = 3.0).
- β_t = Local or mixture calibration factor.
- E = Modulus.
- σ_m = Mixture tensile strength, psi.

The stress intensity factor, K , has been incorporated in the MEPDG through the use of a simplified equation developed from theoretical finite element studies (Equation I-9).

$$K = \sigma_{tip} (0.45 + 1.99(C_o)^{0.56}) \quad (I-9)$$

Where:

- σ_{tip} = Far-field stress from pavement response model at depth of crack tip, psi.
- C_o = Current crack length, ft.

The degree of cracking is predicted by the MEPDG using an assumed relationship between the probability distribution of the log of the crack depth to HMA layer thickness ratio and the percent of cracking. Equation I-10 shows the expression used to determine the extent of thermal cracking.

$$TC = \beta_{t1} N \left[\frac{1}{\sigma_d} \text{Log} \left(\frac{C_d}{h_{HMA}} \right) \right] \quad (I-10)$$

Where:

TC	=	Observed amount of thermal cracking, ft/mi.
β_{1l}	=	Regression coefficient determined through field validation.
$N(z)$	=	Standard normal distribution evaluated at (z) .
σ_d	=	Standard deviation of the log of the depth of cracks in the pavement.
C_d	=	Crack depth, in.
h_{HMA}	=	Thickness of surface layer, in.

The MEPDG transverse cracking transfer function has been found to be acceptable for flexible pavements in northern climates, and is recommended for use in Montana for evaluating different pavement design strategies and mixtures. This procedure requires extensive and complicated mixture characterization tests, as well as detailed climatic data. Thus, it is not recommended for pavement management purposes, but should be evaluated for use in selecting HMA mixtures for different areas in Montana.

As tabulated in Table I-7, there are more than just a few sections that do not exhibit transverse cracking. Conversely, many of the sections located outside Montana do exhibit high amount of transverse cracks. This observation will need to be considered when verifying and revising the calibration coefficients for the thermal cracking model between the Montana and other agency test sections.

I-3.4 SURFACE DISTORTION – RUTTING

Surface distortion in the form of rutting can be caused by two mechanisms; permanent deformation in the HMA layers and in the unbound layers. The approach presented in the MEPDG is based upon incremental rut depth and was found to be reasonably accurate for HMA mixtures but overestimated rutting in the unbound layers. Both mechanisms are recommended for use in Montana for evaluating flexible pavement designs.

Table I-7 tabulates the rut depths measured along each test section. With the exception of the SPS-5 experiment, few of the test sections have average rut depths exceeding 0.5 inches. Conversely, many of the test sections located outside Montana have rut depths in excess of 0.5 inches (refer to Table I-8). This observation again suggests a systematic difference in HMA mixture quality between Montana sections and those located in adjacent areas. This potential difference in material quality between the Montana and other agency test sections will need to be carefully considered in verifying and calibrating the distortion transfer functions. Chapter 7 within this volume addresses this material quality issue.

I-3.4.1 Permanent Deformation in HMA Layers

Rutting is estimated for each sub-season at the mid-depth of each sub-layer within the pavement system. The permanent deformation for a given season is the sum of the permanent deformation within each layer. The field calibrated form of the final lab expression selected for use in the MEPDG is given below (see Equation I-11).

$$\Delta_{p(HMA)} = \epsilon_{p(HMA)} h_{HMA} = \beta_{1r} k_z \epsilon_{r(HMA)} 10^{-3.35412} N^{0.4791 * \beta_{2r}} T^{1.5606 * \beta_{3r}} \quad (I-11a)$$

Where:

- $\Delta_{p(HMA)}$ = Accumulated permanent or plastic vertical deformation in the HMA layer/sublayer, in.
 $\epsilon_{p(HMA)}$ = Accumulated permanent strain, in/in.
 $h_{(HMA)}$ = Total HMA thickness, in.
 $\epsilon_{r(HMA)}$ = Resilient strain, in/in.
 $\beta_{1r}, \beta_{2r}, \beta_{3r}$ = Local or mixture field calibration constants; all of these constants were set to 1.0 for the global calibration efforts completed under NCHRP Projects 1-37A(ARA 2004a,b,c,d) and 1-40D (NCHRP 2006).

k_z = Depth confinement factor.
 $k_z = (C_1 + C_2 D)0.328196^D$ (I-11b)

$C_1 = -0.1039(H_{HMA})^2 + 2.4868H_{HMA} - 17.342$ (I-11c)

$C_2 = 0.0172(H_{HMA})^2 - 1.7331H_{HMA} + 27.428$ (I-11d)

D = Depth below the surface, in.
 H_{HMA} = Total HMA thickness, in.

- N = Number of load repetitions.
 T = Mixing temperature, °F.

I-3.4.2 Permanent Deformation in Unbound Layers

Equation I-12 shows the mathematical equation used to calculate plastic deformation within the unbound layers.

$$\Delta_p = \beta_{s1} k_{s1} \epsilon_v h_p \left(\frac{\epsilon_o}{\epsilon_r} \right) e^{-\left(\frac{\rho}{N} \right)^\beta} \quad (I-12a)$$

Where:

- Δ_p = Permanent deformation for the layer/sublayer, in.
 N = Number of axle load applications.
 ϵ_o, β, ρ = Material properties.
 ϵ_r = Resilient strain imposed in laboratory test to obtain material properties ϵ_o, β , and ρ .
 ϵ_v = Average vertical resilient strain in the layer/sublayer as obtained from the primary response model.
 h_p = Thickness of the unbound layer/sublayer, in.
 K_{s1} = Global calibration coefficients, $k_{s1}=1.673$ for granular materials and 1.35 for fine-grained materials.
 β_{s1} = Local calibration constant for the rutting in the unbound layers. The local calibration constant was set to 1.0 for the global calibration effort.

$\text{Log } \beta = -0.61119 - 0.017638(W_c)$ (I-12b)

$$\rho = 10^9 \left(\frac{C_o}{(1 - (10^9)^\beta)} \right)^{\frac{1}{\beta}} \quad (I-12c)$$

$$C_o = \text{Ln} \left(\frac{a_1 M_r^{b_1}}{a_9 M_r^{b_9}} \right) \quad (I-12d)$$

W_c = Water content, %.

M_r = Resilient modulus of the unbound layer or sublayer, psi.

$a_{1,9}$ = Regression constants, $a_1=0.15$ and $a_9=20.0$.

$b_{1,9}$ = Regression constants, $b_1=0.0$ and $b_9=0.0$.

As noted above, the model used to predict the plastic deformations in the unbound layers was found to over predict rut depths in the foundation or subgrade soil (*Von Quintus et al. 2005b*). As a potential alternate, it is recommended that the modified Corps of Engineers limiting strain criteria (Equation I-13) be used to ensure that there is sufficient cover above any unbound layer. This assumption implies that the structural layers above the subgrade or foundation will be constructed so that only negligible rutting will occur within those layers. This criterion is recommended for use in categorizing the pavement structures at a site with or without sufficient cover to protect the foundation soils.

$$N_f = 1.259 \times 10^{-11} (M_R)^{0.955} (\epsilon_v)^{-4.082} \quad (I-13)$$

Where:

N_f = Allowable number of load applications to rutting criteria.

M_R = Resilient modulus of the unbound layer or soil.

ϵ_v = Vertical strain computed at the surface of the unbound layer or soil.

I-3.5 HMA MIXTURE DISINTEGRATION DISTRESSES

I-3.5.1 Raveling

Raveling is not predicted in the MEPDG, but is considered in a few ME based procedures (*Von Quintus et al. 1991*). As stated previously, about 20 percent of the test sections exhibit various amounts of raveling (refer to Table I-7). However, most of the sections that exhibit some amount of raveling were from the SPS-5 experiment. Conversely, over 40 percent of test sections in adjacent States exhibit raveling (refer to Table I-8). This larger percentage could be attributable to differences in mixture design, construction specification, and quality assurance procedures and enforcement. Few of the LTPP test sections located outside of Montana have the HMA mixture property (IDT strain at failure) to estimate the potential for this distress. Thus, it is recommended that this distress not be considered for use in pavement design or management.

I-3.5.2 Block Cracking

Block cracking is not predicted in any known ME based procedure. Block cracking was exhibited on only a few of the test sections (refer to Table I-7). Thus, it is recommended that this distress not be considered for use in pavement design or management.

I-3.6 SMOOTHNESS – LONGITUDINAL PROFILES

The MEPDG prediction model for smoothness or increasing roughness is recommended for use in Montana, because it is based on hundreds of test sections placed around the U.S. and was found to have reasonable error terms (see Equations I-14a to I-14c). No other models were found to provide the accuracy considering the diverse pavements and site conditions within the LTPP database. These equations were developed from data collected within the LTPP program for the MEPDG:

Models for New HMA Pavements and HMA Overlays of Flexible Pavements

$$IRI = IRI_o + 0.0150(SF) + 0.400(FC) + 0.0080(TC) + 40.0(RD) \quad (I-14a)$$

and

Models for HMA Overlays of Rigid Pavements

$$IRI = IRI_o + 0.00825(SF) + 0.575(FC) + 0.0014(TC) + 40.8(RD) \quad (I-14b)$$

Where:

- IRI* = International Roughness Index.
- IRI_o* = Initial IRI after construction, in/mi.
- FC* = Area of fatigue cracking (combined alligator and longitudinal cracking in the wheel path), percent of total lane area.
- TC* = Length of transverse cracking, ft/mi.
- RD* = Average rut depth, inches.
- SF* = Site Factor (*SF* Equation I-14c shows the parameters used to determine a site factor for each test section.

$$SF = Age(0.02003(PI + 1) + 0.007947(Rain + 1) + 0.000636(FI + 1)) \quad (I-14c)$$

Where:

- Age* = Pavement age, years.
- PI* = Percent plasticity index of the soil.
- FI* = Average annual freezing index, °F days.
- Rain* = Average annual rainfall, in.

I-3.7 SUMMARY – HMA MIXTURE PROPERTIES FOR DISTRESS TRANSFER FUNCTIONS

Table I-9 summarizes the performance indicator prediction models recommended for use in evaluating trial pavement designs and for pavement management purposes. These prediction models need to be verified and the global calibration factors confirmed or revised to ensure

reliable use in Montana. Tables I.10 and I-11 list the material properties and climatic parameters that are needed in support of these models, respectively.

Table 1-9 Performance Indicator Prediction Models Considered for Use in Montana

Distress/Performance Indicator		Evaluating Design Strategies	Forecasting Performance for Pave. Management
Load Related Cracking	Alligator Cracking	Yes	Yes
	Longitudinal Cracking in Wheel Path	Yes, but only if standard error is reduced	No
Non-Load Related Cracking	Transverse (Thermal) Cracks	Yes	No
	Block Cracking	No	No
Surface Distortion	HMA Rutting	Yes	No
	Aggregate Base	Yes	No
	Subgrade Rutting	Yes	Yes, but based on vertical strain to categorize structure.
HMA Disintegration	Raveling	No	No
Smoothness	IRI	Yes	Yes

Table I-10 Material Properties Needed for Performance Indicator Prediction Models

Layer/Material	Property	Input Level	Purpose
HMA	Dynamic Modulus	1	Used for fatigue & rutting predictions.
	IDT Creep Compliance	1,2	Used for transverse cracking predictions.
	IDT Strength	1,2	
	IDT Strain at Failure		Information purposes for calibration.
	Air Voids	1,2,3	Used for calculating dynamic modulus & predicting fatigue cracking.
	Effective Asphalt Content by Volume	1,2,3	
	Density	1,2,3	Used to estimate coefficient of thermal contraction.
	Gradation	2,3	Used for calculating dynamic modulus.
	Asphalt Performance Grade	3	Used to provide default values for other input parameters.
Unbound Aggregate Base & Subgrade Soil	Resilient Modulus	1	Used to predict fatigue cracking and rutting.
	Dynamic Cone Penetrometer	2	Estimate resilient modulus of unbound layers and subgrade.
	Deflection Basins	1,2,3	Determine modulus of layer in existing pavements.
	Gradation	1,2,3	Used to estimate water content over time.
	Water Content	1,2,3	Estimate resilient modulus over time.
	Dry Density	1,2,3	Estimate resilient modulus over time.
	Soil-Water Characteristic Curve	1,2,3	Estimate resilient modulus & changes in water content over time.
	Atterberg Limits	1,2,3	
	Gradation	1,2,3	Used to provide default values for other input parameters.
	Classification	1,2,3	
CTB	Flexural Strength	1,2,3	Used to estimate fatigue cracking.
	Elastic Modulus	1,2,3	Used to estimate fatigue cracking.
	Compressive Strength	2	Used to estimate flexural strength.

Table I-11 Climatic Parameters and Information Needed for Performance Indicator Prediction Models

Climatic Parameter	Purpose	Used For:	
		Evaluating Design Strategies	Forecasting for Pave. Management
Weather Stations	Used to predict temperature and water content of pavement layers.	Yes	No
Annual Rainfall	Used to predict IRI with time.	Yes	Yes
Average Annual Freezing Index	Used to predict IRI with time.	Yes	Yes

CHAPTER I-4 CLIMATE CHARACTERIZATION

Extensive and detailed climatic data are required to use the MEPDG in predicting pavement distress. These data include hourly temperature, precipitation, wind speed, relative humidity, and cloud cover. These data are used to predict the temperature and moisture content in each of the pavement layers (*Larson and Dempsey 1997*), as well as provide some of the inputs to the site factor parameter for the smoothness prediction models (Equation I-14b).

All of these climate data are available from weather stations, generally located at airfields around the United States (U.S.). The MEPDG has an extensive number of these weather stations embedded in the software for ease of use and implementation.

One or more weather stations are selected as close to the project as possible to provide hourly temperature, precipitation, wind speed, relative humidity, and cloud cover information. Each weather station is defined and located based on Longitude and Latitude. Table I-12 lists the Montana weather stations that are currently available in the MEPDG software database. The stations without missing data are recommended for use in evaluating trial designs and were used in the performance analysis of test sections located in Montana and adjacent States and Canadian provinces. Other weather stations located in adjacent States but near a project location should be considered for use in Montana.

Table I-12 Weather Stations that are Available in the MEPDG Software for Montana

City	Latitude (Degrees.Minutes)	Longitude (Degrees.Minutes)	Elevation, ft.	Number of Months Available
Baker	46.22	-104.15	2963	97*
Billings	45.49	-108.32	3582	116
Bozeman	45.47	-111.09	4468	116
Butte	45.58	-112.30	5539	64
Cut Bank	48.37	-112.23	3855	62
Dillon	45.16	-112.33	5221	105
Glasgow	48.13	-106.37	2271	116
Great Falls	47.28	-111.23	3673	116
Havre	48.34	-109.47	2584	116
Helena	46.37	-111.58	3867	116
Lewistown	47.03	-109.28	4146	63
Livingston	45.42	-110.27	4655	65
Miles City	46.26	-105.53	2630	64
Missoula	46.55	-114.05	3202	114
Wolf Point	48.05	-105.34	1984	90

* Weather station has missing month within the database.

Stations with missing months and data may cause the MEPDG software to crash or get hung up in the climatic computations. Only one of the Montana weather stations has missing data – Baker.

A single weather station was selected for projects within close proximity (e.g., 25 miles) to a particular test section. When weather stations were unavailable, up to six surrounding weather stations were selected and combined into a virtual weather station for that project. This creation

of a virtual weather station is done automatically by the software after selection by the user. There are several weather stations in the surrounding States of Idaho, North Dakota, South Dakota, and Wyoming for projects located near State lines. These stations were used in creating some of the virtual weather stations for a particular test section.

Tables I-13 and I-14 list the longitude, latitude, and elevation for the test sections located in Montana and adjacent States and Canadian provinces that were used in this study, respectively.

Table I-13 Latitude, Longitude, and Elevation of the Test Sections Located in Montana for Selecting Weather Stations

Test Section	Latitude (Degrees.Minutes)	Longitude (Degrees.Minutes)	Elevation, ft.
Condon, North	47.33	-113.44	3650
Deer Lodge/Beckhill	46.28	-112.43	4436
Geyser	47.14	-110.28	4270
Hammond NW	45.19	-105.09	3280
Lavina, West	46.18	-109.05	3516
Perma	47.30	-114.36	2820
Roundup, East	46.27	-108.31	3200
Wolf Point, South	47.57	-105.31	2310
Silver City, West	46.45	-112.11	4360
Fort Belknap	48.25	-108.23	2314
Lothair, East	48.29	-111.12	3290
Baum Road	46.32	-111.43	4280
Vaughn North	47.38	-111.35	3770
30-0113 to 30-0124	47.4	-111.5	3343
30-0501 to 30-0509	45.8	-110.0	4072
30-0805 and 30-0806	46.1	-112.9	4200
30-0901 to 30-0903	47.4	-111.5	3343
30-1001	47.2	-110.5	4196
30-6004	46.4	-105.1	2766
30-7066	45.8	-110.0	4072
30-7075	45.7	-108.6	3177
30-7076	45.1	-107.4	3750
30-7088	45.8	-110.0	4072
30-8129	46.3	-109.1	4440

Table I-14 Latitude, Longitude, and Elevation of the Test Sections Located in States and Canadian Provinces Adjacent to Montana for Selecting Weather Stations

Agency	Test Section	Latitude (Degrees.Minutes)	Longitude (Degrees.Minutes)	Elevation, ft.
Idaho	16-1001	44.6	-116.8	3232
	16-1007	42.6	-114.7	3771
	16-1009	42.5	-113.4	3025
	16-1010	43.7	-112.1	4775
	16-1020	42.7	-114.4	4097
	16-1021	43.6	-111.9	4849
	16-5025	42.4	-112.2	4979
	16-6027	42.4	-111.4	6056
	16-9032	47.6	-116.9	2602
16-9034	48.4	-116.5	2119	
North Dakota	38-2001	47.9	-97.4	922
South Dakota	46-0600	45.5	-98.1	1317
	46-0800	45.9	-100.4	1680
	46-7049	43.0	-97.4	974
	46-9106	45.9	-102.2	2405
	46-9187	44.8	-102.1	2360
	46-9197	44.1	-98.5	1450
Wyoming	56-1007	44.5	-108.9	5204
	56-2015	41.6	-104.9	5814
	56-2017	43.6	-105.7	5210
	56-2018	43.0	-106.7	5545
	56-2019	44.2	-105.4	4577
	56-2020	44.9	-107.2	4022
	56-2037	41.7	-107.7	7085
	56-6029	42.7	-110.9	6404
	56-6031	43.1	-108.5	5472
	56-6032	43.5	-110.8	6165
	56-7772	43.7	-108.3	4677
	56-7773	42.7	-106.5	5538
56-7775	42.0	-109.6	6433	
Alberta	81-0500	53.6	-116.0	2900
	81-0900	49.8	-113.3	3100
	81-1803	53.3	-111.4	2123
	81-1804	53.3	-113.6	2301
	81-1805	50.9	-113.9	3379
	81-2812	51.7	-113.2	2975
	81-8529	51.0	-115.0	4197
Saskatchewan	90-1802	50.2	-102.3	2112
	90-6400	50.4	-102.3	1967
	90-6405	51.9	-105.3	1785
	90-6410	52.1	-106.6	1680
	90-6412	52.1	-106.6	1678
	90-6420	50.2	-102.3	2112
90-6801	50.4	-102.3	1965	

CHAPTER I-5 TRUCK TRAFFIC CHARACTERIZATION

Current Montana procedures for analyzing traffic data for pavement design and management includes calculating truck equivalency factors to determine the number of 18-kip Equivalent Single Axle Loads (ESALs) over the design/analysis period. The number of ESALs is determined from truck equivalency factors derived or estimated from weigh-in-motion data measured on roadways in Montana.

The number of ESALs is not a required input to the MEPDG. The input is the actual or an estimate of the actual single, tandem, and tridem axle load distributions themselves. This section of the report summarizes the truck traffic inputs used for evaluating the applicability of the global calibration factors included in the distress transfer functions. A detailed analysis of the truck traffic data and Weigh in Motion (WIM) measurements is presented in detail in Part III of Volume III (*Von Quintus and Moulthrop 2007b*).

Overall, 21 Montana WIM sites (see Figure I-6) were used to determine the variability of truck volumes and loading patterns. The MEPDG includes 17 different groups of normalized truck volume and loading patterns. These groups are referred to in the MEPDG as Truck Traffic Classification (TTC) groups. The purpose of the analysis completed within this study was to compare those default axle load and truck volume distributions included in the MEPDG, and hopefully reduce the number of groups that describe that variation in truck volumes, as well as axle loads that can be expected in Montana.

In summary, MDT has a well developed traffic monitoring program that should serve as the basis for its use of the MEPDG. The current traffic monitoring program should provide the detailed traffic inputs that are needed for ME based design methods. This chapter is grouped by the different input categories related to truck traffic: Truck Category, Wheel and Axle Load Configurations, Volume Distributions, and Axle Load Distributions.

I-5.1 TRUCK CATEGORIES

A significant number of double-bottom trailers use Montana roadways, based on the WIM data. These multi-trailer trucks need to be tracked and considered separately in pavement design. As a result it is recommended that Montana use three truck categories for design evaluations; single unit trucks, combination trucks, and multi-trailer trucks. These three categories were used in verifying and calibrating the distress transfer functions in the MEPDG. The remaining sections of this chapter use these categories in establishing the truck traffic inputs for use in Montana.

I-5.2 WHEEL AND AXLE LOAD CONFIGURATIONS

Numerous input parameters are required to estimate the number of individual axle loads for calculating incremental damage and permanent deformation within each pavement layer. As an example, these input parameters include directional and lane distribution factors, speed, dual tire spacing, axle spacing, and many others. Table I-15 lists and defines the general truck traffic input parameters and default values that were used in the calibration of the distress transfer functions.

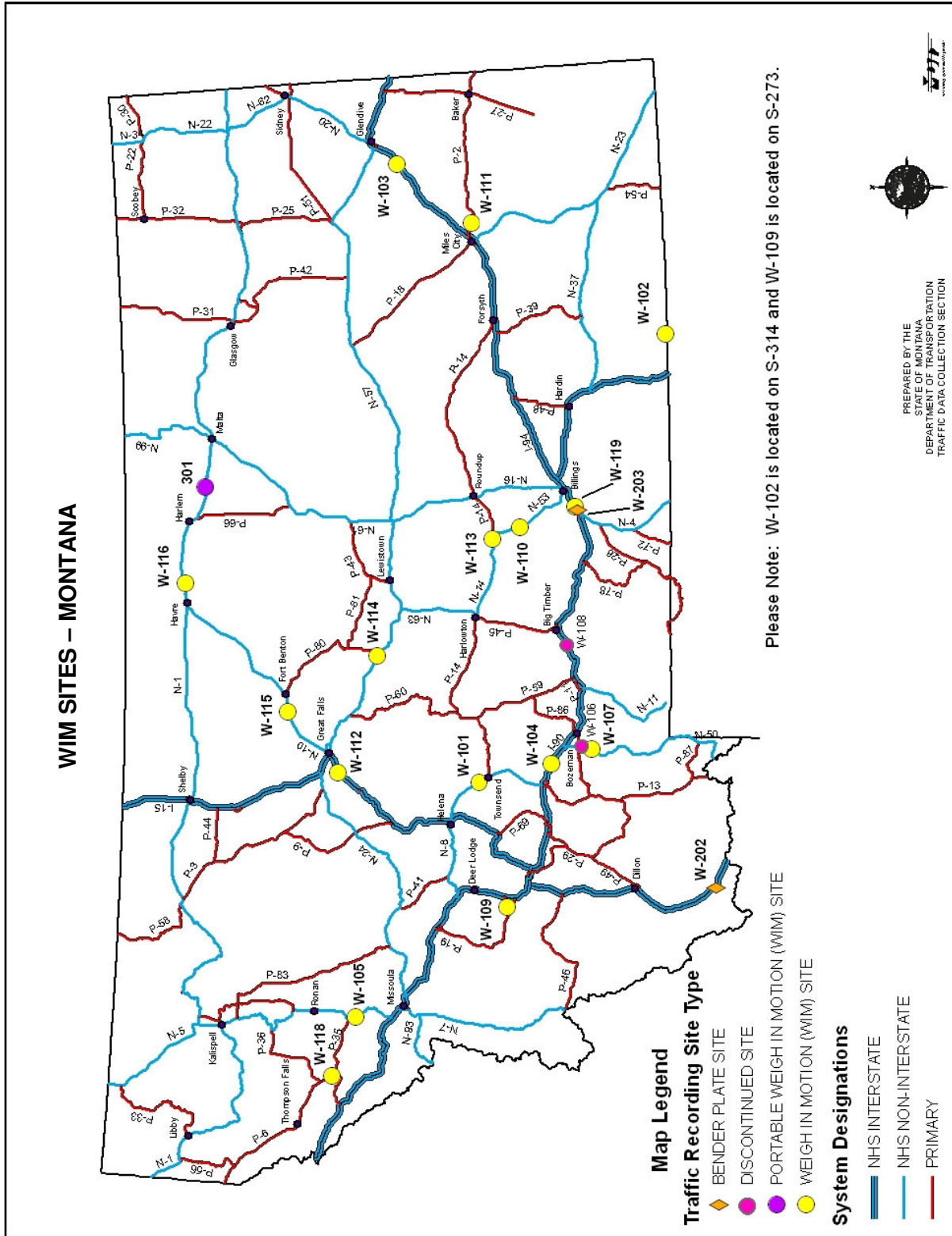


Table I-15 Summary of Truck Traffic Input Parameters and Values Used in Verification and Calibration of the Distress Transfer Functions for Montana

Input Parameter		Value		
Initial Two-Way Average Annual Daily Truck Traffic (AADTT)		Site specific		
Number of Lanes – One Direction		Site specific		
Percent Trucks in Design Lane		Site specific, based on number of lanes in each direction		
Percent Trucks in Design Direction	Default value selected	Dependent on primary truck type using facility and type of facility, (50 to 60 %)		
Operational Speed		Site specific, posted speed limit		
Lane Width		Site specific		
Growth Factor		Site specific, historical values of AADTT or ESALs used to determine growth		
Number of Axles per Truck Class	Truck Class	Axle Type		
		Single	Tandem	Tridem
	4	1.5	0.5	0.0
	5	2.0	0.0	0.0
	6	1.0	1.0	0.0
	7	1.0	0.0	1.0
	8	2.5	0.5	0.0
	9	1.0	2.0	0.0
	10	1.0	1.0	1.0
	11	4.75	0.25	0.0
	12	4.0	1.0	0.0
13	3.0	1.75	0.25	
Axle Spacing	Default values	Tandem	Tridem	Quad
		51.6	49.2	49.2
Dual Tire Spacing	Default value	12		
Tire Pressure	Default value	120		

I-5.3 TRUCK VOLUME DISTRIBUTIONS AND PATTERNS

I-5.3.1 Truck Classification Volume Distribution Factors

The 21 WIM sites in Montana were reviewed and used to determine the variability of truck volumes and loading patterns. In summary, Class 9 trucks generally contribute the vast majority of truck traffic loads, while truck Class 13 supplies a significant secondary load. The only deviation from this observation was for the WIM sites located on county roads or those with low truck volumes. For these roadways, truck Class 6 made up a significant portion of the truck traffic. Therefore, truck Classes 6, 9, and 13 were used to determine the normalized truck volume distributions and how those distributions might change between different roadways.

For roadways where sufficient truck volume data is unavailable to estimate the truck loadings and patterns, the distributions recommended for use in design are included in Table I-16. These groups were used in the verification and calibration portion of this study for those test sections located in Montana without sufficient truck traffic data. For the test sections located

outside Montana, the same truck classification groupings were assumed, with the exception for those test sections with sufficient truck volume data measured at the site.

Table I-16 Primary Truck Type Normalized Volume Distribution Factors Recommended for Use in Montana

Roadway Description	Primary Vehicle Class	Percentage of Trucks That Class	Applicable TTC Group
Interstate Highways & Primary Arterials, Heavier Volumes	9	75	TTC-11
	13	15	
	10	5	
Primary & Secondary Arterials, Moderate Volumes	9	65	TTC-5
	13	20	
	10	10	
Secondary Arterials, Lower Volumes	9	45	TTC-8
	13	15	
	5,6	5	
Local Routes with Low Truck Volumes	6, 5	55	TTC-15
	9	30	
	13	5	

The percentages listed in Table I-16 are preliminary and should be evaluated in future calibration updates conducted by the MDT. Specifically, these truck volume patterns should be expanded and improved with additional WIM and truck volume data measured over time.

I-5.3.2 Seasonal Distribution Factors

For the initial testing and calibration of the MEPDG distress transfer functions, it is recommended that Montana develop and apply seasonal monthly distribution factors for three categories of trucks. If sufficient data exists for a specific site or test section, the site specific monthly distribution values can be used. At present, however, there is insufficient data to be confident in site specific monthly distribution values for the individual test sections in Montana and adjacent States and Canadian provinces. Thus, the statewide average values for the three truck categories were used for all of the Montana test sections.

The statewide monthly volume factor averages are provided in Table I-17, which were used for all of the test sections located in Montana. For all test sections in adjacent States and Canadian provinces, the seasonal monthly distribution factors were all set to 1.0 (the recommended default values in the MEPDG). There were insufficient data from LTPP to determine regional values for the individual agencies.

Table I-17 Recommended Monthly Distribution Factors for Use in Montana

Month	Single Unit Trucks (Truck Class 5 or 6)	Combination Trucks (Truck Class 9 or 10)	Multi-Trailer Trucks (Truck Class 13)
January	0.84	0.91	0.99
February	0.79	0.92	0.89
March	0.76	0.94	0.88
April	0.86	0.99	0.999
May	1.10	1.06	1.03
June	1.30	1.09	0.96
July	1.43	1.02	0.92
August	1.39	1.06	1.11
September	1.14	1.00	1.09
October	1.06	1.15	1.12
November	0.87	1.00	1.00
December	0.76	0.84	0.87

NOTE: The values included within this table were used as the monthly distribution factors for each type of truck class noted within the columns. In other words, the monthly distribution factors listed for single unit trucks were used for truck Classes 4, 5, 6, and 7.

I-5.4 AXLE LOAD DISTRIBUTIONS AND PATTERNS

An analysis was conducted to determine whether the axle load spectra values computed from the Montana WIM data are significantly different from the default axle load spectra data contained in the MEPDG. The MEPDG defaults are based on averages of many WIM sites throughout the U.S. averaged by vehicle class and axle type. The issue was approached by analyzing the axle weight data for the primary truck classes.

Analysis of the WIM data suggests that many of Montana WIM stations are in general agreement with the defaults in the MEPDG. The use of four Truck Weight Road Group (TWRG) categories is recommended for use in Montana. These four groups are listed below:

- Primarily Loaded Trucks
- Bimodal Loaded Condition – Heavy Distribution
- Bimodal Loaded Condition – Even Distribution
- Lightly Loaded Trucks

However, considerable drift appears in the weights reported in the 2000-2001 data for a number of the WIM scales in Montana. This drift can result in substantial shifts in the calculated pavement damage for a given number of trucks. It is unclear whether these reported weights are correct or the data provided had some scale calibration problems. As a result, the axle weight default factors for each axle type were used in the verification and calibration study. It is recommended that Montana check their ongoing calibration process to confirm the accuracy and reliability of the axle weight data collected by its WIM scales. In the meantime, the TTC groups designated in the MEPDG that are similar to the above four groups were used in the verification and calibration study.

The axle weight default values included in the MEPDG have been independently checked by other agencies that are considering their use in design. Several of these agencies include

Mississippi, Missouri, and Utah. Thus far, it has been reported that the default normalized axle weight distributions are reasonable. This is the reason why the default normalized distributions were used in Montana.

CHAPTER I-6 MATERIALS CHARACTERIZATION

Early in the development stage of the MEPDG, it was recognized by the NCHRP 1-37A (*ARA 2004a,b,c,d*) project team and NCHRP that some agencies will purchase all of the necessary field and laboratory test equipment to implement the guide, while other agencies will continue to use correlations and “best-guessed” values for inputs to the program. The MEPDG has a unique hierarchical input scheme. Table I-1 provided a definition of each input level. This hierarchical input scheme was developed to facilitate implementation by the diverse procedures and policies that exist across the U.S. This input scheme is especially important for the materials characterization.

MDT has no immediate plans to purchase the laboratory test equipment to measure the required material properties. Like many other State agencies, MDT plans to continue with their current field and laboratory test procedures for new pavement and rehabilitation designs. Thus, one of the objectives of this project was to recommend methods that MDT can use to estimate the material properties required for ME based pavement design methods using their day to day testing procedures.

Chapter I-2 summarized the different field and laboratory tests that were used to characterize the layer of each test section (refer to Table I-6), and Table I-10 listed the material properties needed for executing the MEPDG. These material properties have a significant impact on the distress transfer functions discussed in Chapter I-3. The purpose of this chapter is two-fold, as listed below.

- Present the results of the field and laboratory tests and the analyses completed to determine the material properties for each test section used in the verification and calibration process. All test data were entered into the MDT database for future use.
- List the default values recommended for use in Montana for each material property input parameter.

I-6.1 FIELD INVESTIGATIONS

A field investigation is an important step in pavement evaluation and in calibrating distress transfer functions. For all of the LTPP test sections in Montana and in the adjacent States and Canadian provinces, this step was completed when the test sections were nominated for that program. For the non-LTPP test sections, a field investigation was included for three reasons.

1. Visually identify and classify the layers and foundation soil at each of the non-LTPP test sections.
2. Recover cores for volumetric and other laboratory tests. The cores and borings were used to determine the direction of crack propagation and rutting beneath the HMA layers. Field Dynamic Cone Penetrometer (DCP) tests were performed through the

unbound layers at many of the test sections prior to auguring the materials and recovering samples for laboratory tests.

3. Perform FWD tests to measure the load-response characteristics of each test section and to backcalculate the elastic modulus for each pavement layer and the foundation.

I-6.1.1 Material Recovery – Cores and Borings

Borings (Shelby tube and auger samples) and cores were drilled to recover sufficient material for laboratory testing and visually identify the materials and soils at each of the non-LTPP test sections. The results from the laboratory tests performed on the recovered materials are discussed in Section I-6.2.1, Unbound Materials and Soils. The layer thickness and material type recovered from the construction records were confirmed for each non-LTPP test section. The layer thickness, material type, and other information were included in the MDT database created for this project.

A field investigation was used to determine the amount of rutting in the underlying layers for each test section. In summary, most of the rut depths measured at the surface is occurring in the HMA layer. The amount of rutting in the unbound layers for the non-LTPP sites is considered to be immeasurable. Cores were planned to be taken through cracks found at these sites. None of the non-LTPP test sections, however, had any cracking within the wheel paths.

Field investigations were already available from the LTPP program. All of the borings and cores were taken outside the LTPP test section, and none of the cores were taken through cracks. This information was to become available from field forensic studies that were planned for the SPS projects, but those studies were removed from the program because of funding issues. Thus, there is no visual observation on the direction of crack propagation or an estimate of the rutting in individual layers for the LTPP sites.

I-6.1.2 Deflection Basin Tests

FWD deflection basin tests were performed in accordance with the test protocol used for the LTPP program. These deflection basin tests were performed on the LTPP and non-LTPP sites at different time periods during the course of the project to calculate the elastic modulus within different seasons of the year. Deflection basin tests were performed to classify each site in accordance with the procedure recommended for use by Von Quintus and Killingsworth (1998). In summary, all of the sites would be classified as having an elastic or deflection hardening structural response.

The first and second rounds of deflection basin tests were used to backcalculate the layer modulus for each layer of the non-LTPP test sections in Montana. Some discrepancies were noted between the modulus values calculated from Rounds 1 and 2. It was anticipated that there would be some differences between the resulting modulus values from Rounds 1 and 2, because of seasonal differences. However, the differences were significant enough to look for an error or assignable cause. The differences between the values were attributed to the compensating error effect that can occur when back-calculating layer modulus for relatively strong pavement sections (low deflections), pavements built over strong foundations, or areas

with shallow bedrock. These compensating errors usually result in unreasonably high and low elastic modulus values for adjacent layers and/or high root mean squared error (RMSE) terms. The sections with these compensating errors were identified and evaluated to determine the reason for the compensating error. These sections were redone using a different set of layer assumptions to remove the compensating error effect.

I-6.1.3 Backcalculation of Elastic Layer Modulus Values

The elastic layer modulus values were backcalculated from the deflection basin data using two programs – MODULUS and EVERCALC. MDT currently uses the MODULUS program. The EVERCALC program was used as an added check to confirm the modulus values. The elastic layer modulus values calculated from the deflection basins are discussed in Chapter 1-6.3 (this chapter) under each material characterization that was used for verification and calibration.

Table I-18 lists the representative or average modulus values calculated for the test sections located in Montana. Some of the backcalculated values for the unbound layers are extremely high (for example, LTPP Test Section 30-8129). These high values were measured during the winter months and represent a frozen layer. Solutions or backcalculated layer modulus values resulting in an RMSE greater than 3.0 percent were excluded from characterizing the load response of each structural layer. Solutions with RMSE values greater than 3.0 percent are considered too high and may result in inappropriate modulus values.

I-6.1.4 Comparison of FWD Equipment

Two FWDs were used to measure the deflection basins that were used within this study. The equipment used by MDT on a day to day basis is a JILS FWD. The MDT JILS FWD was used to measure the structural response of the non-LTPP sections, while a Dynatest FWD was used on all of the LTPP test sections. It is important to know whether a consistent difference exists between the two FWDs. Any consistent difference will result in an increased standard error of the distress transfer functions. One of the issues addressed within this study was to determine if there is a systematic difference in deflections and backcalculated layer modulus from both pieces of equipment.

A comparison study was performed on the LTPP sections in Great Falls and Big Timber (May 6-May 19, 2004) in which Montana LTPP sections were tested in parallel with the MDT and LTPP FWD equipment. The purpose of this comparison testing was to identify any bias between the two FWDs used to measure deflection data on different test sections used on this project. The hypothesis was that there is no bias between the two FWDs.

Deflection basin data were measured at 416 locations (station/lane) for four drop heights (load Levels: 6, 9, 12, and 16 kip) and 9 sensors. The LTPP and MDT FWDs had the same number of sensors and same sensor spacing. Plots of deflections measured with the LTPP FWD versus the MDT FWD are graphically shown in Figures I-7 through I-9, while the comparison of the backcalculated layer modulus values are shown in Figures I-10 through I-12. The comparisons in measured deflection and backcalculated modulus values between the MDT and LTPP FWDs resulted in the following general conclusions.

Table I-18 Summary of Backcalculated Elastic Layer Modulus Values for Each of the Test Sections Located in Montana

Section Identification	Temp. °F	Backcalculated Layer Modulus, ksi				
		HMA	Base		Subbase	Subgrade
			Material	Modulus		
Condon	46*	1117	Cold-In Place Recycled HMA	45.2	22.5	39.3
	50*	1304		34.2	56.2	42.4
	49	1522		34.4	30.3	49.1
	79	664		36.8	25.2	36.6
	84	602		50.0	20.7	38.3
Deer Lodge / Beckhill	51*	2507	Cold-In Place Recycled HMA	87.1	53.3	41.1
	54*	2982		75.4	57.2	51.7
	47	2297		194.0	46.8	51.0
	54	1777		197.0	50.5	52.1
Fort Belknap	26*	4008	Cement Aggregate Mixture	930.0	47.1	50.6
	47*	3844		606.0	45.0	56.0
	38	2888		2347.0	104.5	54.6
	59	2008		527.0	73.4	41.9
	76	869		1713.0	44.5	76.9
Geyser	42*	3465	Cement Aggregate Mixture	887.0	32.9	56.9
	45*	2241		943.0	23.9	48.1
	40	2494		885.0	20.3	94.0
	42	2743		736.0	30.1	57.2
	96	815		1377.0	16.7	76.5
Hammond	50*	1205	Cement Aggregate Mixture	803.0	9.5	13.4
	78*	839		654.0	37.1	40.8
	54	1800		575.0	26.0	42.0
	55	2320		350.0	32.0	48.0
	72	1350		312.0	41.0	38.0
Lavina	34*	4500	Cement Aggregate Mixture	234.0		25.6
	43*	2400		220.0		17.3
	62	2878		304.0		20.3
	71	1081		198.0		16.7
	86	884		262.0		19.5
Perma	52*	2581	Cement Aggregate Mixture	123.0	30.3	19.3
	70*	1600		759.0	34.7	34.7
	58	1904		722.0	12.2	20.1
	83	1688		278.0	20.6	18.3
	85	1229		177.0	40.1	17.2
Roundup	42*	4800	Cement Aggregate Mixture	398.0		24.5
	47*	4800		414.0		23.2
	61	4212		486.0		19.5
	81	2763		487.0		16.3
	87	2285		528.0		17.0
Silver City	36*	2728	Aggregate Base, Crushed Gravel	35.2		31.6
	41*	1558		14.6		15.9
	43	1577		21.5		31.4
	61	937		52.6		24.1
	84	932		21.8		29.8
Wolf Point	24*	2840	Cement Aggregate Mixture	475.0		37.7
	60*	1906		387.0		18.4
	62	2100		582.0		23.8
	66	1700		575.0		17.6
Vaughn North	50	1415	Crushed Gravel	81.6	70.1	46.8
	92	464		43.2	20.5	36.1

*Designates Round 1 and 2 tests that were performed in 2001 and 2002. The other deflection tests were performed in 2003 through 2005.

Table I-18 Summary of Backcalculated Elastic Layer Modulus Values for Each of the Test Sections Located in Montana, Continued

Section Identification	Temp., F	Backcalculated Layer Modulus, ksi				
		HMA	Base		Subbase	Subgrade
			Material	Modulus		
30-0506, Overlay	76	378		16.2	23.2	23.2
30-0507, Overlay	65	417	Soil-Aggregate Mix Coarse Grained	20.1	26.9	24.1
30-0509, Overlay	49	1402		12.2	47.7	26.6
30-0509, Overlay	81	244		12.2	23.7	24.6
30-7066, Overlay	65	966	Crushed Gravel	15.6		20.0
30-7075, Overlay + Asphalt Treated Base	77	934	Subbase	13.6	38.4	17.9
30-7076, Overlay + Asphalt Treated Base	75	434	Subbase	8.7	10.6	16.9
30-7088, Overlay	55	1047	Crushed Gravel	21.3	11.5	22.5
30-8129	32	3128	Crushed Gravel	2178.0	170.0	24.7
	35	6706		390	47.5	18.7
	42	4170		65.5	18.7	50.5
	56	1772		18.8	12.2	12.0
	68	1101		16.9	18.0	11.8
	99	526		20.3	12.1	11.7
	100	580		23.5	13.9	11.8

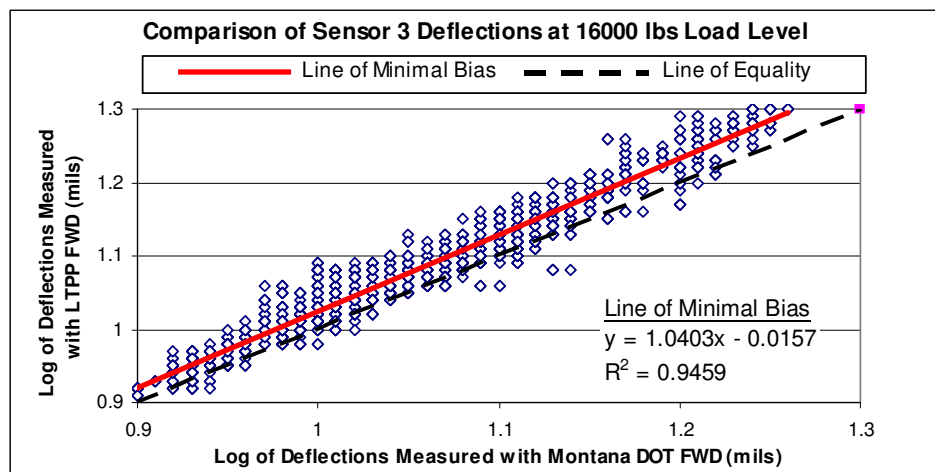
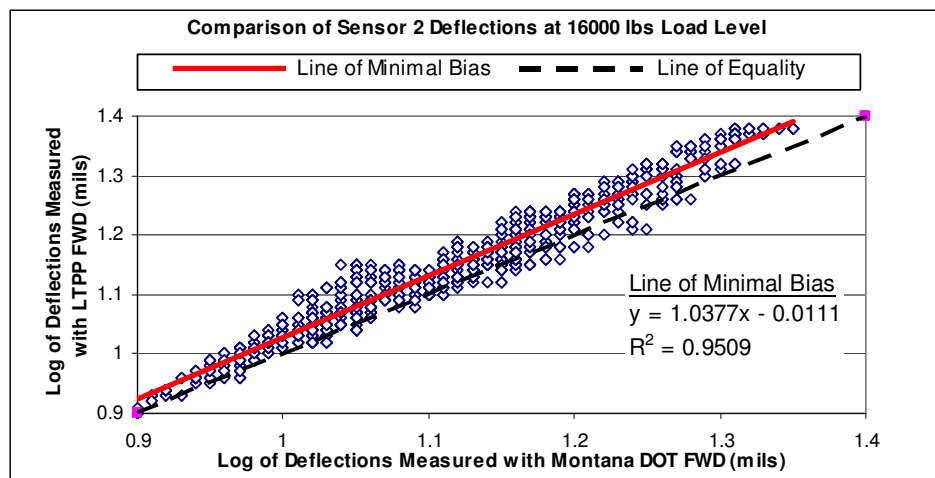
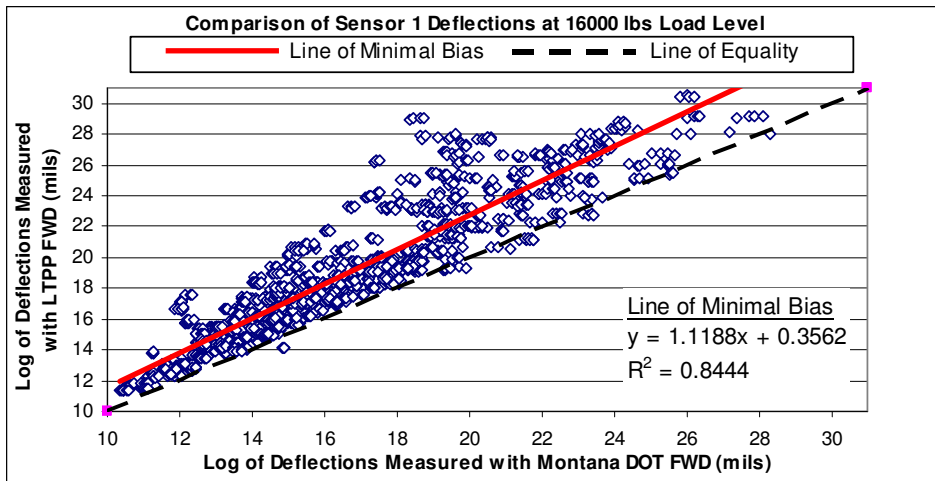


Figure I-7 Comparison of the deflections measured by the LTPP Dynatest and MDT JILS FWDs at Sensors 1, 2, and 3 for the 16 kip test load.

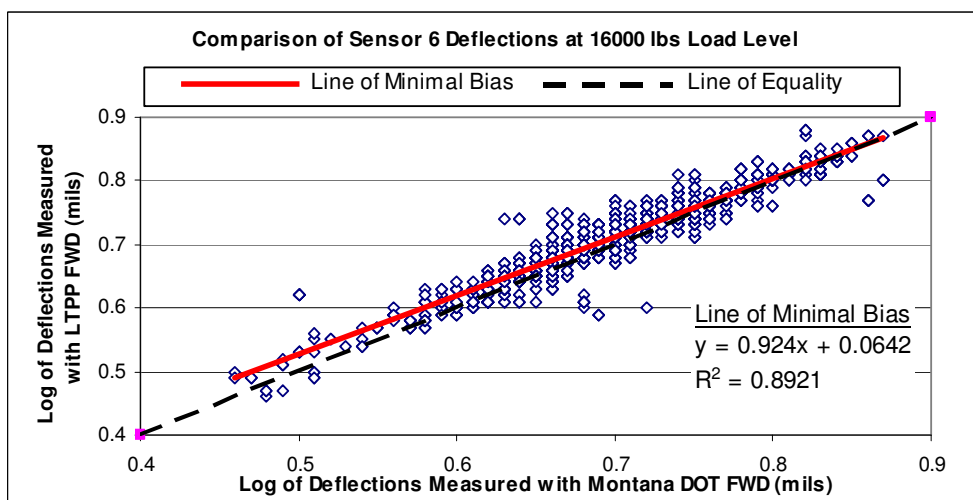
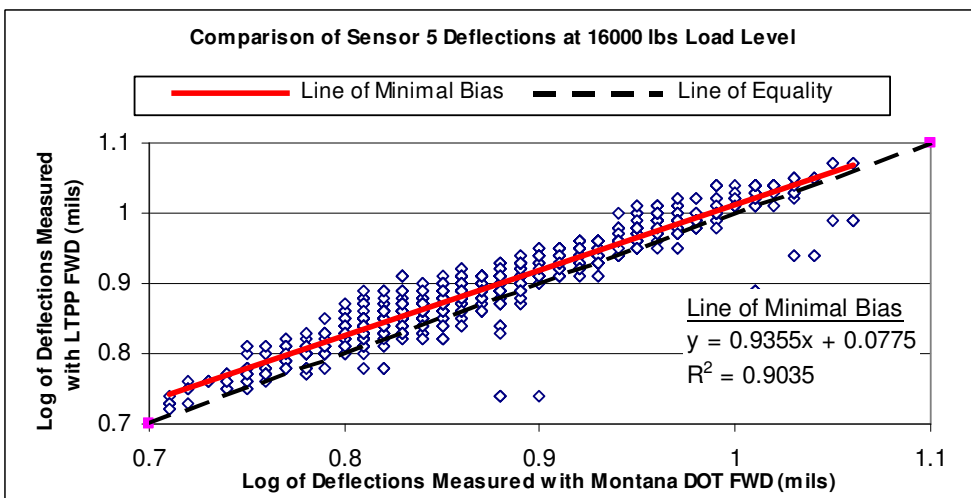
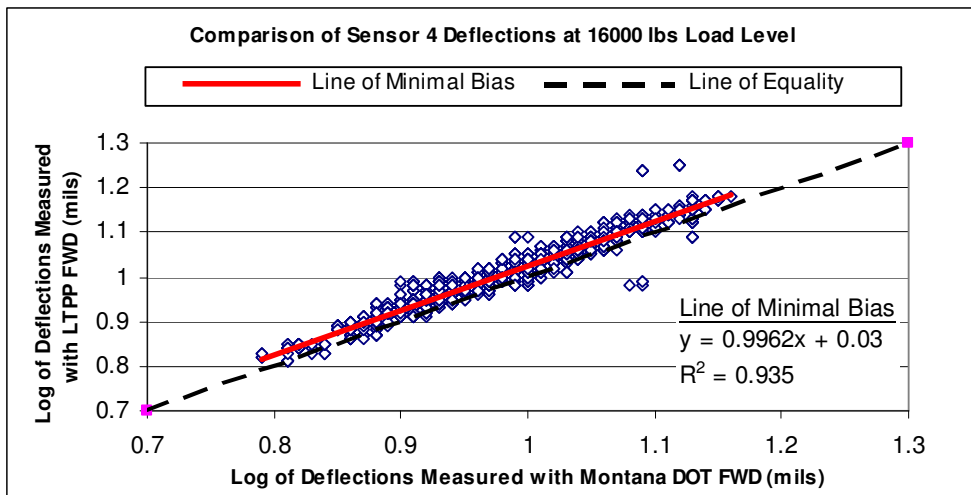


Figure I-8 Comparison of the deflections measured by the LTPP Dynatest and MDT JILs FWDs at Sensors 4, 5, and 6 for the 16 kip test load

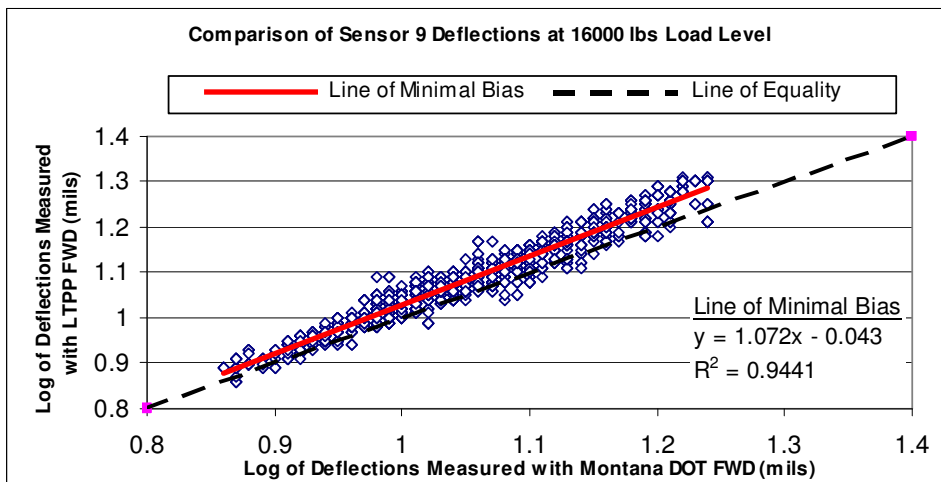
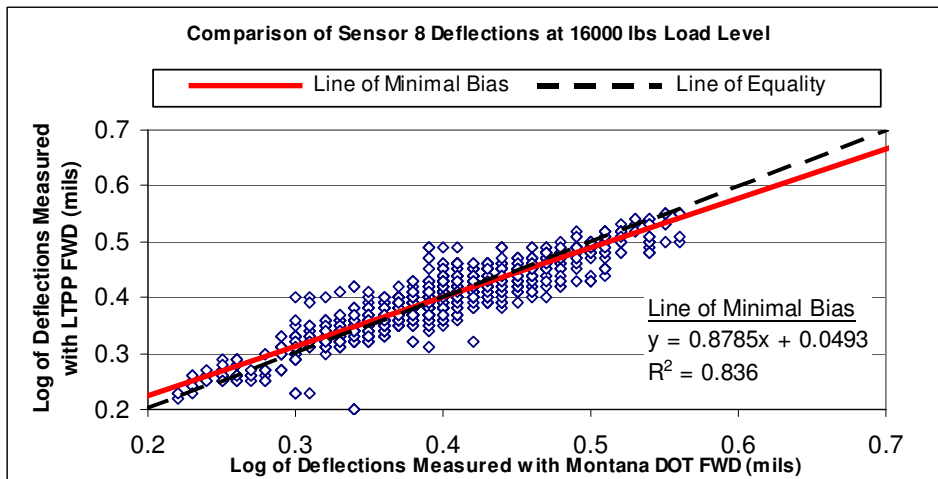
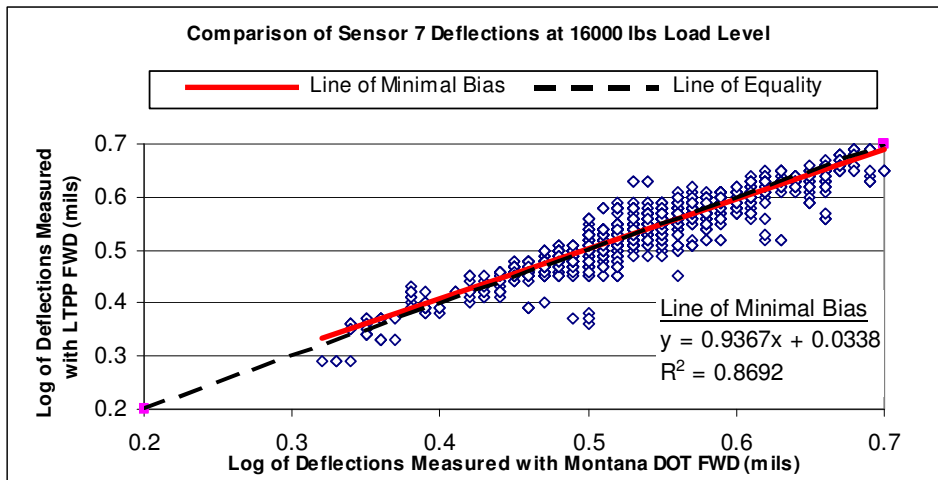


Figure I-9 Comparison of the deflections measured by the LTPP Dynatest and MDT JILs FWDs at Sensors 7, 8 and 9 for the 16 kip test load.

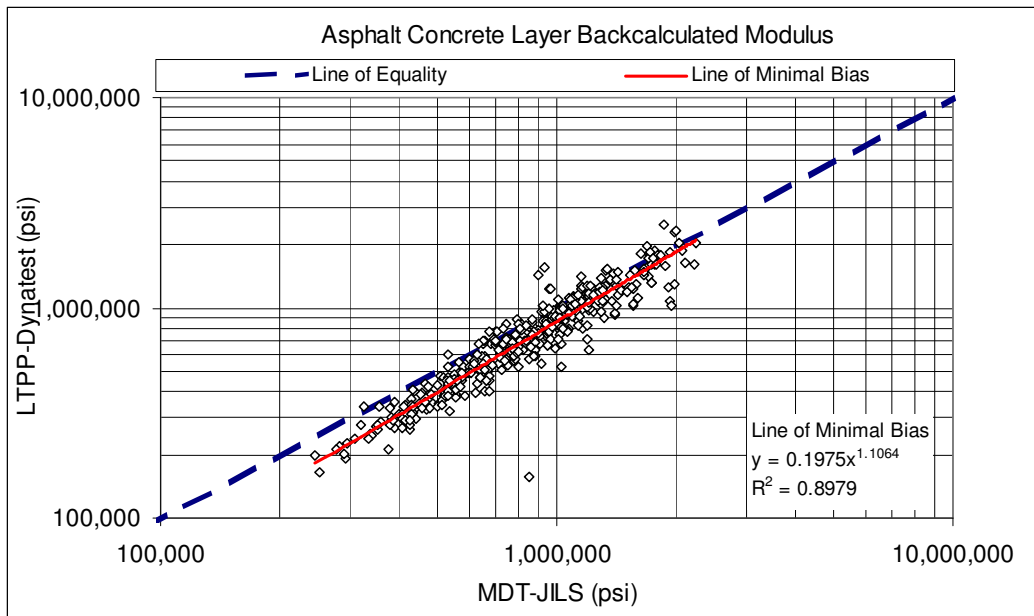


Figure I-10 Graphical comparison of the backcalculated HMA layer modulus values for the JILS and Dynatest FWDs that were used to measure deflection basins within this study.

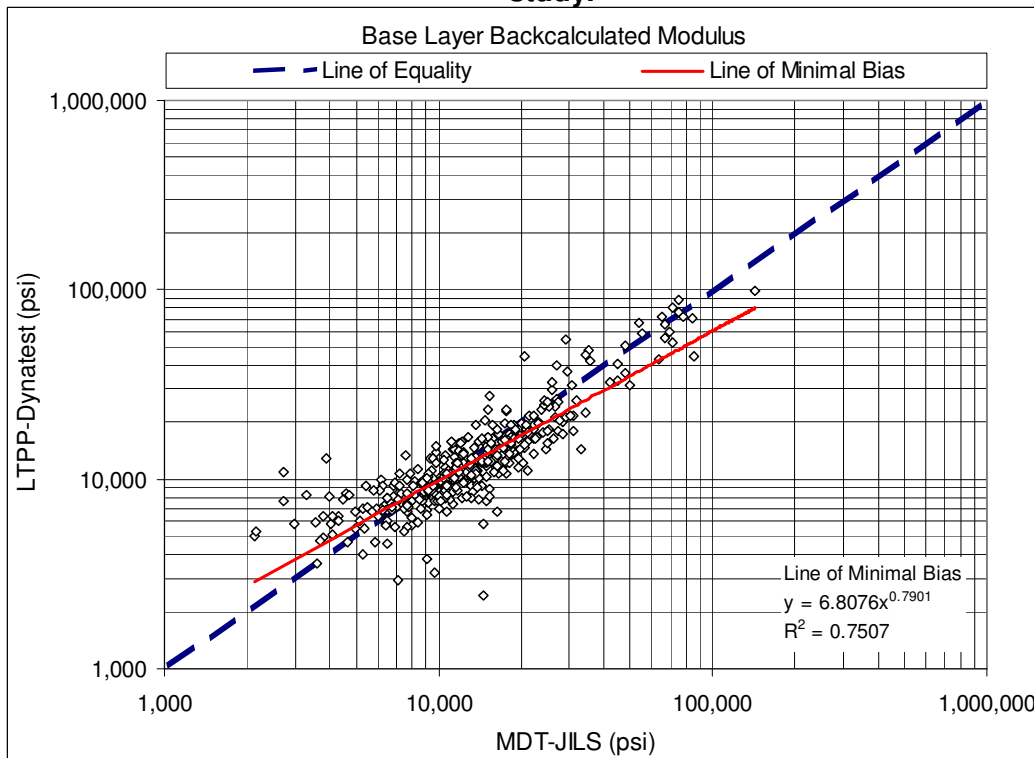


Figure I-11 Graphical comparison of the backcalculated crushed aggregate base modulus values for the JILS and Dynatest FWDs that were used to measure deflection basins within this study.

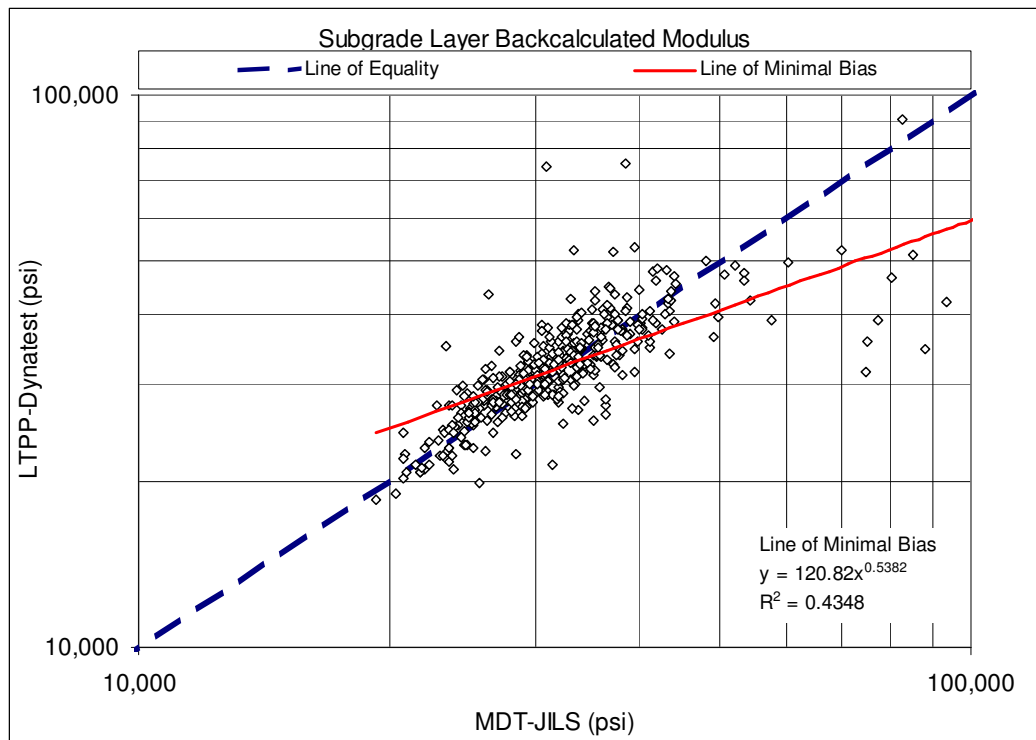


Figure I-12 Backcalculated subgrade modulus.

The LTPP FWD consistently measured higher deflections for all sensors and all drop heights compared to the MDT FWD. The bias was higher for Sensor 1 and that bias decreased as the distance from the load (Sensor 1) increased (refer to Figures I-7 through I-9).

A bias was found between the two FWDs for the modulus of the HMA layer (refer to Figure I-10). The ratio E_{MDT}/E_{LTPP} for the HMA layer ranges from a value of 1.5 at 300,000 psi to 1.0 at 2,000,000 psi. A simple correlation was developed and is given in Equations I-15 and I-16).

$$E_{LTPP} = 0.1975 \cdot E_{MDT}^{1.1064} \tag{I-15}$$

Where:

E_{LTPP} = Layer modulus measured with LTPP FWD.

E_{MDT} = Layer modulus measured with MDT FWD.

$$(R^2 = 0.90) \tag{I-16}$$

Where:

R = Correlation coefficient.

This bias for the HMA layers is not considered significant for the calibration study, because the MEPDG uses the dynamic modulus values measured in the laboratory or calculated from the Witczak regression equation (Witczak et al. 2002). The backcalculated elastic modulus values for the HMA layer, however, are used in the rehabilitation designs to determine the damage modulus of the existing HMA layers. The bias and its effect are discussed in Chapter I-6.2.3 and I-6.3.3 (this chapter), the sections on HMA materials characterization for calibration.

Figure I-12 shows a comparison of the backcalculated subgrade or foundation modulus from the deflection basins measured with the JILS and Dynatest FWDs. The FWD comparison study resulted in a poor correlation between the two FWDs when looking at the backcalculated modulus of the subgrade soil.

Most of the data-points are concentrated along the line of equality, with the exception of a limited number of data-points corresponding to modulus values higher than 50,000 psi from the MDT JILs FWD. Figure I-12 suggests that a reasonable agreement between the two FWDs exists, but for modulus values lower than 50,000 psi. The high values (greater than 50,000 psi) are considered outliers, because most modulus values for the subgrade soils are below 50,000 psi (refer to Table I-18). To evaluate the effect of removing these data points on the correlation, the reduced data set are compared in Figure I-13. As shown, the coefficient of determination R^2 increases from 0.43 in Figure I-12 to 0.69 in Figure I-13.

The purpose of this comparison was to investigate if bias exists between the two FWDs, and as shown in Figures I-10 through I-13, there is no significant bias (i.e., data-points are concentrated on the line of equality and equally distributed on both side of the equality line). The R^2 value of 0.69 shows that there is scatter in the data and that the correlation is not perfect, in which case the R^2 value would be 1. The sources of scatter most likely come from both pieces of equipment and there is no indication or reason to state that one is better or more accurate than the other.

I-6.1.5 Profile Measurements

Longitudinal and transverse profile measurements along each LTPP test section were made with the dip stick and LTPP profilometer, whereas, only the Montana profilometer was used in measuring the longitudinal and transverse profiles of the non-LTPP test sections. The transverse profiles were used to estimate the magnitude and variability of the rut depths along each test section. The rut depths estimated from the wire line, as recorded within the LTPP database, were used within this study. The IRI values calculated from the longitudinal profiles were used within this study for each test section.

As for the FWD comparisons, profile measurements were made on a few test sections with both the Montana profilometer used for their pavement management database and the LTPP profilometer operated by Nichol's Engineering for the LTPP Western Region. These data were too few and contain too much variability to determine if there was any statistical difference between the two profile measurement devices. MDT should consider expanding this comparison to ensure that the IRI values determined with the Montana profilometer are comparable with the LTPP profilometer. Within this study, it is assumed that they are comparable.

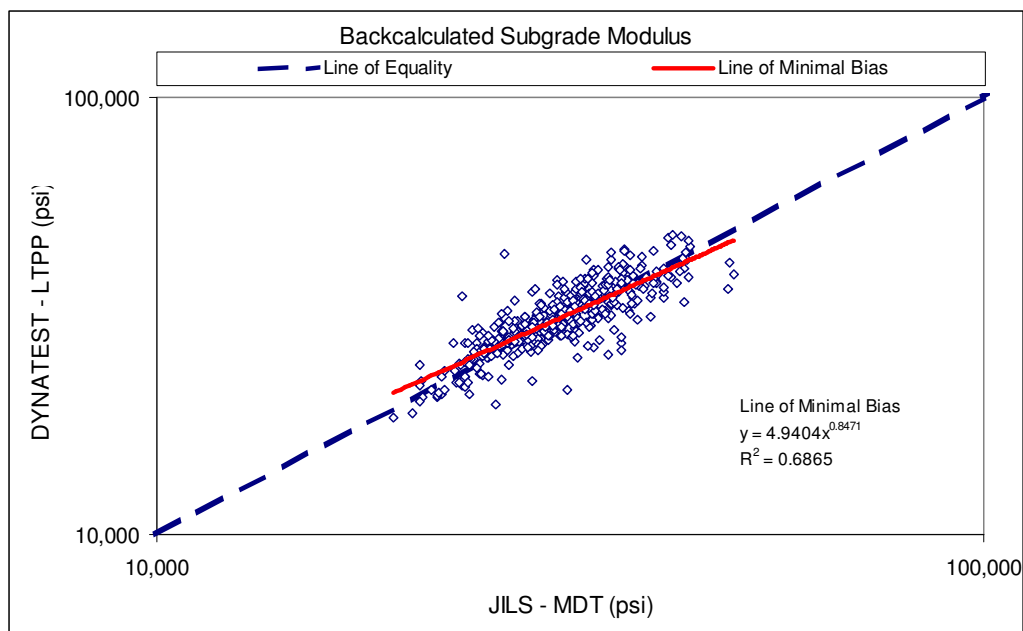


Figure I-13 Comparison of backcalculated subgrade modulus from the deflection basins measured with the Dynatest and JILs FWDs (reduced data).

I-6.1.6 Dynamic Cone Penetrometer Tests

DCP tests were performed by MDT at selected locations along the non-LTPP test sections. Results and use from the DCP tests will be discussed in Chapter 1-6.3.1 (this chapter) under unbound materials. DCP tests were not performed on any of the unbound layers and foundation for the LTPP test sections, because they were not included in the LTPP test program.

I-6.2 LABORATORY TESTS

Selected laboratory materials tests were performed to measure the properties needed for the MEPDG distress transfer functions. Table I-6 listed the laboratory tests planned for each of the non-LTPP sites. Laboratory tests for the materials included in the LTPP sites were already completed under the LTPP program and were beyond the scope of work for this project. All material test results for the LTPP test sections were extracted from DataPave. This section of Chapter I-6 overviews and presents the results of the laboratory tests for each material.

I-6.2.1 Unbound Materials and Soils

The objective for testing the unbound materials was to obtain repeated load resilient modulus (M_r) for each unbound base and subgrade material that was sampled. Testing was completed at

the optimum moisture content. The moisture-density relationship for each unbound material was determined prior to M_r testing. Once the optimum moisture content was determined, sample preparation for the M_r testing was completed. Each sample was tested in accordance with the LTPP protocol (AASHTO T 307) (AASHTO 2006b).

Classification Testing of Unbound Materials

Atterberg Limits and gradation tests were performed on unbound materials recovered at each test section. Table I-19 summarizes the classification tests and the results for the aggregate base materials for Montana LTPP sections only. Table 20 summarizes the classification tests for LTPP and non-LTPP sections and includes the results for the foundation soils.

Physical/Volumetric Properties

Most of the subgrade soils encountered at the non-LTPP sites are coarse-grained or soils with low cohesion and recovering undisturbed samples from the Shelby tubes for accurate density determination was not possible, so the average dry density was not measured. Moisture content tests were also planned (refer to Table I.6) for the unbound layers and subgrade soil, but were omitted from the laboratory test plan. Water from the wet coring process infiltrated the unbound aggregate base layer and upper soil preventing an accurate determination of the moisture content of these layers. As a result, moisture density tests were run on the recovered materials, and samples using the optimum moisture content and maximum dry density were used to mold specimens for resilient modulus testing. This sampling event was not considered detrimental to the calibration process because the inputs to the MEPDG are the in place moisture content and dry density at the time of construction. Moisture-density curves were derived for each of the seventeen materials tested prior to resilient modulus testing. A modified compactive effort (AASHTO T 180) (AASHTO 2006a) was used for the coarse-grained materials, while a standard compactive effort (AASHTO T 99) (AASHTO 2006a) for fine-grained soils. The optimum moisture content and maximum dry density obtained for each material is given in Tables I-21 and I-22. Table I-21 provides the test results for the aggregate base layers, while Table I-22 provides the results for the foundation soils.

Table I-19 Summary of Results from the Classification Tests Performed on the Base Materials Recovered from the LTPP Test Sections in Montana

Test Section	Layer	Atterberg Limits		Gradation, Sieve Size, Percent Passing, %					
		Liquid Limit	Plasticity Index	¾ in.	3/8 in.	#4	#40	#80	#200
Crushed Gravel									
30-0117	Layer 2		NP	89	70	53	26	16	10.4
30-0121	Layer 2		NP	85	58	41	18	11	7.3
30-0805	Layer 2		NP	91	71	54	22	15	11.0
30-0806	Layer 2		NP	91	72	52	23	16	11.9
30-0806	Layer 2		NP	93	73	52	22	15	10.6
30-0903	Layer 2		NP	100	80	62	30	15	8.2
30-0502	Layer 3		NP	97	73	51	26	16	11.2
30-0506	Layer 3		NP	92	72	52	23	14	8.9
30-0508	Layer 3		NP	100	81	62	31	19	12.7
30-6004	Layer 3		NP	93	80	64	32	21	13.2
30-7066	Layer 3		NP	100	85	63	22	14	10.1
30-7075	Layer 3	17	3	69	50	34	19	10	5.7
30-7075	Layer 3		NP	56	40	29	18	10	5.7
30-7088	Layer 3		NP	100	80	60	28	18	11.1
30-8129	Layer 2		NP	97	63	35	15	10	6.8
30-8129	Layer 2		NP	95	64	43	21	12	7.5
Soil-Aggregate Mixture; Predominately Coarse Grained Soil									
30-0502	Layer 2	20	8	70	50	38	20	12	8.1
30-0506	Layer 2		NP	74	55	42	20	12	7.8
30-0508	Layer 2		NP	74	57	47	28	17	11.3
30-1001	Layer 2	22	9	82	64	46	29	21	15.9
30-1001	Layer 3	22	12	84	52	30	15	12	9.9
30-1001	Layer 3	21	14	81	57	40	18	13	10.5
30-6004	Layer 2		NP	90	75	57	34	27	19.1
30-6004	Layer 2		NP	96	87	73	53	38	23.6
30-7066	Layer 2		NP	86	61	42	22	16	11.7
30-7066	Layer 2		NP	75	54	42	20	12	8.4
30-7075	Layer 3	17	3	69	50	34	19	10	5.7
30-7075	Layer 3		NP	56	40	29	18	10	5.7
30-7075	Layer 2	22	8	60	48	39	32	23	13.9
30-7076	Layer 3		NP	97	93	87	69	44	17.1
30-7076	Layer 3		NP	95	89	80	78	57	20.9
30-7076	Layer 2		NP	92	81	71	70	53	24.3
30-7076	Layer 2		NP	100	95	95	90	61	25.2
30-7088	Layer 2		NP	82	59	42	22	16	10.6
30-7088	Layer 2		NP	75	57	46	23	15	9.5

Table I-20 Summary of Results from the Classification Tests Performed on the Subgrade Soils Recovered from the LTPP and Non-LTPP Test Sections in Montana

Test Section	Soil Class	Atterberg Limits		Gradation, Sieve Size, Percent Passing, %					
		Liquid Limit	Plasticity Index	¾ in.	3/8 in.	#4	#40	#80	#200
30-0113	A-1-a		NP	82	65	53	31	15	8.7
30-0113	A-1-a		NP	88	64	45	20	12	8.2
30-0805	A-1-a		NP	75	58	44	19	13	9.2
30-0806	A-1-a		NP	70	54	41	16	11	7.5
30-0806	A-1-a		NP	65	54	42	19	12	8.6
30-0901	A-1-a		NP	69	52	40	22	9	6.1
30-0902	A-1-a		NP	62	45	35	23	7	4.6
30-0903	A-1-a		NP	61	46	34	16	7	5.2
30-0113	A-1-b		NP	79	65	53	31	18	10.2
30-0113	A-2-4		NP	100	100	100	98	61	27.8
30-0116	A-2-4		NP	100	98	97	96	62	23.5
30-0116	A-2-4		NP	100	99	97	92	66	32.1
30-0117	A-2-4		NP	100	100	99	98	68	23.1
30-0117	A-2-4		NP	100	99	98	97	56	16.1
30-0119	A-2-4		NP	99	99	98	97	67	20.8
30-0119	A-2-4		NP	100	100	98	94	65	28.8
30-0122	A-2-4		NP	100	100	99	98	79	23.1
30-0122	A-2-4		NP	100	100	100	98	48	14.7
30-7088	A-2-6	24	9	99	91	78	71	52	31.8
30-0506	A-2-6	28	12	82	74	66	52	43	32.6
30-7075	A-2-6	26	14	84	60	41	40	38	27.7
30-7088	A-2-6	24	12	86	66	46	35	29	21.3
30-0124	A-4		NP	100	99	99	98	75	35.8
30-0502	A-6	28	14	87	80	75	64	57	41.6
30-0508	A-6	27	16	83	62	45	44	43	38.9
30-1001	A-6	33	19	99	95	86	63	55	47.2
30-1001	A-6	36	20	85	76	64	49	42	36.5
30-6004	A-6	29	15	98	96	93	87	79	64.1
30-6004	A-6	30	15	94	93	91	88	82	69.1
30-7066	A-6	32	19	97	95	91	77	66	56.3
30-7066	A-6	32	18	94	92	90	81	69	54.7
30-8129	A-6	31	17	97	92	85	72	66	55.2
30-8129	A-6	31	15	97	90	84	76	72	60.3
Baum									
Condon	A-2-4*								
Deer Lodge	A-1-b*								
Ft. Belknap	A-2-4*								
Geyser	A-2-4*								
Hammond	A-4*								
Lavina	A-4*								
Lothair									
Perma	A-6*								
Roundup	A-6*								
Silver City	A-2-4*								
Vaughn									
Wolf Point	A-4*								

* Visual classifications only for non-LTPP test sections.

Table I-21 Summary of Moisture-Density and Resilient Modulus Test Results for the Unbound Aggregate Base Materials Recovered from the LTPP and Non-LTPP Test Sections in Montana

Test Section	Layer	Maximum Dry Density, pcf	Optimum Water Content, %	Resilient Modulus, ksi*
Crushed Gravel				
30-0113	Layer 2	135	7	24.08
30-0113		142	6	
30-0117		142	6	18.86
30-0121		143	6	21.90
30-0502		143	4	19.00
30-0506		142	5	17.99
30-0508		142	6	22.63
30-0805		142	7	20.31
30-0806		140	6	25.38
30-0806		141	6	23.64
30-6004		131	10	
30-7066		140	7	
30-7075		141	6	
30-7075		142	4	
30-7088		138	6	
30-8129		139	7	
30-8129		138	6	
Beckhill/Deer Lodge		146	5.5	30.39
Silver City		142	6	28.94
Geyser		141	6.5	26.79
Vaughn North				29.21
Vaughn North				33.70
Soil-Aggregate Mixture; Predominately Coarse-Grained				
30-0502		149	6	
30-0506		139	7	
30-0508		141	7	
30-1001		143	5	
30-1001		141	6	
30-1001		142	5	
30-6004		126	11	11.75
30-7066		144	6	
30-7066		142	5	
30-7075		132	10	
30-7076		112	16	8.99
30-7076		114	14	9.72
30-7076		111	15	
30-7076		114	13	
30-7088		139	6	
30-7088		140	6	
Condon		136	7.5	27.01
Fort Belknap		136	7	25.49
Hammond		125.8	12.4	22.44
Perma		130.5	9.5	14.83
Vaughn North				38.86
*Resilient modulus values reported above represent those measured at a confining pressure of 10 psi and a repeated vertical stress of 10 psi. The values used in Figures I-21 and I-22 use a different stress state.				

Table I-22 Summary of Moisture-Density and Resilient Modulus Test Results for the Subgrade Soils Recovered from the LTPP and Non-LTPP Test Sections in Montana

Test Section	Material/Soil	Maximum Dry Density, pcf	Optimum Water Content, %	Resilient Modulus, ksi*
Condon	Silty Gravel w/Sand	143.5	6	20.21
30-0805	Poorly Graded Gravel w/Silt	135	7	
30-0806	Poorly Graded Gravel w/Silt	136	7	
30-0806	Poorly Graded Gravel w/Silt	136	8	
Beckhill/Deer Lodge	Clayey Gravel w/Sand	134	7.5	24.36
Ft. Belknap	Silty Sand w/Gravel	134	7.5	11.21
Geyser	Silty Gravel w/Sand	127	9.5	27.04
Perma	Clay w/Gravel	129.5	9.5	18.82
Lavina	Sandy Silt w/Gravel	127	10	25.46
Silver City	Silty Sand w/Gravel	120.5	12.5	19.19
30-0502	Clayey Gravel w/Sand	119	13	
30-0506	Clayey Gravel w/Sand	120	12	
30-0508	Clayey Gravel w/Sand	122	12	
30-7088	Clayey Sand w/Gravel	120	13	
30-7088	Clayey Sand w/Gravel	118	14	
30-8129	Gravelly Lean Clay w/Sand	120	10	
30-8129	Gravelly Lean Clay w/Sand	117	11	
30-7066	Sandy Clay w/Gravel	118	11	
30-7066	Sandy Clay w/Gravel	118	11	
Roundup	Silty Clay w/Gravel	118	16.5	19.33
Wolf Point	Sandy Clay w/Gravel	117	14	26.16
Hammond	Sandy Clay w/Gravel	117	13	34.81
Vaughn North	Sandy Clay			13.93
Vaughn North	Sandy Clay			16.62
30-7075	Clayey Gravel	114	15	
30-1001	Clayey Gravel w/Sand	118	11	
30-1001	Clayey Gravel w/Sand	107	17	
30-6004	Sandy Lean Clay	112	16	
30-6004	Sandy Lean Clay	111	16	
30-7076	Sandy Silt			
30-0113	Poorly Graded Sand w/Silt			7.69
30-0113	Poorly Graded Sand w/Silt	101	14	5.08
30-0116	Poorly Graded Sand w/Silt	111	14	6.38
30-0116	Poorly Graded Sand w/Silt	106	17	6.24
30-0117	Poorly Graded Sand w/Silt	111	13	6.67
30-0117	Poorly Graded Sand w/Silt	109	14	6.24
30-0119	Poorly Graded Sand w/Silt	110	14	7.98
30-0119	Poorly Graded Sand w/Silt	108	13	6.53
30-0122	Poorly Graded Sand w/Silt	105	16	6.38
30-0122	Poorly Graded Sand w/Silt	98	17	6.38
30-0124	Poorly Graded Sand w/Silt	103	14	6.24
30-0124	Poorly Graded Sand w/Silt			6.67

*Resilient modulus values reported above represent those measured at a confining pressure of 4 psi and a repeated vertical stress of 4 psi. The values included in Figures I-21 and I 22 use a different stress state.

Resilient Modulus Testing

Unbound materials from the 10 non-LTPP sites selected in the experimental factorial (Condon, Deer Lodge, Fort Belknap, Geyser, Hammond, Lavina, Perma, Roundup, Silver City, and Wolf Point) were tested in accordance with AASHTO T 307 (*AASHTO 2006b*). Figures I-14 through I-18 show some examples from the repeated load resilient modulus tests performed on the unbound aggregate base materials and subgrade soils recovered from selected test sections (Beckhill/Deer Lodge, Fort Belknap, and Roundup). These tests cover the range from strong to weaker materials recovered from the non-LTPP test sections in Montana.

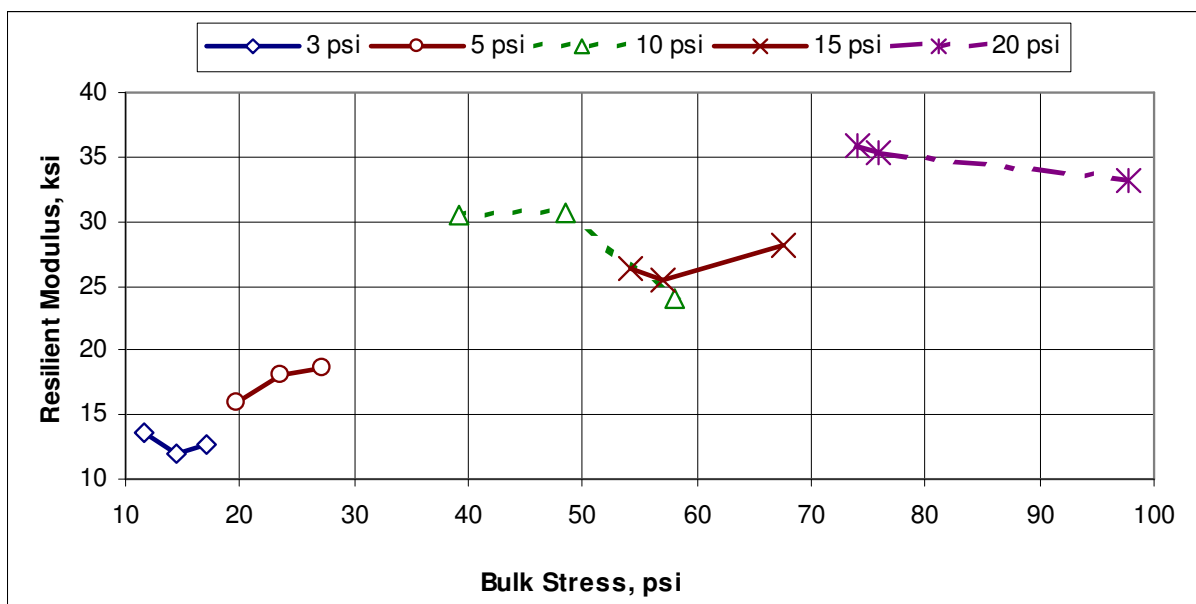


Figure I-14 Summary of repeated load resilient modulus test for the crushed gravel recovered from the Beckhill / Deerlodge test section.

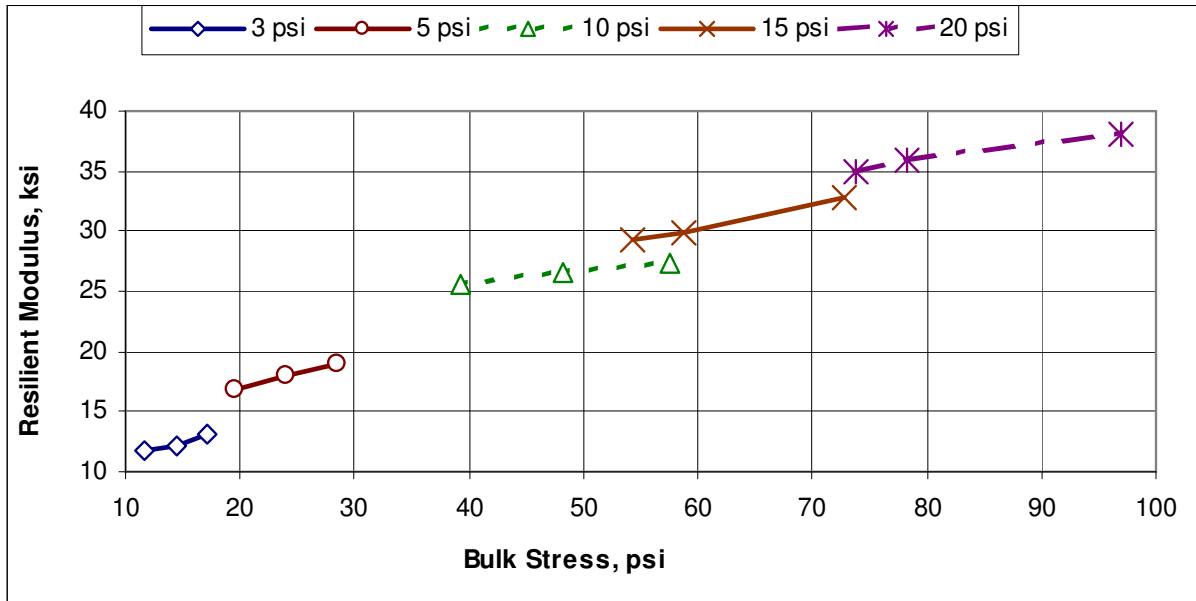


Figure I-15 Summary of repeated load resilient modulus test for the soil-aggregate base mixture recovered from the Fort Belknap test section.

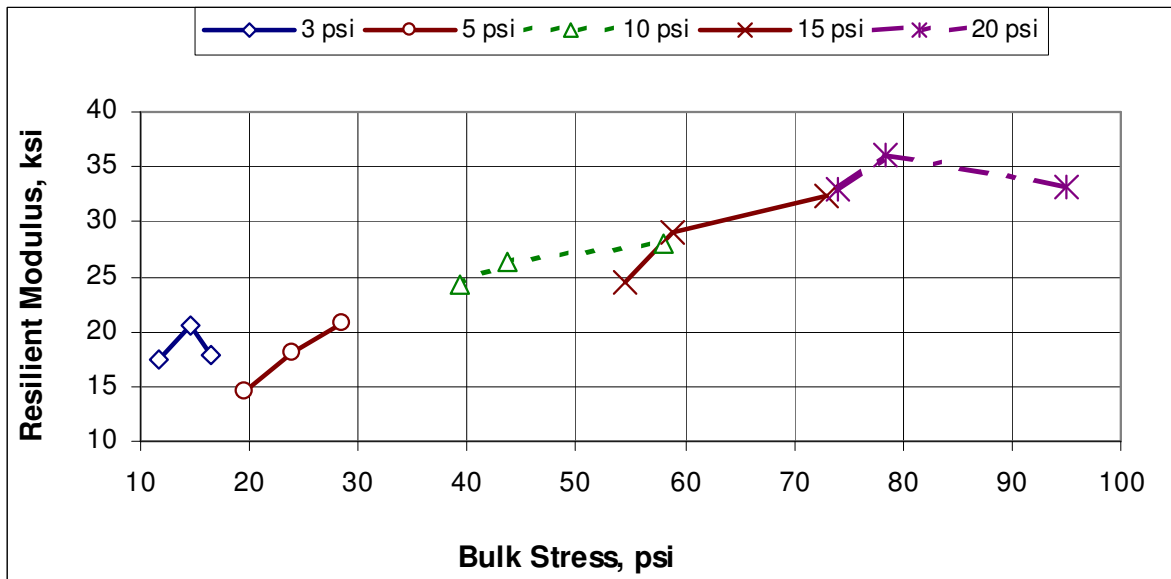


Figure I-16 Summary of repeated load resilient modulus test for the clayey gravel with sand soil recovered from the Beckhill / Deerlodge test section.

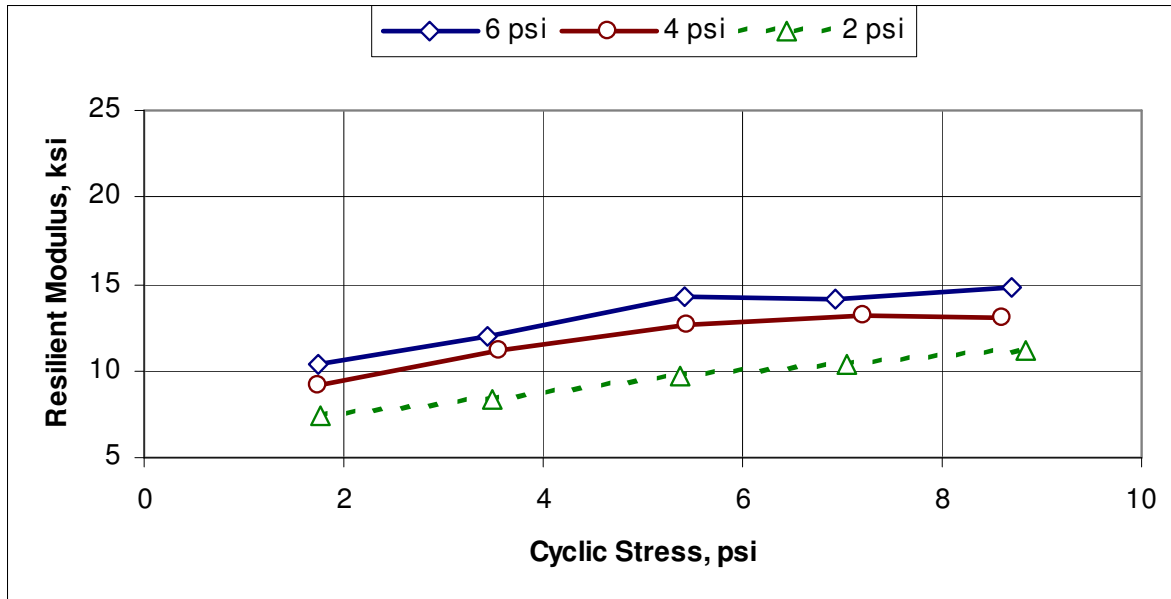


Figure I-17 Summary of repeated load resilient modulus test for the silty sand with gravel soil recovered from the Fort Belknap test section.

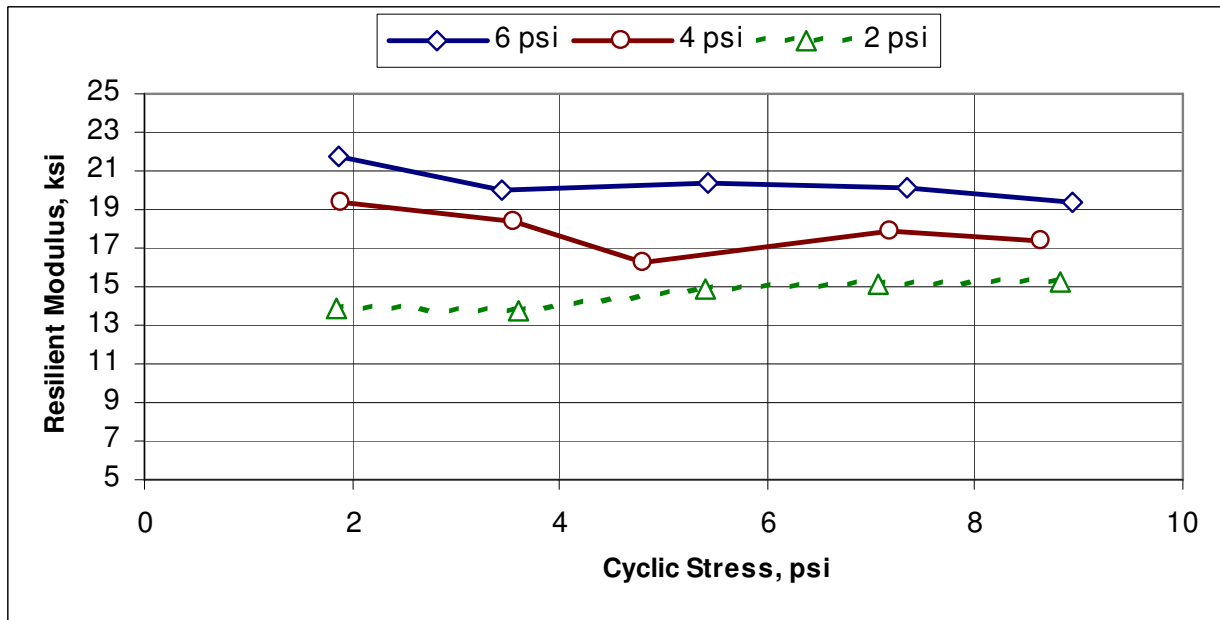


Figure I-18 Summary of repeated load resilient modulus test for the silty clay with gravel soil recovered from the Roundup test section.

Resilient modulus tests were unavailable for some of the LTPP sites (refer to Tables I-21 and I-22). For these sites, equations were used to estimate the regression constants of the resilient modulus constitutive equation included in the MEPDG procedure (*Von Quintus and Yau 2001*). The resilient modulus constitutive equation recommended by the MEPDG for stress-dependent resilient modulus is given in Equation I-17.

$$M_R = k_1 \cdot p_a \cdot \left(\frac{\theta}{p_a} \right)^{k_2} \cdot \left(\frac{\tau_{oct}}{p_a} + 1 \right)^{k_3} \quad (I-17a)$$

Where:

$$\begin{aligned} M_R &= \text{Resilient modulus.} \\ k_1, k_2, k_3 &= \text{Regression constants.} \\ p_a &= \text{Atmospheric pressure, psi.} \\ \theta &= \text{Bulk stress:} \\ &\quad \theta = \sigma_1 + \sigma_2 + \sigma_3. \end{aligned} \quad (I-17b)$$

$$\begin{aligned} \tau_{oct} &= \text{Octahedral shear stress:} \\ &\quad \tau_{oct} = \frac{1}{3} \cdot \sqrt{(\sigma_1 - \sigma_2)^2 + (\sigma_1 - \sigma_3)^2 + (\sigma_2 - \sigma_3)^2} \end{aligned} \quad (I-17c)$$

$$\sigma_1, \sigma_2, \sigma_3 = \text{Major, intermediate and minor principal stresses.}$$

All resilient modulus test data were fit using that constitutive equation, which has been referred to as the “universal” resilient modulus constitutive equation. The following provides an example for determining the *k*-constants of that constitutive equation for the test results for the Condon crushed gravel base material, as illustrated in Figure I-19.

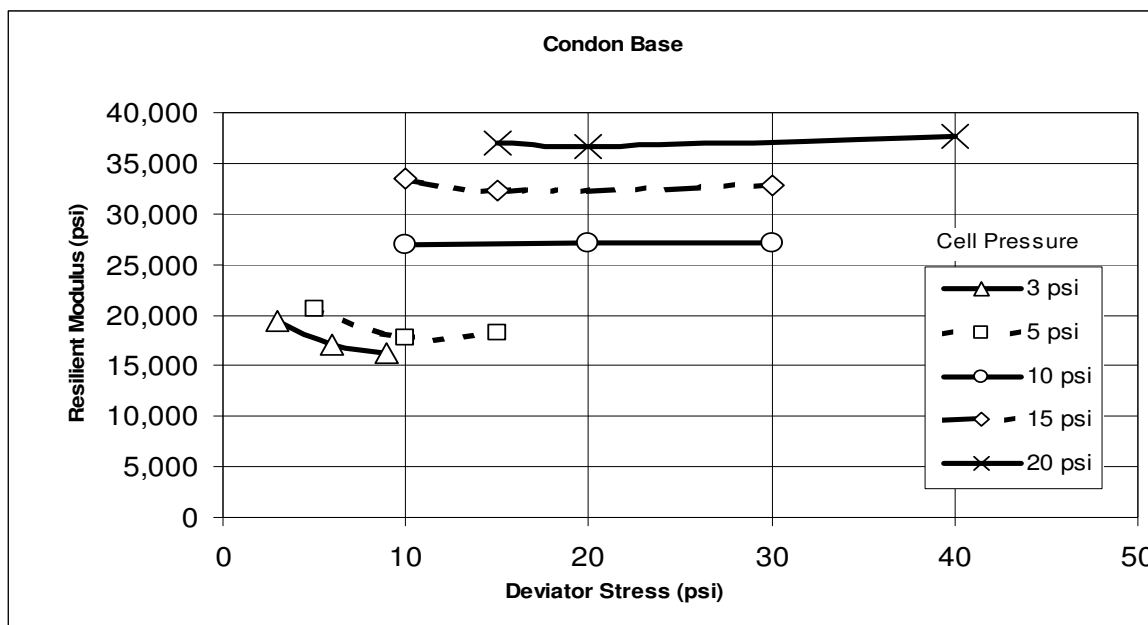


Figure I-19 Graphical presentation of the results from the resilient modulus test performed on the crushed gravel base material recovered from the Condon test section.

For the Condon Base, depending on the repeated stress and confining pressure applied, the modulus ranges from 15,000 psi at the lowest confining pressure (3 psi) to 37,000 psi at the highest confining pressure (20 psi). As illustrated in Figure I-19, resilient modulus is a function of stress and a predictive equation is needed to estimate modulus values at states of stress other than those applied during the laboratory test. The algorithm used to obtain the values of the k_1 , k_2 and k_3 regression constants for each resilient modulus test is listed below on a step-by-step basis.

1. Arrange laboratory test data on three columns as follows: Deviator stress (psi), Confining Pressure (psi) and Resilient Modulus (M_R) (psi).
2. Calculate in the next three columns: Bulk Stress (Equation I-17b), Octahedral Shear Stress (Equation I-17c), and $\log(M_R)$.
3. Insert initial (guess) values for the regression constants k_1 (use 1,000), k_2 (use 0.5) and k_3 (use -0.5).
4. Calculate in a 7th column the predicted resilient modulus, using Equation I-17a.
5. Calculate in a 8th column the squared errors: $(\log(\text{column 7}) - \log(M_R))^2$.
6. Calculate the sum of all terms in column 8 ($SES = \text{sum of errors squared}$).
7. Calculate the standard deviation of terms in column $\log(M_R)$ and label S_y .
8. Calculate the standard error of estimate Se as $(SES/(n-3))^{0.5}$ where n is the number of data points.
9. Calculate in a separate cell the ratio Se/S_y .
10. Calculate R^2 as $1 - (Se/S_y)^2$.
11. In Excel, use Solver (from the Tools menu) to “minimize” Se/S_y “by changing cells” k_1 , k_2 and k_3 .
12. End.

An example Excel spreadsheet that was developed using instructions for Steps 1 to 12 above is given in Figure I-20, and the results of fitting the data are included in Table I-23 for all resilient modulus tests. For comparison, the regression parameters presented in Table I-23 were used to estimate the resilient modulus at two typical states of stress, one for subgrades, and one for base materials, graphically shown in Figures I-21 and I-22. The resilient modulus values shown in Figures I-21 and I-22 are different than those included in Tables I-21 and I-22, because they represent different stress states. A single stress state was used for comparison purposes between different soil types and test sections.

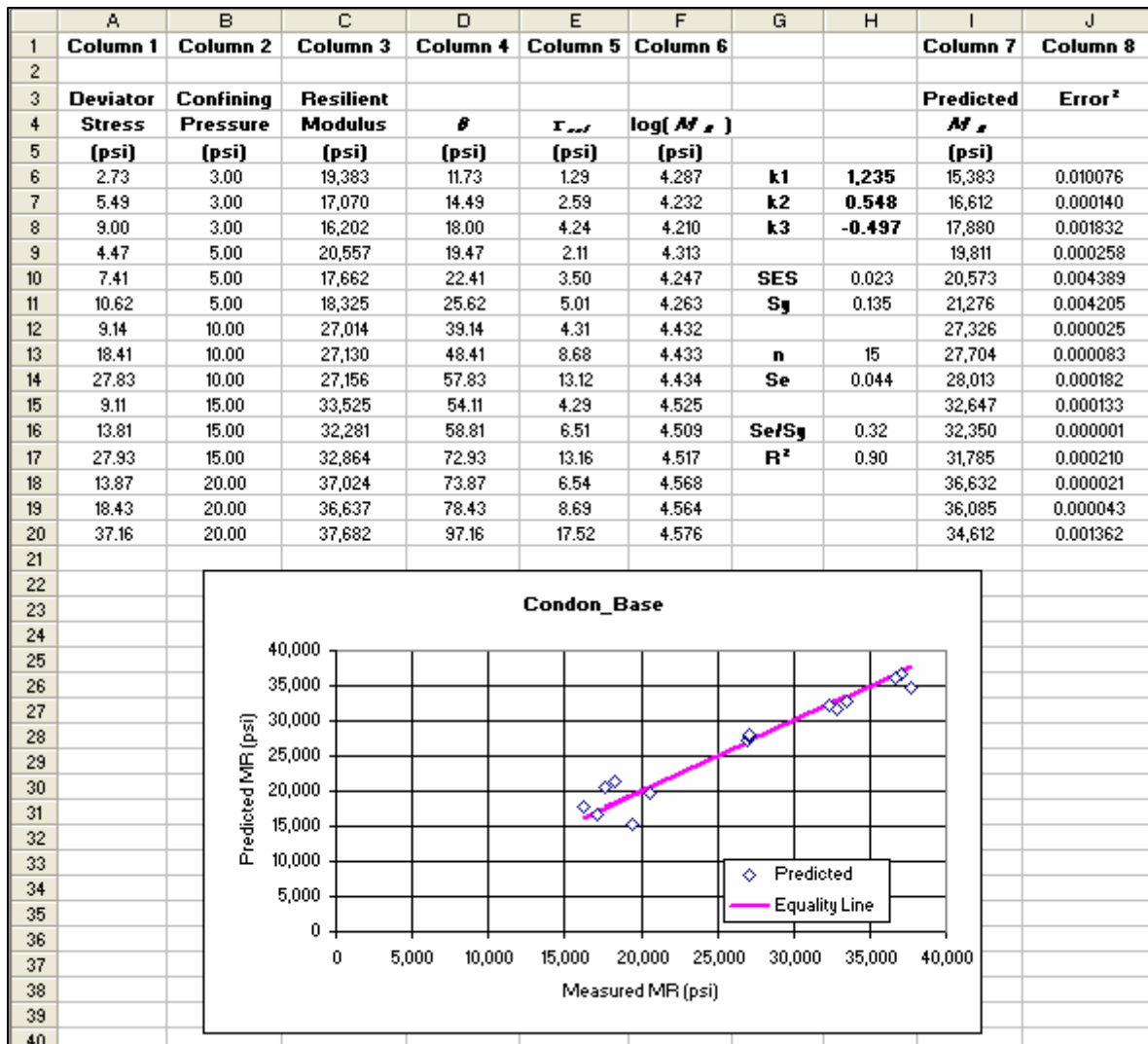


Figure I-20 Example Excel spreadsheet for completing the resilient modulus regression analysis to determine the coefficients and exponents of the universal constitutive equation (refer to Equation I-17a).

Table I-23 Summary of the Regression Constants from the Constitutive Equation for the Repeated Load Resilient Modulus Test Results for the Non-LTPP Sites

Material	Test Section	Constitutive Equation Constants			R ²
		k ₁	k ₂	k ₃	
Aggregate Base and Subbase Materials					
Base; Crushed Gravel	Beckhill/Deer Lodge	995	0.655	-0.533	0.89
	Geyser	1172	0.599	-0.474	0.96
	Silver City	1091	0.648	-0.363	0.99
	Baum Road	1697	0.637	-2.489	0.96
	Lothair Road	1325	0.650	-2.078	0.95
	Vaughn North-A	1135	0.570	-0.240	0.99
	Vaughn North-B	1157	0.720	-0.290	0.99
	Vaughn North-C	784	0.640	0.020	1.00
	Vaughn North-D	826	0.560	0.260	1.00
	Vaughn North-E	837	0.570	0.240	1.00
Base; Soil-Aggregate Mixture	Condon	1235	0.548	-0.497	0.90
	Fort Belknap	928	0.671	-0.326	0.99
	Hammond	896	0.586	-0.204	0.98
	Perma	803	0.565	-0.871	0.88
	Lothair Road	456	0.864	-2.108	0.93
	Vaughn North-B	1350	0.540	0.000	0.99
	Vaughn North-C	1162	0.560	0.050	1.00
	Vaughn North-D	1409	0.520	-0.110	0.99
Vaughn North-E	1510	0.610	-0.130	0.99	
Soils					
Soil; Clayey Gravel w/Sand	Beckhill/Deer Lodge	1134	0.346	0.128	0.81
Silty Gravel w/Sand	Condon	1568	1.007	-1.689	0.97
	Geyser	1911	0.433	-0.317	0.96
Silty Sand w/Gravel	Fort Belknap	632	0.450	-0.926	0.94
	Silver City	1548	0.491	-2.087	0.96
Coarse-Grained Soil	Baum Road	705	0.201	-1.098	0.76
	Lothair Road	610	0.102	-0.991	0.79
Sandy Silt w/Gravel	Lavina	1825	1.130	-2.659	0.94
Silty Clay W/Gravel	Roundup	1350	0.455	-1.160	0.93
Sandy Clay w/Gravel	Wolf Point	1765	0.332	-1.000	0.71
	Hammond	2669	0.764	-3.796	0.84
Clay w/Gravel	Perma	1435	0.555	-2.539	0.94
Sandy Clay	Vaughn North-B	1083	0.400	-2.920	0.94
	Vaughn North-C	1294	0.360	-2.620	0.98

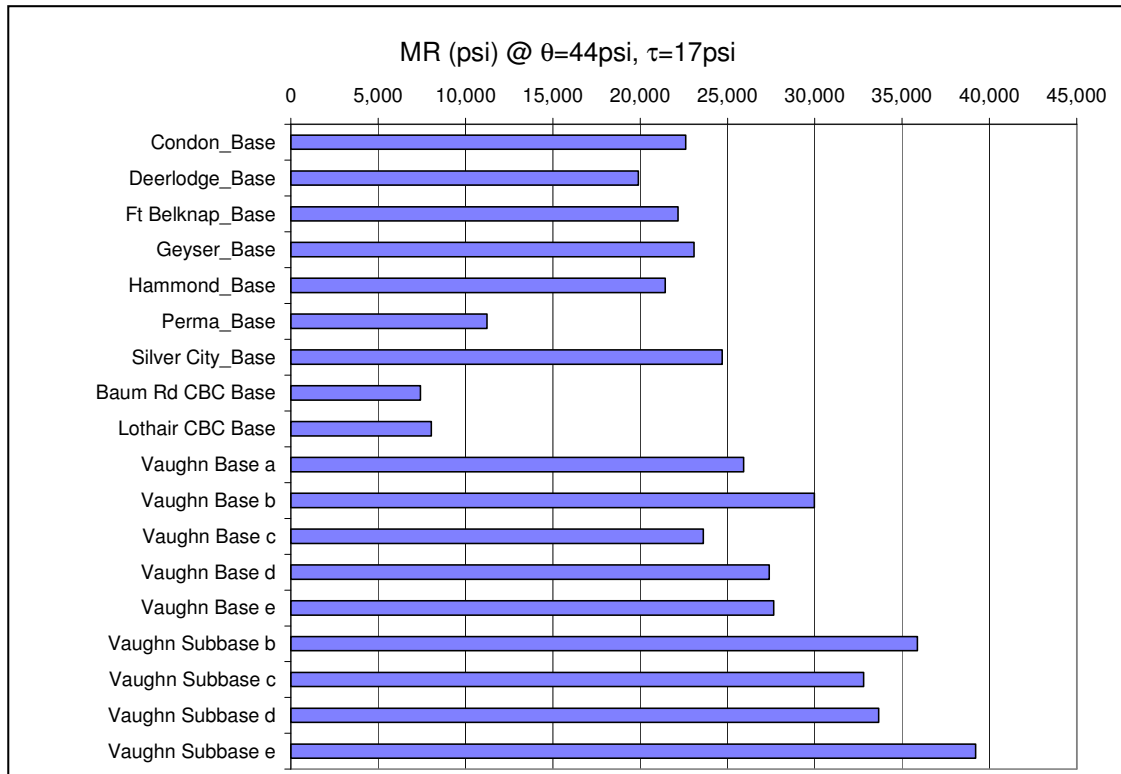


Figure I-21 Resilient Modulus at Typical State of Stress for All MDT Base Materials

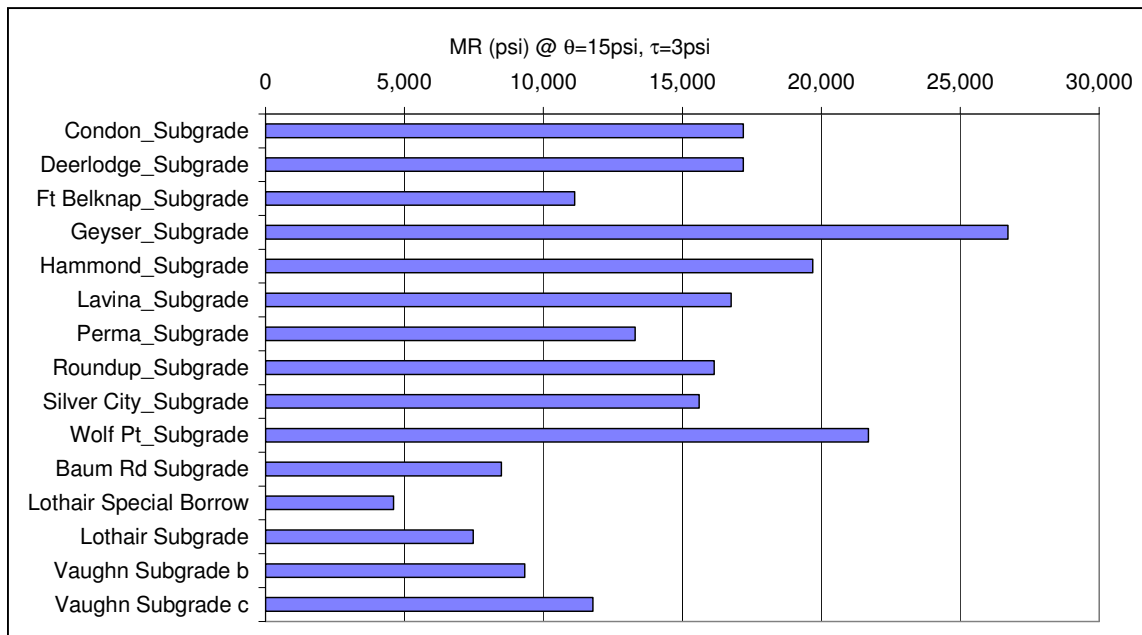


Figure I-22 Resilient Modulus at Typical State of Stress for All MDT Subgrades.

I-6.2.2 Cement Treated Base Materials

The non-LTPP sites with CTB or Cement Aggregate Mixtures (CAM) include Fort Belknap, Geysler, Hammond, Lavina, Perma, Roundup, and Wolf Point. The CAM layers at these sites were cored to recover 6-inch samples for laboratory tests to obtain the elastic modulus and compressive strength of the material, as listed in Table I-6. However, adequate samples for laboratory testing were not obtained for one of the seven sites – Fort Belknap. The CAM crumbled during the coring process at this site.

Five samples from the remaining six sites that had CAM layers were tested in accordance with American Society for Testing and Materials (ASTM) 469. One extra sample was provided from each site to determine the ultimate strength before running the elastic modulus tests. As required by the elastic modulus test protocol, the six inch diameter cores were reduced to four inch diameter test specimens. Some of the 6 inch cores, however, fell apart during the four inch coring process. The cores that began to fall apart were from those layers with lower cement contents, and thus, lower tensile strengths. In fact, the compressive strength and elastic modulus tests could only be measured on cores recovered from three of the sites – Geysler, Hammond, and Wolf Point.

For the remaining three sites IDT and seismic tests were performed on pieces of the cores that were testable. To ensure consistency between the different modulus tests, the indirect tensile test was used to measure the elastic modulus of the Geysler, Hammond, and Wolf Point CAM layers. The test results or mixture properties were found to be highly variable within a project. It is expected that some freeze-thaw damage has occurred within these CAM layers resulting in high variability in the measured strength and modulus. In addition, non-uniform distribution of the cement can also increase the variability of these materials.

Table I-24 summarizes the laboratory test results for the CAM recovered from the non-LTPP test sections, while Figure I-23 provides a comparison of the elastic modulus values measured from the laboratory seismic and indirect tensile tests. The limited comparison summarized in Table I-24 and Figure I-23 shows that the results of the seismic testing are different from the results of traditional indirect tensile and compressive tests. Although there are only two sites with both indirect tensile and compressive elastic modulus values, the elastic modulus values are similar. The elastic modulus values were found to be somewhat low and highly variable. The compressive strengths are relatively high for the elastic modulus values measured with the other tests. The characterization of the CAM layers relative to the calibration and validation of the MEPDG is discussed in the Section I-6.2.3 of this chapter.

I-6.2.3 HMA Mixtures

Table I-6 overviewed the tests planned for the HMA mixtures sampled at each of the non-LTPP test sections. These mixture tests included both volumetric and engineering property tests in support of the MEPDG distress transfer functions. The engineering properties include the dynamic modulus, creep compliance, and tensile strength. Volumetric tests for the HMA mixtures placed at the LTPP test sections are available within the LTPP program and were extracted from the LTPP database – DataPave. Engineering property tests for the dynamic

modulus, creep compliance, and tensile strength of the HMA mixtures, however, are unavailable in the LTPP database. Thus, these properties need to be determined using other methods (from regression equations or correlations) for the LTPP sites located in Montana and in adjacent States and Canadian provinces for the validation and calibration of the MEPDG distress transfer functions.

As noted in Chapter I-2 different diameter cores were recovered at each site. Some of the smaller cores were used for volumetric analyses, while some of the larger cores were used to measure the engineering properties and gradations of the aggregate blends. Plant mix seals and other thin layers were not tested. The following testing regime was performed on the cores recovered at each non-LTPP site.

Table I-24 Summary of CAM Properties Measured in the Laboratory on Cores or Portion of Cores Recovered from the Non-LTPP Sites in Montana

Site	Core Portion	Modulus, ksi				Compressive Strength, psi
		Indirect Tensile (IDT)	IDT Average	Seismic	Compressive	
Hammond	#1 Top	585	755	425 1243 923	550	1490 1810
	#2 Top	812				
	#2 Bottom	932				
	#3 Top	689				
Lavina	#1 Top	979	863	2810 1364 577		
	#1 Bottom	956				
	#2 Top	698				
	#2 Bottom	764				
	#3	917				
Perma	#1	668	661	318 683 330		
	#2	1072				
	#2	245				
Roundup	#1 Top	891	868	1557 471 1072		
	#2	781				
	#3	931				
Wolf Point	#2 Top	1461	1243	799 533	1600 1550	2670 2530
	#2 Bottom	1184				
	#3 Top	1096				
	#3 Bottom	1231				
Geyser					500	790
					850	880
					800	1020

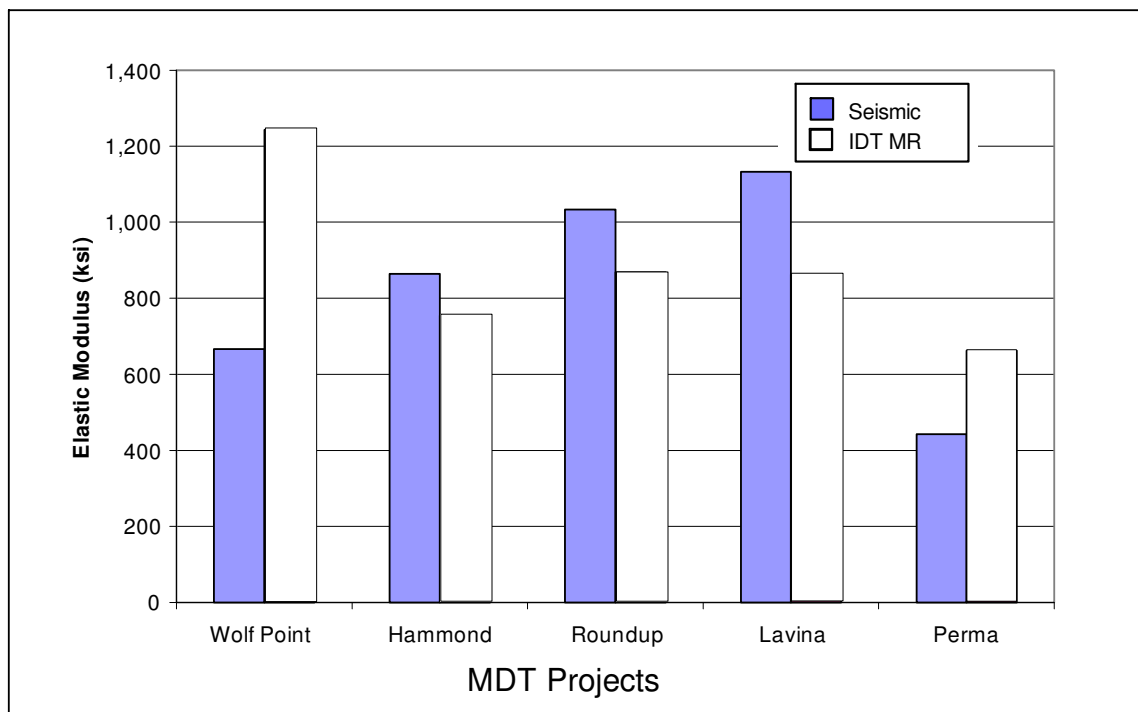


Figure I-23 Comparison of the elastic modulus values measured with the seismic and indirect tensile tests.

1. Twelve cores were split into two groups with approximately equal air voids, both range and average. For most projects this included six cores per group, except Wolf Point had one visually damaged core, Fort Belknap had two visually damaged cores and, Perma had one visually damaged 6-inch and two 4-inch diameter cores.
2. Three cores were selected from each group that spanned the range of air void contents. IDT creep tests were performed at 0, -10, and -20°C on these three cores. Creep tests were performed on the same cores across the temperature regime to obtain good master curves. An additional three creep tests were performed if there was high variability in the data.
3. Three cores were selected from the second group of cores that spanned the range of air void contents. IDT modulus tests were performed at 4, 16, and 27°C on these cores. Again, the modulus tests were performed at different temperatures on the same cores to get good modulus-temperature relationships. Up to three more modulus tests were performed if there was high variability in the data.
4. IDT strength tests were performed at 0, -10, and -20°C using three cores. Cores were selected for this group that has air void contents that spanned the range and have the same average. In selecting the cores, any of the untested cores or the previously tested

creep and modulus cores was used for strength tests, provided they were not damaged during the creep and modulus testing.

This provided a simple and efficient approach to obtain the data needed for validation and calibration for the non-LTPP sites in Montana.

Supplemental Test Sections

Three Superpave supplemental test sections were selected to include projects constructed with Superpave-designed HMA mixtures. The purpose of adding these sections was to incorporate pavements constructed with current MDT mixture design procedures. Three projects were selected and sampled under this project and are defined as the Baum Road site, the Lothair East site, and the Vaughn North site. The Fort Belknap site was overlaid with a leveling and surface or wearing course. The sampling included asphalt binder, aggregate stockpiles, and HMA. MDT sampled the subgrade and subbase materials from the Vaughn North site, and sampled subgrade from the Lothair East site. Geographical Positioning System (GPS) readings were taken at each location so that the sites could be easily identified.

Binder test results from Trumbull (Granite City, Illinois) for the three Superpave mixture tests were completed and the test results entered into the database. HMA cores were not available for the indirect tensile modulus, tensile strength, and creep compliance for the Baum Road and Lothair East sites. Gradation, volumetric and asphalt properties can be used to predict the stiffness of the HMA layer using the dynamic modulus predictive equation included in the MEPDG.

HMA Property Predictive Equations for Montana Mixtures

The indirect tensile strength and creep compliance at low temperatures are required inputs for the MEPDG to predict the amount of low temperature cracking. These properties were measured on the HMA mixtures sampled at each of the non-LTPP test sites, but are unavailable for the LTPP sites, as noted above. In addition, the tensile strain at failure was planned for use to improve on the calibration of the fracture related models. Thus, the indirect tensile strength, tensile strain at failure, creep compliance, and modulus were measured over a range of temperatures using two specimens per temperature (twelve cores per material). This test program was completed to develop correlations and determine the indirect tensile strain at failure and creep compliance for the HMA mixtures placed at the other LTPP sites located in Montana.

The test results for the advanced asphalt materials testing are summarized in Tables I-25 through I-27. Table I-25 provides a summary of the HMA modulus, Table I-26 provides a summary of the indirect tensile strength and tensile strain at failure, and Table I-27 provides the creep compliance for the different test temperatures. Using these data, correlations or regression equations were developed to determine those HMA properties not readily available as default values in the MEPDG. The following provides some correlations and comparisons of the HMA mixtures sampled from Montana.

- Most of these mixes are believed to have better fatigue characteristics than what has been reported on other mixtures sampled and tested at different facilities based on the

HMA resilient modulus and indirect tensile strain at failure. Figure I-24 compares the fracture properties for typical Montana mixtures to those of a standard mix. The data used to prepare this figure was taken from Tables I-25 and I-26. As shown, the Montana HMA mixtures generally have better fracture characteristics than typically used in pavement design methods. This type of relationship can be used to estimate the tensile strain at failure for use in improving the calibration of the fracture distresses, if needed. It is expected that the lower air voids for these HMA mixtures contribute to the improved fracture properties. The only HMA that falls below the line representative of the standard mixture is the binder mixture that was sampled from the Vaughn North Superpave supplemental test section. The binder course contained a PG 58-28 binder and the surface course contained a 70-28 binder. This HMA mixture is believed to have inferior fracture properties for the lower temperature, as compared to the other mixtures tested. The reason for the inferior fracture properties is unknown at this time.

- Figure I-25 shows that there is a good relationship between the elastic modulus and tensile strength of the HMA mixtures, as measured with the indirect tensile test. Similar relationships have been found from other projects. This relationship can be used to estimate the tensile strength of the HMA mixtures from the dynamic modulus for those LTPP test sections where sufficient test data do not exist in the LTPP database.
- Figures I-26 and I-27 show that the creep compliance of the HMA mixtures can be estimated using the elastic modulus of the mixture. The data used to prepare these figures were taken from Table I-27. The variability within the correlation does increase with creep loading time, but that variability is considered acceptable to estimate this mixture property when laboratory tests are unavailable. This relationship can be used to estimate the creep compliance of the HMA mixtures from the dynamic modulus for those LTPP test sections where sufficient test data do not exist in the LTPP database. Similar to the tensile strain at failure, the creep compliance values measured on typical Montana HMA mixtures are representative of mixtures resistant to thermal cracking.
- Another important observation from the field cores: the average air voids measured on the recovered cores are low, which suggests that the mixes were adequately compacted during construction. Lower air voids would definitely improve the fracture resistance (fatigue and thermal cracking) of the mixture. In summary:
 - Five sites have air voids less than 3 percent.
 - Three sites have air voids between 3 to 5 percent.
 - Two sites have air voids just slightly greater than 5 percent.

Table I-25 Summary of Laboratory Measured IDT Resilient Modulus for the HMA Mixtures Sampled from the Non-LTPP Test Sections in Montana

Test Section	Statistics	Air Voids, %	Total Resilient Modulus, ksi		
			4 °C	16 °C	27 °C
Condon	Average	2.7	1,426	603	259
	Std. Dev., ksi	1.9	61.6	51.8	29.4
	COV, %	71.5	4.2	8.6	11.4
Beckhill/Deer Lodge	Average	5.1	1,287	495	192
	Std. Dev., ksi	0.6	100.4	60.2	30.5
	COV, %	12.4	7.8	12.2	15.9
Fort Belknap	Average	3.2	2,102	774	357
	Std. Dev., ksi	1.3	534.1	71.0	59.0
	COV, %	41.5	25.4	9.2	16.5
Hammond	Average	1.9	1,944	916	382
	Std. Dev., ksi	0.6	389.1	172.5	78.7
	COV, %	31.6	20.0	18.8	20.6
Geyser	Average	5.2	1,620	489	231
	Std. Dev., ksi	1.4	494.6	93.3	66.5
	COV, %	26.6	30.5	19.1	28.8
Lavina	Average	2.3	2,040	1,058	700
	Std. Dev., ksi	0.6	324.8	64.3	219.8
	COV, %	27.8	15.9	6.1	31.4
Perma	Average	4.3	1,510	602	271
	Std. Dev., ksi	2.1	447.5	36.7	26.3
	COV, %	49.2	29.6	6.1	9.7
Roundup	Average	2.8	2,728	1,174	546
	Std. Dev., ksi	0.9	598.3	56.2	37.9
	COV, %	33.3	21.9	4.8	6.9
Silver City	Average	3.1	1,896	667	292
	Std. Dev., ksi	1.2	445.0	123.2	76.6
	COV, %	39.5	23.5	18.5	26.2
Wolf Point	Average	2.1	1,937	658	241
	Std. Dev., ksi	0.7	207.3	104.2	60.6
	COV, %	32.2	10.7	15.8	25.2
Vaughn N., Binder	Average	1.7	2,244	1,086	393
	Std. Dev., ksi	0.35	101.4	97.8	47.0
	COV, %	20.3	4.5	9.0	11.9
Vaughn N., Surface	Average	1.7	1,891	907	346
	Std. Dev., ksi	0.4	78.1	43.2	25.2
	COV, %	20.3	4.1	4.8	7.3

Std. Dev. = Standard Deviation
COV = Coefficient of Variation

Table I-26 Summary of Laboratory Measured Tensile Strengths and Tensile Strain at Failure for the HMA Mixtures Sampled from the Non-LTPP Test Sections in Montana

Test Section	Sample	Air Voids, %			Tensile Strength, psi			Tensile Strain at Failure, mils/in.		
		4 °C	16 °C	27 °C	4 °C	16 °C	27 °C	4 °C	16 °C	27 °C
Condon	1	4.6	3.7	2.6	410	144	84	3.4	7.8	9.6
	2	0.8	0.8	1.7	424	160	84	5.7	5.8	13.1
	Average	2.7	2.3	2.2	417	152	84	4.5	6.8	11.4
Beckhill/Deer Lodge	1	4.5	4.6	4.7	446	204	92	4.5	7.4	14.3
	2	5.7	5.3	5.0	430	191	93	4.3	7.8	12.9
	Average	5.1	5.0	4.9	438	197	92	4.4	7.6	13.6
Fort Belknap	1	4.6	2.8	2.8	389	153	58	2.9	8.5	12.7
	2	2.0	4.4	3.1	488	144	95	3.3	9.0	10.4
	Average	3.3	3.6	2.9	439	149	77	3.1	8.8	11.6
Hammond	1	1.2	1.4	1.6	543	235	88	3.4	4.2	8.0
	2	2.4	2.1	2.0	554	216	123	2.5	5.2	6.5
	Average	1.8	1.7	1.8	548	225	106	2.9	4.7	7.3
Geyser	1	3.8	4.7	5.5	458	157	76	5.5	8.2	12.8
	2	6.3	6.3	5.3	337	145	80	5.7	9.8	13.2
	Average	5.1	5.5	5.4	397	151	78	5.6	9.0	13.0
Lavina	1	2.9	2.3	2.5	414	210	116	4.3	12.4	14.6
	2	1.6	2.6	2.4	464	236	141	4.6	5.3	6.4
	Average	2.3	2.5	2.4	439	223	128	4.5	8.8	10.5
Perma	1	6.4	4.0	4.4	450	197	94	3.8	10.3	11.3
	2	2.1	3.6	3.3	535	202	86	3.6	9.3	12.5
	Average	4.3	3.8	3.9	493	200	90	3.7	9.8	11.9
Roundup	1	1.9	3.4	2.7	508	210	117	3.6	6.1	5.7
	2	3.8	2.6	3.2	461	235	101	3.2	3.8	19.0
	Average	2.8	3.0	3.0	484	223	109	3.4	5.0	12.4
Silver City	1	4.3	2.1	2.2	482	147	62	4.4	9.0	11.2
	2	1.8	3.4	3.3	465	196	85	3.5	6.2	10.1
	Average	3.1	2.7	2.7	474	171	74	4.0	7.6	10.6
Wolf Point	1	2.7	1.4	1.8	483	151	65	2.6	8.1	16.0
	2	1.4	1.7	2.0	528	151	68	4.2	10.4	11.6
	Average	2.1	1.5	1.9	506	151	67	3.4	9.2	13.8
Vaughn N., Binder	1	2.1	1.7	1.7	589	291	112	2.1	4.5	8.5
	2	1.4	2.1	1.9	669	288	108	1.0	3.4	7.8
	Average	1.8	1.9	1.8	629	290	110	1.6	4.0	8.2
Vaughn N., Surface	1	3.1	2.3	2.5	593	306	125	3.3	6.5	15.0
	2	2.2	3.1	2.5	536	305	142	4.8	6.7	8.7
	Average	2.7	2.7	2.5	565	306	134	4.1	6.6	11.9

Table I-27 Summary of the Laboratory Creep Compliance Tests for HMA Mixtures Recovered from the Non-LTPP Test Sections Located in Montana

Temp., °F:	-4			14			32		
	Creep Comp., 1/psi	m(t)	μ(t)	Creep Comp., 1/psi	m(t)	μ(t)	Creep Comp., 1/psi	m(t)	μ(t)
Site: CONDON									
10	2.87E-07	0.129	0.149	5.61E-07	0.246	0.413	8.56E-07	0.320	0.413
13	2.95E-07	0.130	0.149	6.04E-07	0.252	0.413	9.46E-07	0.331	0.413
16	3.02E-07	0.131	0.149	6.37E-07	0.257	0.413	9.96E-07	0.339	0.413
20	3.11E-07	0.131	0.149	6.70E-07	0.263	0.413	1.09E-06	0.347	0.413
25	3.18E-07	0.132	0.149	7.17E-07	0.268	0.413	1.18E-06	0.356	0.413
32	3.34E-07	0.133	0.149	7.59E-07	0.274	0.413	1.28E-06	0.366	0.413
40	3.46E-07	0.133	0.149	8.11E-07	0.279	0.413	1.38E-06	0.375	0.413
50	3.58E-07	0.134	0.149	8.68E-07	0.285	0.413	1.51E-06	0.383	0.413
63	3.72E-07	0.134	0.149	9.34E-07	0.290	0.413	1.66E-06	0.392	0.413
79	3.84E-07	0.135	0.149	1.00E-06	0.296	0.413	1.82E-06	0.401	0.413
100	3.89E-07	0.136	0.149	1.05E-06	0.301	0.413	1.98E-06	0.410	0.413
Site: DEER LODGE/BECKHILL									
10	3.34E-07	0.104	0.220	5.40E-07	0.201	0.294	1.20E-06	0.355	0.294
13	3.45E-07	0.104	0.220	5.75E-07	0.208	0.294	1.33E-06	0.368	0.294
16	3.51E-07	0.103	0.220	6.02E-07	0.214	0.294	1.45E-06	0.377	0.294
20	3.59E-07	0.103	0.220	6.19E-07	0.221	0.294	1.54E-06	0.388	0.294
25	3.68E-07	0.102	0.220	6.37E-07	0.227	0.294	1.70E-06	0.398	0.294
32	3.76E-07	0.101	0.220	6.95E-07	0.234	0.294	1.88E-06	0.410	0.294
40	3.91E-07	0.101	0.220	7.39E-07	0.241	0.294	2.06E-06	0.421	0.294
50	4.02E-07	0.100	0.220	7.83E-07	0.247	0.294	2.28E-06	0.431	0.294
63	4.10E-07	0.100	0.220	8.32E-07	0.254	0.294	2.53E-06	0.442	0.294
79	4.22E-07	0.099	0.220	8.89E-07	0.261	0.294	2.82E-06	0.453	0.294
100	4.22E-07	0.099	0.220	9.25E-07	0.267	0.294	3.09E-06	0.464	0.294
Site: SILVER CITY									
10	2.94E-07	0.156	0.217	4.88E-07	0.186	0.223	1.13E-06	0.337	0.223
13	3.02E-07	0.146	0.217	5.02E-07	0.195	0.223	1.23E-06	0.349	0.223
16	3.14E-07	0.139	0.217	5.25E-07	0.202	0.223	1.32E-06	0.359	0.223
20	3.22E-07	0.131	0.217	5.61E-07	0.210	0.223	1.42E-06	0.369	0.223
25	3.30E-07	0.123	0.217	5.89E-07	0.218	0.223	1.55E-06	0.379	0.223
32	3.44E-07	0.114	0.217	6.21E-07	0.226	0.223	1.73E-06	0.390	0.223
40	3.55E-07	0.106	0.217	6.57E-07	0.234	0.223	2.87E-06	0.401	0.223
50	3.61E-07	0.098	0.217	6.94E-07	0.242	0.223	2.09E-06	0.411	0.223
63	3.69E-07	0.090	0.217	7.35E-07	0.250	0.223	2.29E-06	0.421	0.223
79	3.86E-07	0.082	0.217	7.85E-07	0.257	0.223	2.54E-06	0.432	0.223
100	3.83E-07	0.074	0.217	8.22E-07	0.266	0.223	3.78E-06	0.442	0.223
Site: ROUNDUP									
10	2.46E-07	0.094	0.204	3.89E-07	0.195	0.268	7.44E-07	0.299	0.268
13	2.55E-07	0.098	0.204	4.09E-07	0.203	0.268	8.04E-07	0.321	0.268
16	2.58E-07	0.102	0.204	4.36E-07	0.210	0.268	8.57E-07	0.339	0.268
20	2.65E-07	0.105	0.204	4.52E-07	0.218	0.268	9.32E-07	0.358	0.268
25	2.69E-07	0.108	0.204	4.76E-07	0.225	0.268	1.01E-06	0.377	0.268
32	2.77E-07	0.112	0.204	4.99E-07	0.234	0.268	1.12E-06	0.399	0.268
40	2.85E-07	0.116	0.204	5.19E-07	0.241	0.268	1.22E-06	0.418	0.268
50	2.91E-07	0.119	0.204	5.54E-07	0.248	0.268	1.35E-06	0.437	0.268
63	3.01E-07	0.123	0.204	5.82E-07	0.256	0.268	1.49E-06	0.457	0.268
79	3.09E-07	0.126	0.204	6.25E-07	0.264	0.268	1.66E-06	0.476	0.268
100	3.13E-07	0.130	0.204	6.69E-07	0.272	0.268	1.83E-06	0.497	0.268

Table I-27 Summary of the Laboratory Creep Compliance Tests for HMA Mixtures Recovered from the Non-LTPP Test Sections Located in Montana, Continued

Temp., °F:	-4			14			32		
Loading Time, Sec.	Creep Comp., 1/psi	m(t)	μ(t)	Creep Comp., 1/psi	m(t)	μ(t)	Creep Comp., 1/psi	m(t)	μ(t)
Site: LAVINA									
10	3.40E-07	0.107	0.244	4.62E-07	0.134	0.175	9.30E-07	0.333	0.175
13	3.51E-07	0.114	0.244	4.72E-07	0.149	0.175	1.04E-06	0.340	0.175
16	3.61E-07	0.119	0.244	4.95E-07	0.161	0.175	1.10E-06	0.346	0.175
20	3.68E-07	0.125	0.244	5.09E-07	0.173	0.175	1.19E-06	0.352	0.175
25	3.80E-07	0.131	0.244	5.38E-07	0.186	0.175	1.26E-06	0.358	0.175
32	3.91E-07	0.138	0.244	5.61E-07	0.200	0.175	1.40E-06	0.365	0.175
40	4.03E-07	0.143	0.244	5.85E-07	0.213	0.175	1.51E-06	0.371	0.175
50	4.08E-07	0.149	0.244	6.13E-07	0.226	0.175	1.63E-06	0.377	0.175
63	4.27E-07	0.155	0.244	6.60E-07	0.239	0.175	1.79E-06	0.383	0.175
79	4.48E-07	0.161	0.244	6.89E-07	0.252	0.175	1.96E-06	0.389	0.175
100	4.59E-07	0.168	0.244	7.21E-07	0.266	0.175	2.11E-06	0.396	0.175
Site: WOLF POINT									
10	1.97E-07	0.124	0.182	4.10E-07	0.246	0.263	1.25E-06	0.448	0.263
13	1.99E-07	0.132	0.182	4.29E-07	0.261	0.263	1.43E-06	0.463	0.263
16	2.11E-07	0.138	0.182	4.68E-07	0.272	0.263	1.55E-06	0.474	0.263
20	2.14E-07	0.145	0.182	4.83E-07	0.284	0.263	1.74E-06	0.487	0.263
25	2.18E-07	0.151	0.182	5.17E-07	0.297	0.263	1.92E-06	0.500	0.263
32	2.33E-07	0.159	0.182	5.66E-07	0.310	0.263	2.19E-06	0.514	0.263
40	2.40E-07	0.165	0.182	6.05E-07	0.322	0.263	2.46E-06	0.526	0.263
50	2.50E-07	0.172	0.182	6.39E-07	0.335	0.263	2.77E-06	0.539	0.263
63	2.63E-07	0.178	0.182	6.98E-07	0.347	0.263	3.12E-06	0.552	0.263
79	2.72E-07	0.185	0.182	7.66E-07	0.360	0.263	3.57E-06	0.565	0.263
100	2.78E-07	0.192	0.182	8.12E-07	0.373	0.263	3.99E-06	0.578	0.263
Site: FORT BELKNAP									
10	2.53E-07	0.125	0.196	4.38E-07	0.207	0.223	9.23E-07	0.292	0.223
13	2.57E-07	0.130	0.196	4.61E-07	0.221	0.223	9.84E-07	0.316	0.223
16	2.67E-07	0.135	0.196	4.83E-07	0.232	0.223	1.08E-06	0.335	0.223
20	2.78E-07	0.139	0.196	5.24E-07	0.244	0.223	1.16E-06	0.356	0.223
25	2.84E-07	0.144	0.196	5.47E-07	0.257	0.223	1.24E-06	0.376	0.223
32	2.96E-07	0.149	0.196	5.78E-07	0.270	0.223	1.38E-06	0.399	0.223
40	2.98E-07	0.154	0.196	6.19E-07	0.282	0.223	1.53E-06	0.420	0.223
50	3.11E-07	0.158	0.196	6.51E-07	0.294	0.223	1.68E-06	0.440	0.223
63	3.23E-07	0.163	0.196	7.05E-07	0.306	0.223	1.84E-06	0.461	0.223
79	3.42E-07	0.168	0.196	7.55E-07	0.319	0.223	2.05E-06	0.482	0.223
100	3.67E-07	0.173	0.196	8.00E-07	0.331	0.223	2.23E-06	0.504	0.223
Site: PERMA									
10	3.04E-07	0.091	0.190	4.81E-07	0.143	0.229	9.02E-07	0.279	0.229
13	3.18E-07	0.094	0.190	5.06E-07	0.160	0.229	9.77E-07	0.299	0.229
16	3.21E-07	0.097	0.190	5.22E-07	0.173	0.229	1.04E-06	0.314	0.229
20	3.31E-07	0.100	0.190	5.47E-07	0.187	0.229	1.12E-06	0.331	0.229
25	3.33E-07	0.103	0.190	5.83E-07	0.201	0.229	1.20E-06	0.348	0.229
32	3.40E-07	0.106	0.190	5.93E-07	0.216	0.229	1.31E-06	0.367	0.229
40	3.55E-07	0.109	0.190	6.23E-07	0.230	0.229	1.45E-06	0.384	0.229
50	3.62E-07	0.113	0.190	6.53E-07	0.244	0.229	1.58E-06	0.400	0.229
63	3.72E-07	0.116	0.190	6.99E-07	0.258	0.229	1.72E-06	0.418	0.229
79	3.77E-07	0.119	0.190	7.40E-07	0.272	0.229	1.89E-06	0.435	0.229
100	3.75E-07	0.122	0.190	7.85E-07	0.287	0.229	2.02E-06	0.453	0.229

Table I-27 Summary of the Laboratory Creep Compliance Tests for HMA Mixtures Recovered from the Non-LTPP Test Sections Located in Montana, Continued

Temp., °F:	-4			14			32		
Loading Time, Sec.	Creep Comp., 1/psi	m(t)	μ(t)	Creep Comp., 1/psi	m(t)	μ(t)	Creep Comp., 1/psi	m(t)	μ(t)
Site: GEYSER									
10	4.30E-07	0.086	0.277	7.47E-07	0.195	0.305	1.47E-06	0.342	0.305
13	4.46E-07	0.102	0.277	7.84E-07	0.210	0.305	1.60E-06	0.353	0.305
16	4.55E-07	0.115	0.277	8.20E-07	0.221	0.305	1.72E-06	0.363	0.305
20	4.65E-07	0.128	0.277	8.76E-07	0.234	0.305	1.87E-06	0.372	0.305
25	4.82E-07	0.142	0.277	9.06E-07	0.247	0.305	2.07E-06	0.382	0.305
32	4.95E-07	0.157	0.277	9.74E-07	0.261	0.305	2.25E-06	0.393	0.305
40	5.14E-07	0.170	0.277	1.05E-06	0.274	0.305	2.46E-06	0.403	0.305
50	5.39E-07	0.184	0.277	1.10E-06	0.286	0.305	2.67E-06	0.413	0.305
63	5.63E-07	0.198	0.277	1.19E-06	0.299	0.305	2.95E-06	0.423	0.305
79	5.85E-07	0.212	0.277	1.26E-06	0.312	0.305	3.27E-06	0.433	0.305
100	6.09E-07	0.226	0.277	1.31E-06	0.326	0.305	3.52E-06	0.444	0.305
Site: HAMMOND									
10	2.54E-07	0.067	0.144	4.20E-07	0.199	0.239	8.72E-07	0.360	0.239
13	2.60E-07	0.079	0.144	4.37E-07	0.206	0.239	9.52E-07	0.364	0.239
16	2.63E-07	0.088	0.144	4.53E-07	0.211	0.239	1.03E-06	0.368	0.239
20	2.72E-07	0.098	0.144	4.77E-07	0.217	0.239	1.11E-06	0.371	0.239
25	2.78E-07	0.108	0.144	4.98E-07	0.222	0.239	1.19E-06	0.375	0.239
32	2.83E-07	0.119	0.144	5.39E-07	0.229	0.239	1.34E-06	0.379	0.239
40	2.89E-07	0.129	0.144	5.59E-07	0.234	0.239	1.44E-06	0.383	0.239
50	3.01E-07	0.139	0.144	5.91E-07	0.240	0.239	1.59E-06	0.386	0.239
63	3.07E-07	0.149	0.144	6.29E-07	0.246	0.239	1.73E-06	0.390	0.239
79	3.21E-07	0.159	0.144	6.70E-07	0.252	0.239	1.90E-06	0.394	0.239
100	3.35E-07	0.170	0.144	7.03E-07	0.258	0.239	2.04E-06	0.398	0.239
Site: VAUGHN NORTH, Binder									
10	1.82E-07	0.08	0.21	2.42E-07	0.17	0.16	6.30E-07	0.34	0.16
13	1.94E-07	0.08	0.21	2.59E-07	0.18	0.16	6.95E-07	0.35	0.16
16	1.84E-07	0.07	0.21	2.68E-07	0.20	0.16	7.41E-07	0.36	0.16
20	1.92E-07	0.07	0.21	2.82E-07	0.21	0.16	7.97E-07	0.37	0.16
25	1.94E-07	0.07	0.21	2.96E-07	0.23	0.16	8.74E-07	0.37	0.16
32	1.98E-07	0.06	0.21	3.07E-07	0.25	0.16	9.60E-07	0.38	0.16
40	2.04E-07	0.06	0.21	3.27E-07	0.26	0.16	1.03E-06	0.39	0.16
50	2.02E-07	0.05	0.21	3.50E-07	0.28	0.16	1.13E-06	0.39	0.16
63	2.10E-07	0.05	0.21	3.67E-07	0.29	0.16	1.25E-06	0.40	0.16
79	2.08E-07	0.05	0.21	3.96E-07	0.31	0.16	1.37E-06	0.41	0.16
100	2.00E-07	0.04	0.21	4.22E-07	0.33	0.16	1.49E-06	0.41	0.16
Site: VAUGHN NORTH, Surface									
10	2.26E-07	0.13	0.20	3.28E-07	0.20	0.30	7.64E-07	0.31	0.30
13	2.31E-07	0.12	0.20	3.49E-07	0.21	0.30	8.23E-07	0.32	0.30
16	2.32E-07	0.12	0.20	3.63E-07	0.22	0.30	8.88E-07	0.33	0.30
20	2.39E-07	0.11	0.20	3.84E-07	0.22	0.30	9.62E-07	0.34	0.30
25	2.45E-07	0.10	0.20	3.98E-07	0.23	0.30	1.03E-06	0.35	0.30
32	2.58E-07	0.10	0.20	4.23E-07	0.23	0.30	1.13E-06	0.36	0.30
40	2.62E-07	0.09	0.20	4.51E-07	0.24	0.30	1.22E-06	0.37	0.30
50	2.68E-07	0.09	0.20	4.83E-07	0.25	0.30	1.32E-06	0.38	0.30
63	2.75E-07	0.08	0.20	4.97E-07	0.25	0.30	1.45E-06	0.39	0.30
79	2.79E-07	0.08	0.20	5.29E-07	0.26	0.30	1.58E-06	0.40	0.30
100	2.73E-07	0.07	0.20	5.43E-07	0.27	0.30	1.71E-06	0.40	0.30

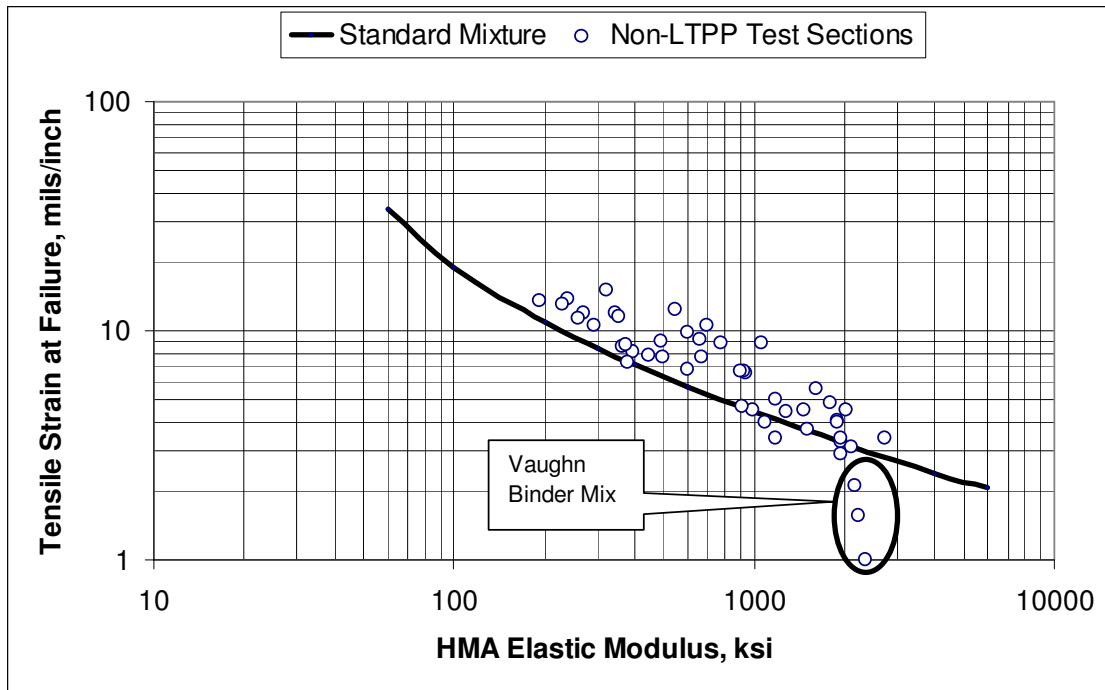


Figure I-24 Relationship between the elastic modulus and tensile strain at failure as measured from the indirect tensile strength test for the HMA mixtures recovered from the non-LTPP test sections in Montana (data taken from Tables I-25 and I-26).

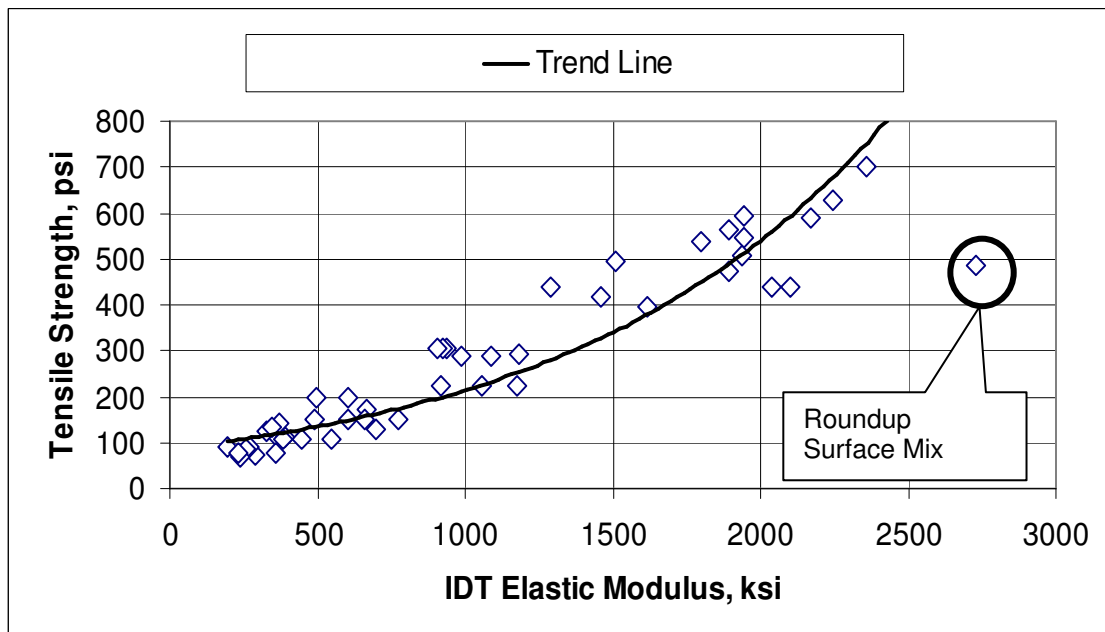


Figure I-25 Relationship between the elastic modulus and the tensile strength of the HMA mixtures recovered from the non-LTPP test sections in Montana (data taken from Tables I-25 and I-26).

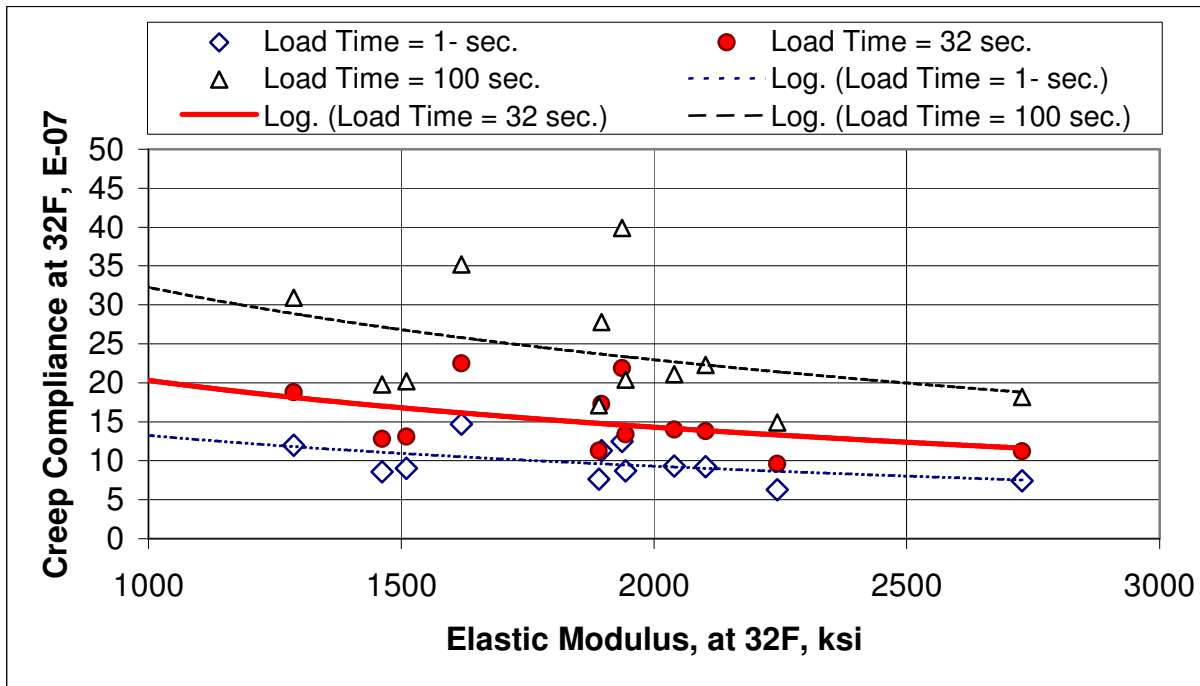


Figure I-26 Relationship between the IDT elastic modulus measured at 32°F and the tensile creep compliance measured at 4°F for different loading times of the HMA mixtures recovered from the non-LTPP test sections in Montana.

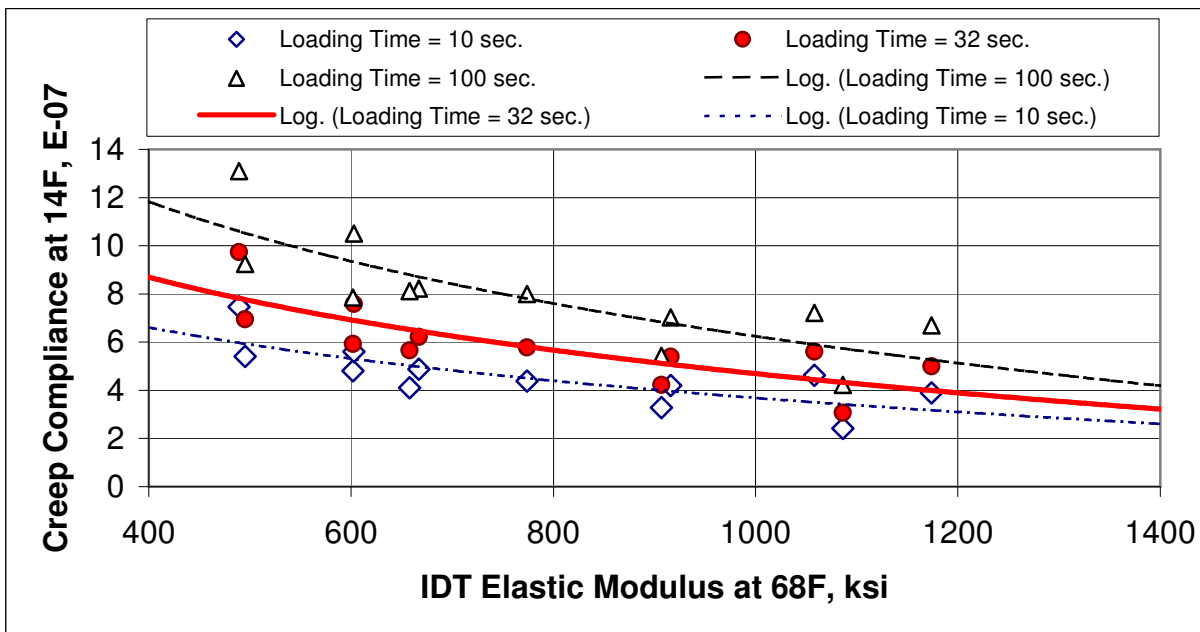


Figure I-27 Relationship between the IDT elastic modulus measured at 68°F and the tensile creep compliance measured at 14°F for different loading times of the HMA mixtures recovered from the non-LTPP test sections in Montana.

As noted above, the tensile strength, tensile strain at failure, and creep compliance are not available on any of the HMA mixtures included in the LTPP database. Thus, correlations are needed to estimate those properties rather than just accepting the default values included in the MEPDG. Predictive equations were developed for the IDT elastic modulus and tensile strain at failure. The IDT modulus can then be used to estimate the indirect tensile strength and creep compliance using Figures I-25 through I-27.

The predictive equation for the indirect tensile modulus of Montana HMA mixtures is provided by Equation I-18. The parameters and “goodness of fit” statistics obtained for the regression equation to predict the indirect tensile modulus for Montana’s typical HMA mixtures from the volumetric properties and temperature are given in Table I-28.

$$\log M_R = k_1 + k_T \cdot T + k_{V_a} \cdot V_a \quad (I-18)$$

Where:

- M_R = Diametral or indirect tensile resilient modulus (psi) voids.
- T = Temperature, °F.
- V_a = Air voids, %.
- k_1, k_T, k_{V_a} = Regression constants, shown in Table I-28.

Table I-28 IDT Resilient Modulus Model Parameters for the Non-LTPP HMA Mixtures Sampled from the Montana Test Sections

Test Section	Coefficients of Equation I-18			Statistical Parameters	
	k_1	k_T	k_{V_a}	Se/Sy	R ²
Condon	6.321	-0.033	-0.009	0.10	0.99
Beckhill	6.116	-0.036	0.028	0.14	0.98
Fort Belknap	6.590	-0.033	-0.047	0.16	0.97
Geyser	6.629	-0.037	-0.059	0.23	0.95
Hammond	6.610	-0.031	-0.102	0.22	0.95
Lavina	6.270	-0.021	0.046	0.38	0.86
Perma	6.317	-0.032	-0.005	0.24	0.94
Roundup	6.443	-0.030	0.038	0.14	0.98
Silver City	6.145	-0.035	0.082	0.09	0.99
Wolf Point	6.231	-0.040	0.104	0.10	0.99
All Sites	6.510	-0.033	-0.040	0.39	0.84

Following a similar approach, Equation I-19 was developed to predict the tensile strain at failure as measured in the indirect tensile strength test for typical Montana HMA mixtures.

$$\log \epsilon_f = k_1 + k_T \cdot T + k_{V_a} \cdot V_a \quad (I-19)$$

Where:

- ϵ_f = Tensile strain at failure in the indirect tensile strength test (dimensionless).
- k_1, k_T, k_{V_a} = Regression constants, shown in Table I-29.
- T = Temperature, °F
- V_a = Air voids, %.

Table I-29 Tensile Strain at Failure Model Parameters for the Non-LTPP HMA Mixtures Sampled from the Montana Test Sections

Test Section	Coefficients of Equation I-18			Statistical Parameters	
	k_1	k_T	k_{V_a}	Se/Sy	R^2
Condon	-2.630	0.009	-0.001	0.93	0.13
Beckhill	-2.478	0.019	-0.041	0.24	0.94
Fort Belknap	-2.756	0.024	-0.004	0.47	0.78
Geyser	-2.670	0.014	0.025	0.39	0.85
Hammond	-2.686	0.014	-0.025	0.41	0.83
Lavina	-2.346	0.017	-0.137	1.02	-0.04
Perma	-2.664	0.019	-0.006	0.26	0.93
Roundup	-3.119	0.023	0.081	0.71	0.49
Silver City	-2.591	0.013	-0.020	0.83	0.32
Wolf Point	-2.308	0.020	-0.202	0.36	0.87
All Sites	-2.757	0.018	-0.019	0.63	0.61

These two predictive equations are very similar, semi-log form and only temperature and air voids are used as predictor variables. Although the accuracy of the models could be improved by adding aggregate gradation and binder properties as predictor variables, the very good fit observed in the great majority of cases shows that making the models more complex is not necessary.

For the surface layer, the laboratory measured IDT resilient modulus and tensile strain at failure values were used to develop a generalized predictive model for resilient modulus and tensile strain at failure as a function of air voids and temperature. Both models are moderately accurate, with a coefficient of determination R^2 of 0.84 for the IDT resilient modulus, which is presented in Equation I-20, and an R^2 of 0.61 for the tensile strain at failure, which is presented in Equation I-21.

$$M_R = 10^{6.510 - 0.033T - 0.040V_a} \quad (I-20)$$

Where:

- M_R = Resilient modulus.
- T = Temperature, °F.
- V_a = Air voids, %.

$$\epsilon_f = 10^{-2.757 + 0.018T - 0.019V_a} \quad (I-21)$$

Where:

- ϵ_f = Tensile strain at failure.
- T = Temperature, °F.
- V_a = Air voids, %.

Equations I-20 and I-21 can be used to calculate the IDT modulus and tensile strain at failure for those HMA mixtures placed at the LTPP test sections in Montana.

I-6.3 MATERIAL CHARACTERIZATION SUMMARY – LAYER PROPERTIES FOR CALIBRATION AND VALIDATION

This section of Chapter 6 summarizes the layer properties and how those properties were determined or estimated for use in validating and calibrating the MEPDG distress transfer functions for Montana. However, there are many material properties required by the MEPDG that were not included in the materials test program for this project and were not measured within the LTPP program. As an example, these properties include Poisson's ratio, saturated hydraulic conductivity, soil-water characteristics curve, thermal coefficient of contraction for HMA mixtures, thermal conductivity, and heat capacity. For these properties, the default values recommended for use in the MEPDG software (Version 0.900) and used in the updated calibration work under NCHRP Project 1-40D (*NCHRP 2006*) were accepted and used within this study. The following sections summarize the methods to determine the volumetric, strength, and stiffness properties used to validate the MEPDG distress transfer function in Montana.

I-6.3.1 Unbound Materials and Soils

The gradation, in place moisture content and dry density, Atterberg limits, and maximum dry density and optimum moisture content of each unbound layer and the foundation were measured within this project or under the LTPP program. These properties were used directly in the MEPDG to predict the performance of each test section. The maximum dry density and optimum moisture content derived from the moisture-density curves for each base material were used as inputs to the MEPDG. It was assumed that these layers were compacted to 100 percent of the maximum dry unit weight.

The density and moisture content of the foundation or subgrade soils, however, were estimated based on the conditions that existed at the time of construction. In summary, the moisture contents and densities measured at the time of sampling were adjusted or backcasted so that the MEPDG would predict those properties or conditions with time.

The resilient modulus was tested within this project and LTPP. The resilient modulus was determined from both laboratory tests and backcalculated from deflection basin data. The modulus values input into the MEPDG represent laboratory derived values at the time of construction for predicting performance. The resilient modulus for each unbound layer and the foundation were determined using the procedure outlined in the FHWA Design Pamphlets (*Von Quintus and Killingsworth 1997a,b and 1998*). Figure I-28 is a comparison of the modulus values measured in the laboratory and those calculated from the deflection basin data for the same physical condition – same density and moisture content level. As shown, the backcalculated layer modulus values are greater than the values measured in the laboratory for most of the data.

The FHWA Design Pamphlet recommended factors to adjust the backcalculated values to an equivalent laboratory measured value (*Von Quintus and Killingsworth 1997a,b*). These adjustment factors were refined using the data collected in Montana. Table I-30 compares the adjustment factors recommended in the FHWA Design Pamphlet and the adjustment factors derived from the Montana data for the stronger and more coarse-grained soils than were used

in developing the original factors. In addition, the soils recovered from Montana during deflection basin testing were drier relative to the liquid and plastic limits of the soil than used in the FHWA study to estimate the conversion factors between laboratory and in place conditions. The drier condition and coarser materials could explain the difference in the adjustment factors (see Table I-30).

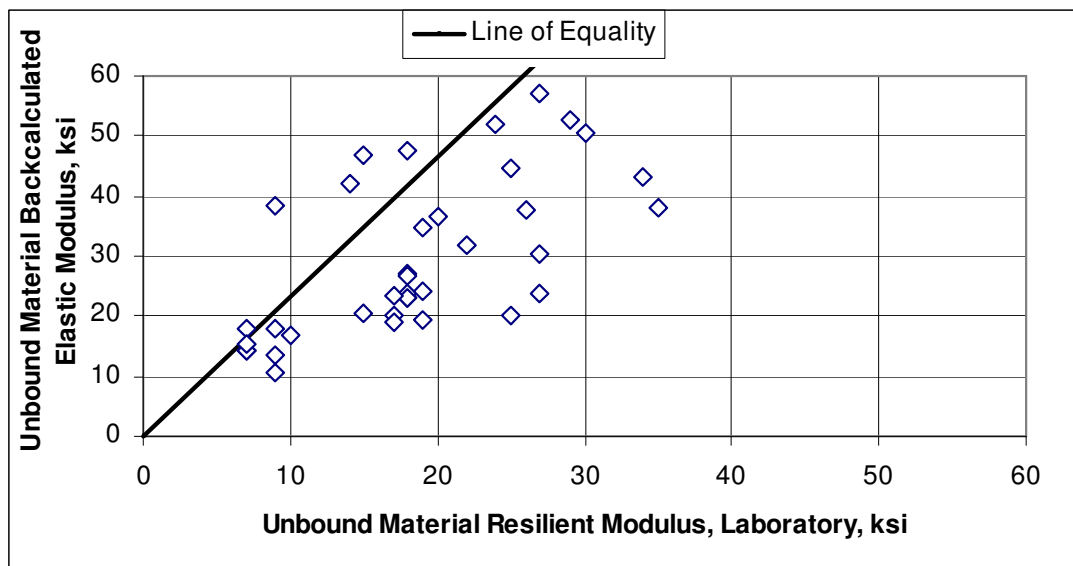


Figure I-28 Comparison of the laboratory measured resilient modulus values to those backcalculated from deflection basins.

Figure I-29 is a comparison of the modulus values measured in the laboratory and those backcalculated but adjusted to laboratory conditions using the factors recommended for use from the Montana data. Thus, all backcalculated layer modulus values from deflection basin data should be adjusted with the factors listed in Table I-30. Laboratory resilient modulus values estimated at the time of construction should be used as the inputs for layer modulus for all unbound layers.

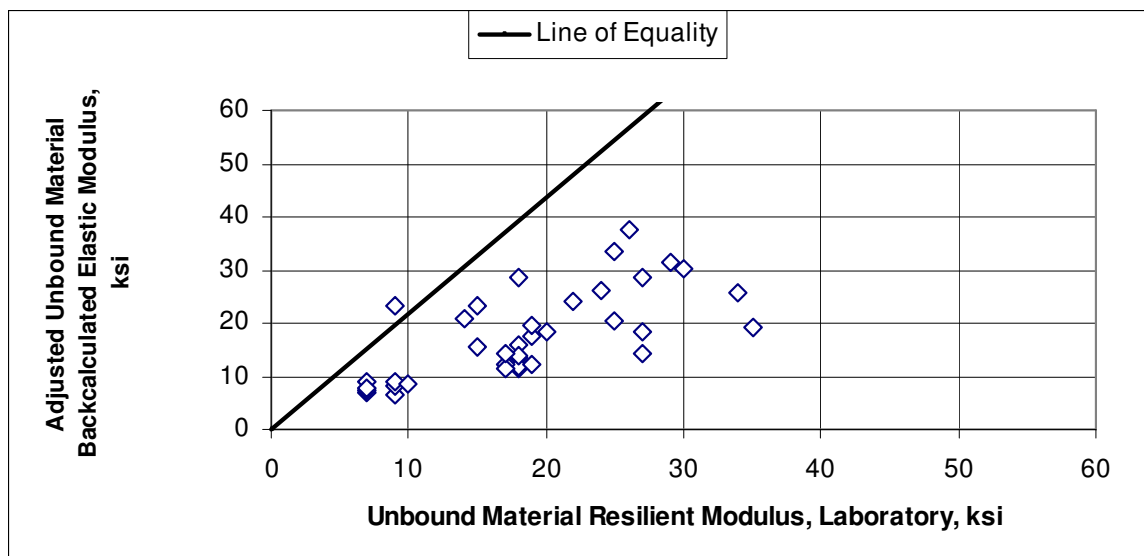


Figure I-29 Comparison of the laboratory measured resilient modulus values to the adjusted backcalculated modulus values from deflection basins using the Montana adjustment factors.

Table I-30 Summary of the Adjustment Factors Recommended for Use in Montana to Convert Backcalculated Layer Modulus Values to Laboratory Equivalent Resilient Modulus Values

Layer & Material Type	Layer Description	Adjustment Factor, C_{FWD} (M_R/E_{FWD})	
		FHWA Pamphlet	Montana Sites
Aggregate Base Layers	Granular base under a PCC surface	1.32	---
	Granular base under a CAM layer; semi-rigid pavement	---	0.75
	Granular base above a stabilized material (a Sandwich Section)	1.43	---
	Granular base under an HMA surface or base	0.62	0.60
Subgrade Soil/Foundation	Soil under a CAM layer; no granular base	---	1.00
	Soil under a semi-rigid pavement with a granular base/subbase	---	0.50
	Soil Under a Stabilized Subgrade	0.75	---
	Soil under a full-depth HMA pavement	0.52	---
	Soil under flexible pavement with a granular base/subbase	0.35	0.50
Cement Aggregate Base Layer	Cement stabilized or treated aggregate layers	---	1.50
HMA Mixtures	HMA surface and base layers; 41 °F	1.00	0.9
	HMA surface and base layers; 77 °F	0.36	0.6
	HMA surface and base layers; 104 °F	0.25	0.5

MDT has used the DCP for pavement evaluations and in estimating the resilient modulus of the unbound materials and soils. Equation I-22 can be used to calculate the resilient modulus from the penetration rate measured with the DCP.

$$M_R = 17.6 \left(\frac{292}{(DPI)^{1.12}} \right)^{0.64} (C_{DCP}) \quad (I-22)$$

Where:

- M_R = Resilient modulus of unbound material, MP_a .
- DPI = Penetration rate or index, mm/blow.
- C_{DCP} = Adjustment factor for converting the elastic modulus to a laboratory resilient modulus value.

DCP tests were performed at most of the non-LTPP test sections in Montana, but that data were unavailable for use in this study. Figure I-30, from NCHRP Project 10-65 (*Von Quintus et al. 2006 Active*), compares the unadjusted and adjusted elastic modulus estimated from the DCP to the resilient modulus values measured in the laboratory for a range of different aggregate base materials and subgrade soils. As shown, the elastic modulus values estimated from the DCP can be used to estimate the resilient modulus values, but require an adjustment to laboratory conditions. The adjustment factors were found to range from 0.34 to 1.90, and were found to be material dependent. Table I-31 lists the DCP adjustment factors for the typical materials and soils encountered in Montana. For soils and conditions not listed in Table I-31, engineering judgment should be used in converting the DCP values to laboratory equivalent resilient modulus values. These adjustment factors should be confirmed in future studies.

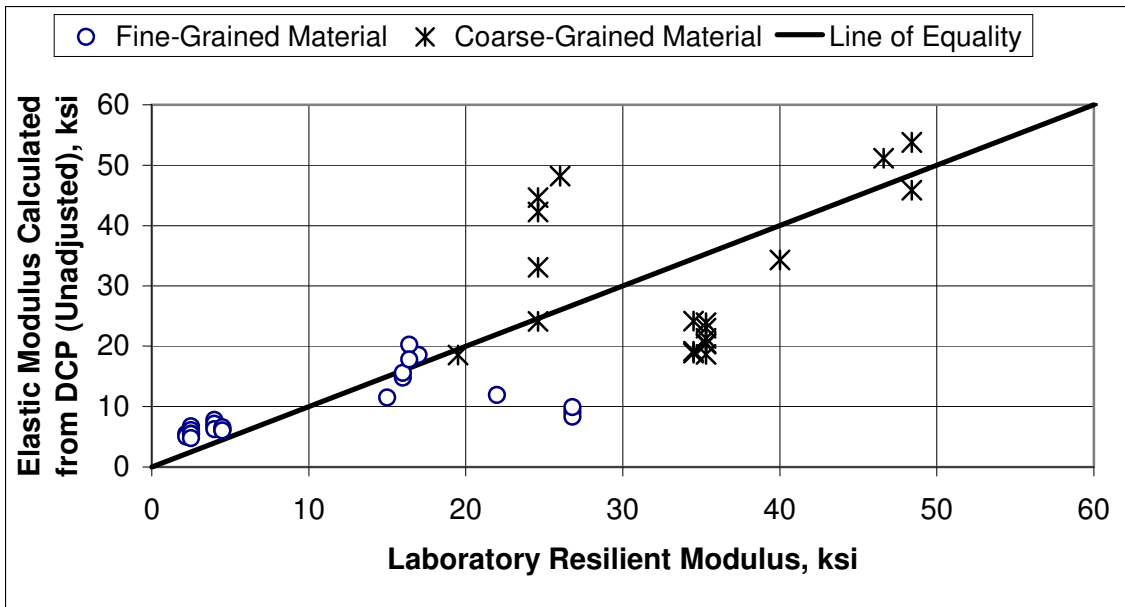


Figure I-30a Elastic modulus values not adjusted to laboratory conditions.

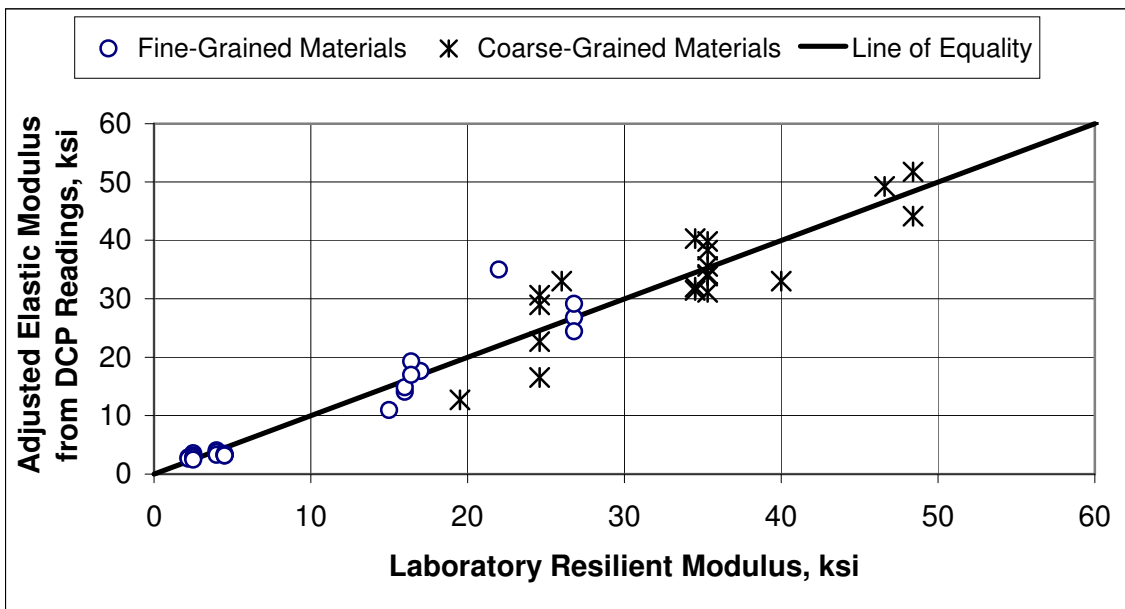


Figure I-30b Elastic modulus values adjusted to laboratory conditions.

Figure I-30 Comparison of the resilient modulus values measured in the laboratory to the in place values estimated with the DCP.

Table I-31 Summary of the DCP Adjustment Factors Recommended for Use in Montana to Convert the Elastic Layer Modulus Values to Laboratory Equivalent Modulus Values

Material/Soil Type		Condition	Adjustment Factor, C_{DCP}
Fine-Grained; Low Plasticity Soil	Clay-Silt	Above Optimum Water Content	1.90
	Soil-Sand Mix	At or Below Optimum Water Content	1.05
	Soil-Aggregate Mix with Large Aggregate	At or Below Optimum Water Content	0.60
Coarse-Grained Material	Soil-Aggregate Mix	At or Below Optimum Water Content	0.60
	Crushed Aggregate	At or Below Optimum Water Content	1.04

In summary, both the backcalculated elastic modulus values from deflection basins measured with the FWD and those estimated from the DCP are considered acceptable for use in estimating the design resilient modulus for use with the MEPDG when adjusted to laboratory conditions. The DCP will result in less error in comparison to the FWD deflection basins for estimating the resilient modulus of the unbound materials and soils, because the DCP values are independent of layer thickness variations (refer to Figures I-29 and I-30b).

I-6.3.2 Cement Aggregate Mixtures

The CAM properties needed for the MEPDG include the elastic modulus and flexural strength of the mixture. The flexural strength can be estimated from the compressive strengths measured in the laboratory. The modulus of the CAM layers was measured in the laboratory and backcalculated from the deflection basin data. Typically, the elastic modulus calculated from deflection basin measurements is assumed to be equal to the laboratory measured values.

Figure I-31 compares the laboratory measured values to those backcalculated from the deflection basins. As shown, there is a bias between the two values; the laboratory measured values are larger than those backcalculated from deflection basin data. It is expected that there are hairline cracks within the CAM layer, caused by freeze-thaw or shrinkage of the material. These cracks are eliminated from the specimens tested in the laboratory because those cracks will prevent the recovery of a testable core, but will reduce the elastic modulus calculated from deflection basin data.

In summary, the hypothesis is that the shrinkage cracks or freeze-thaw damage will reduce the in place modulus of the CAM layer. As a result the backcalculated values need to be adjusted to laboratory test conditions – test specimens without any cracks. Obviously, the adjustment factor should not be applied to newly placed CAM layers or CAM layers without any damage. Unfortunately, there is insufficient data to establish this time dependent adjustment factor. For the validation and calibration, this adjustment factor for CAM layers should only be applied for test sections that have been in place for more than five years.

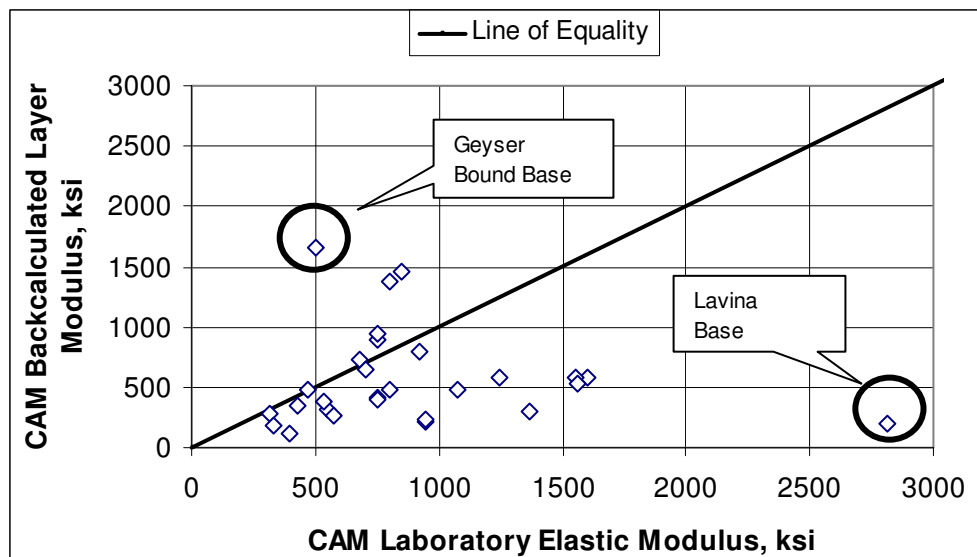


Figure I-31 Comparison of the laboratory measured and backcalculated elastic modulus of the CAM mixtures.

The adjustment factor was varied until the bias was eliminated from the data. The final adjustment factor is listed in Table I-30, and was applied to the backcalculated values. Figure I 32 compares the laboratory measured values to the adjusted backcalculated modulus values. With this adjustment factor of 1.5, the bias has been removed, but the variability is very large. The large variability is probably related to the fact that all CAM layers do not have hairline cracks or freeze-thaw damage. However, it is impossible to identify the areas with cracks without an extensive coring program.

I-6.3.3 HMA Mixtures

The HMA properties needed for the MEPDG include both volumetric and engineering properties at the time of construction. The volumetric properties include air voids, effective asphalt content by volume, gradation, density, and asphalt grade. The volumetric properties were measured on cores recovered from the HMA layers for both the non-LTPP and LTPP test sections. The air voids measured on the cores represent the value years after construction for many of the test sections. These air voids were backcasted to estimate that property after compaction. This back casting process was used during the original and updated calibration studies completed under NCHRP Projects 1-37 (*ARA 2004a,b,c,d*) and 1-40D (*NCHRP 2006*).

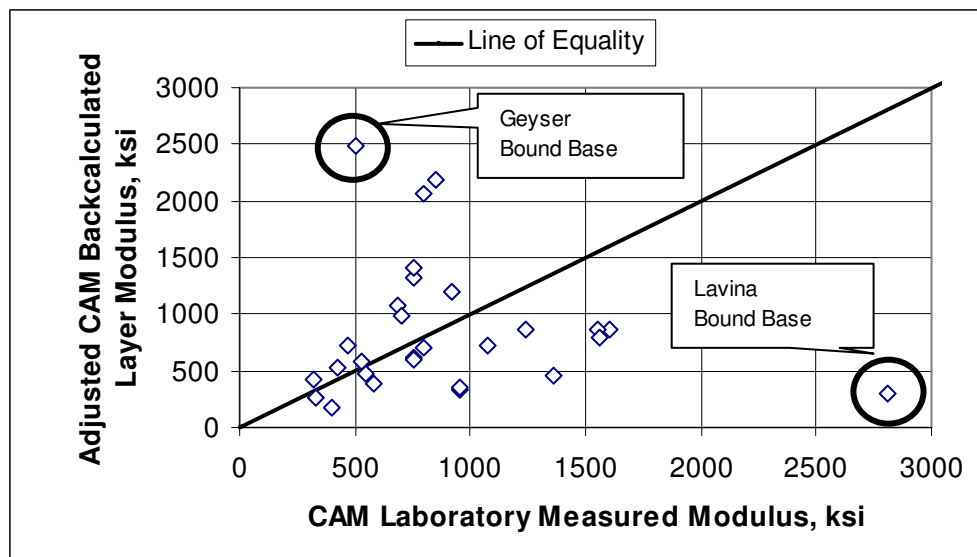


Figure I-32 Comparison of the laboratory measured and adjusted backcalculated elastic modulus of the CAM mixtures.

The engineering properties include the dynamic modulus, creep compliance, and tensile strength of the mixture. The tensile strength and creep compliance are estimated from the IDT HMA modulus values measured on the mixtures, as discussed in Section I-6.2.3 of this chapter. The modulus of the HMA layers was measured in the laboratory and backcalculated from the deflection basin data. Typically, the elastic modulus calculated from deflection basin measurements is assumed to be equal to the laboratory measured values. The FHWA Design Pamphlet, however, recommended adjustment factors for converting backcalculated modulus values to those measured in the laboratory.

Figure I-33 compares the laboratory measured values to those backcalculated from the deflection basins. As shown, there is a bias between the two values; the backcalculated values are larger than those measured in the laboratory at the same temperature. This observation suggests that similar adjustment factors to the FHWA Design Pamphlet should be used so that the laboratory measured and backcalculated values are similar. The adjustment factors were varied to eliminate the bias shown in Figure I-33. The final adjustment factors are listed in Table I-30 for HMA mixtures, and were applied to the backcalculated values.

Figure I-34 compares the laboratory measured values to the adjusted backcalculated modulus values. With this temperature dependent adjustment factors, the bias has been removed, and the variability is less. Thus, the backcalculated modulus values to estimate the damaged modulus for HMA mixtures should be reduced by the adjustment factors included in Table I-30 in defining the damaged modulus. With this adjustment the difference between the JILs and Dynatest FWDs that was identified in the early part of this chapter becomes less and insignificant in terms of predicting performance.

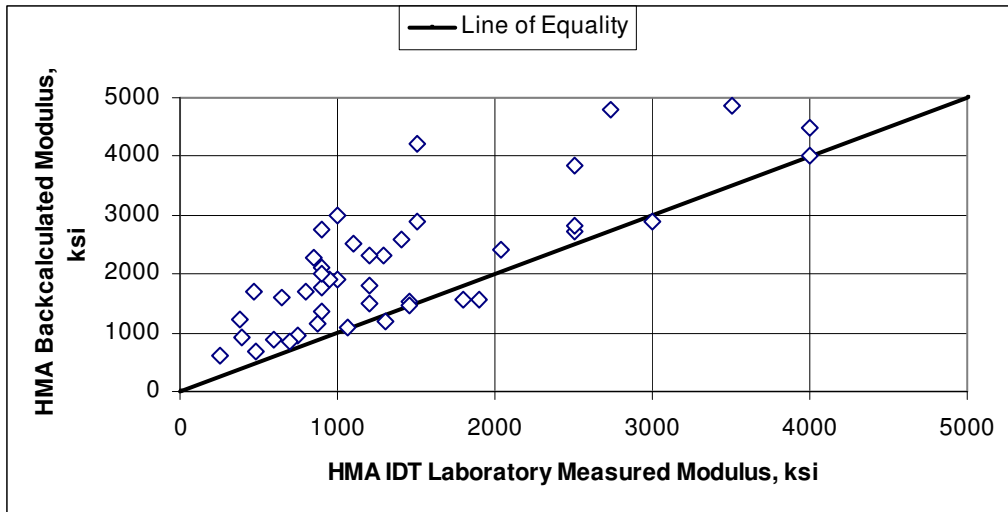


Figure I-33 Comparison of the laboratory measured and backcalculated elastic modulus of the HMA mixtures.

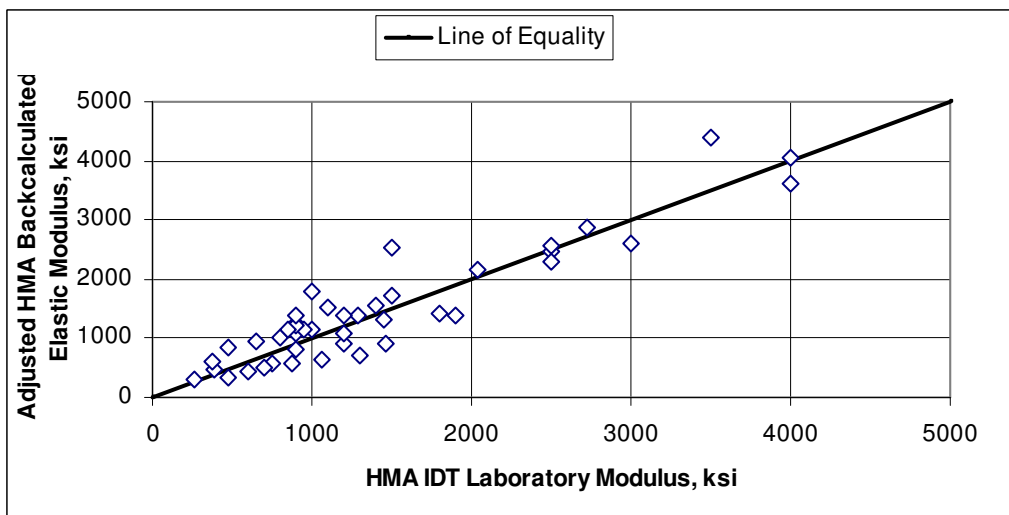


Figure I-34 Comparison of the laboratory measured and adjusted backcalculated elastic modulus of the HMA mixtures.

CHAPTER I-7 CALIBRATION REFINEMENT OF ME PAVEMENT DESIGN PROCEDURES FOR MONTANA

The distress transfer functions embedded in the MEPDG software for flexible pavements were calibrated using many test sections, primarily from the LTPP database. The original calibration of the distress transfer functions was completed under NCHRP Project 1-37A (*ARA 2004a,b,c,d*), and the global calibration coefficients were updated under NCHRP Project 1-40D (*NCHRP 2006*) using the same but an expanded data set; more distress time-history data within the LTPP program.

An independent set of sections or sites were used to verify the predictions from the distress prediction models for both new and rehabilitated flexible pavements under NCHRP Project 1-40B (*Von Quintus et al. 2005b*). The data used for this verification process were taken from the WestTrack experiment, the NCAT rutting and structural experiments (truck trafficking Rounds 1 and 2), the MnRoads first experimental sections, and additional SPS projects within the LTPP program that were not included in the original calibration study. For this independent data set, the MEPDG software was used as is – no changes to the global calibration factors, and the highest level of inputs was used. This set of runs represented the verification runs and became the baseline condition of the prediction models.

Results from these NCHRP 1-40B (*Von Quintus et al. 2005b*) verification runs were used to determine any bias and the standard error, and compare that error to the standard error reported from the original calibration process that was completed under NCHRP Project 1-37A (*ARA 2004a,b,c,d*). Bias was found for most of the distress transfer functions. As part of the NCHRP Project 1-40B (*Von Quintus et al. 2005b*), mixture adjustment factors were recommended for use for both the fatigue cracking and HMA rut depth prediction models. These HMA mixture adjustment factors are planned to be included within Version 1.0 of the MEPDG. Version 1.0 is expected to be released to industry in 2007.

The purpose of this chapter is to identify and discuss the approach used and issues related to the calibration refinement of the MEPDG distress transfer functions for flexible and semi-rigid pavements and HMA overlays constructed in Montana. This calibration refinement procedure used is similar to the procedure that was used within NCHRP Project 1-40B (*Von Quintus et al. 2005b*). Volume III provides a summary of the calibration procedure used within this study and the process that can be used in future updates (*Von Quintus and Moulthrop 2007b*). Volume III includes a User's Guide that MDT can use in future designs.

I-7.1 CALIBRATION APPROACH – STATISTICAL MODELING AND RATIONALITY ASSESSMENT

There are three basic steps in the modeling process, formulation, calibration, and validation. In model formulation, the identification of the most important variables is based on the theoretical consideration or empirical methods (e.g., correlation analyses and graphical comparisons). The degree of interaction between variables and model components is based on sensitivity analysis, while the structure of interaction must be based on theoretical concepts. This step was completed within NCHRP Project 1-37A (*ARA 2004a,b,c,d*) and will not be repeated within this

project. All assumptions made and used in formulating the MEPDG procedure were accepted for use in Montana. The global calibration coefficients included in Version 0.9 of the MEPDG were initially used to predict the distresses and smoothness of the Montana calibration refinement test sections to determine any bias of the prediction models. These runs were considered a part of the validation process, similar to the process used under NCHRP Projects 9-30 (*NCHRP 2003*) and 1-40B (*Von Quintus et al. 2005b*).

In the model validation process, an independent data set is used to predict the distress and compare those values with the observations. The comparison of the predictions and observations are checked for bias and the standard error calculated. If the bias is not larger than included for the original distress transfer functions and the standard error is statistically the same value, the models are assumed to be reliable. This process was used within NCHRP Project 1-40B (*Von Quintus et al. 2005b*).

Results from NCHRP Project 1-40B (*Von Quintus et al. 2005b*) found the models to have significant bias and larger standard errors. As noted above, a mixture adjustment procedure was recommended to eliminate the bias and reduce the standard error for a diverse range of HMA mixtures and pavement structures. However, no semi-rigid pavements and minimal test sections located in a climate similar to Montana's were included within that study. Thus, the NCHRP 1-40B (*Von Quintus et al. 2005b*) calibration process was used as the starting point for checking the bias and standard errors of the distress transfer functions for the climate, HMA mixtures, and pavement structures found in Montana.

In the model calibration-refinement process, agency specific calibration factors were determined for Montana, where applicable. A fitting process of the model constants were evaluated based on a goodness of fit criteria to decide on the best set of values for the coefficients of the model formulated. The methods of evaluation make use of either: 1) the *Analytical* process for models that suggest linear relationship, or 2) the use of *Numerical Optimization* for models that suggest non-linear relationship. The analytical calibration is based on least squares using multiple regression analysis, stepwise regression analysis, principal components analysis, and/or principal component regression analysis. The numerical optimization includes methods such as the steepest descent or pattern search. This calibration process was used within NCHRP Projects 1-37A (*ARA 2004a,b,c,d*) and 1-40D (*NCHRP 2006*). In summary, the analytical process was used for refining the distress transfer functions for use in Montana.

I-7.2 CALIBRATION DATABASE

The first step in any calibration process is to develop or create a database of information that can be used as inputs to the prediction models. The measurements of distress are included within this calibration database. Part IV of Volume II describes the database that was developed for calibrating the distress transfer functions for Montana (*Von Quintus and Moulthrop 2007a*). The following is a listing of the primary steps and activities completed in setting up the database and determining the inputs for the calibration refinement effort.

1. Verification of which LTPP data were missing from the LTPP database. All missing data were identified. As an example, few of the LTPP test sections have creep compliance and tensile strength data. For this missing data, other methods were developed to estimate these properties, as discussed under Chapter I-6.

2. The status of the additional LTPP sections outside of, but adjacent to Montana were verified. Each of the sections was checked for sufficient data so that only those sections with adequate data were utilized.
3. Structured Query Language (SQL) statements were developed for extracting the data required for model calibration from the LTPP IMS. These SQL statements were provided to MDT so that future calibration efforts utilizing updated LTPP data may be streamlined. The data extracted from the LTPP database included materials, traffic, general geometric, and structure data, as well as time-history distress data.
4. Montana climatic data and the climatic stations adjacent to Montana were utilized in the calibration effort. The sites used in the calibration process are included in the MEPDG software.
5. A review of all the LTPP traffic tables was completed and that data was extracted and included in the calibration database. Part III of Volume II provides a discussion and evaluation of the truck traffic data measured along Montana highways for many of the roadways not included within the LTPP program. Most of the sites reviewed could be reduced to four primary truck loading groups. These groups were defined and presented in Part III of Volume III. However, the initial average annual daily truck traffic was unavailable for many of the sites used in the local calibration effort. To determine this input parameter, all truck traffic data were used to back-cast that value, as well as the growth rate. When sufficient data were unavailable for a specific site, a linear growth rate was assumed using truck traffic data from sites located on similar roadways.
6. Volumetric and other mixture properties were unavailable for thin layers. Thin layers were combined with adjacent pavement layers of similar mixtures.
7. Water table depth can be seasonal in some areas in Montana. There was insufficient data and information to quantify the depth during seasonal variations. All depths were assumed to be 20 feet.

I-7.3 PRELIMINARY OBSERVATIONS FROM THE PERFORMANCE DATA

Prior to using the calibration database for refining the agency specific calibration factors, it is important to note some of the preliminary observations within the performance data for the calibration test sections. The following lists and briefly discusses some of the important observations made from the data.

- The average rutting measured on the test sections placed in Montana (0.29 in) is significantly less than the average rutting measured on the test sections in adjacent States (0.50 in). The amount of truck traffic is not significantly less for the test sections in Montana. This difference in rutting is believed to be more related to the HMA mixtures.

- The average length of transverse cracks measured on the Montana test sections (479 ft/mi) is significantly less than the average length measured on the test sections in the adjacent States (2026 ft/mi). The average age of the Montana test sections is less than those in adjacent States, but the length of transverse cracks for the older test sections in Montana is still less than those in the adjacent States. This difference in transverse cracking is believed to be more related to the HMA mixtures.
- The semi-rigid pavements built in Montana are performing significantly better than those placed in adjacent States. For example, none of the Montana semi-rigid pavements have exhibited fatigue cracking, while about 55 percent of the sections located in adjacent States have exhibited fatigue cracking. The amount of fatigue cracking, however, is relatively low with an average area of 1.3 percent. Similarly, about 25 percent of the Montana semi-rigid pavements have exhibited longitudinal cracking, while 100 percent of the sections in adjacent States have exhibited this type of cracking. The average length of longitudinal cracking per project in Montana is 965 ft/mi, while the average length in the adjacent States is 1,576 ft/mi.
- None of the Montana new construction test sections have exhibited any raveling, while over 30 percent of the test sections in the adjacent States have exhibited raveling.
- Another important observation is that many of the older test sections used within this calibration refinement study have different pavement preservation treatments placed early in the life of the pavement structure. Where pavement preservation treatments had been placed early in the pavement's life cycle, the amount of cracking (transverse, longitudinal, and alligator) was less than for the test sections where a pavement preservation treatment had not been placed. This policy or pavement preservation strategy will need to be considered in the calibration refinement process because it represents a confounding factor within the fracture data.
- The HMA overlays placed in Montana have relatively the same types and magnitudes of distress, as well as the same magnitudes of rutting in the test sections located in adjacent areas.
- The test sections with drainage layers have exhibited more fatigue (area or alligator and longitudinal) cracking, but have less transverse cracking. The average rut depth is about the same between the test sections with and without drainage layers.

The key observation from this overall comparison of distress is that the Montana sections for new construction are performing better with less distress. Although the test sections located in adjacent areas might be slightly older, this does not account for the difference in performance. This observation questions the applicability of using the results from test sections in adjacent States for determining agency specific calibration factors for both cracking and rutting. This systematic difference and the use of pavement preservation treatments of some test sections was carefully considered in using the performance data for test sections in adjacent States for developing agency specific calibration factors for use in Montana.

I-7.4 RUT DEPTH PREDICTION MODEL

As noted in Chapter I-3, the MEPDG calculates the rutting within the different layers – HMA layers, unbound aggregate base/subbase layers, and foundation or subgrade. The global calibration factors included in Version 0.9 of the MEPDG were initially used to predict the total rut depth of selected test sections in Montana.

In summary, the MEPDG significantly over predicted the total rut depth, primarily because higher levels of rutting were predicted in the unbound layers and embankment soils. Most of the thicker test sections located in Montana, however, have exhibited only minimal rutting below the HMA layers based on the field investigations conducted as part of this project. This suggests that the calibration coefficients of the rut depth prediction model need to be revised. Engineering judgment and previous experience from NCHRP Project 1-40B (*Von Quintus et al. 2005b*) and other studies was used to adjust the coefficients of the unbound materials and HMA rut depth distress transfer function.

I-7.4.1 Calibration Refinement Process for Predicted Rutting

The Montana sections with negligible rutting in the unbound layers were used to define the agency specific calibration factors for the unbound layers and embankment soils. Negligible rutting was defined as less than 0.05 inches.

As a starting point, the agency specific calibration factors were varied until the rutting in these layers equaled the negligible rut depth. These values were then used to predict the rutting in other test sections where that assumption could not be used. The following lists the agency-specific calibration factors for the unbound layers and embankment soils that were determined from an iterative process to eliminate any bias between the sections located in Montana only.

$$B_{s1} = 0.2 \text{ for coarse-grained soils}$$

$$B_{s2} = 0.2 \text{ for fine-grained soils}$$

The HMA mixture adjustment procedure recommended for use under NCHRP Project 1-40B (*Von Quintus et al. 2005b*) was used to revise the coefficients and exponents of the HMA rut depth transfer function in predicting the HMA rut depth. This procedure is summarized below and provided in detail in Volume III.

1. Determine the gradation index for each HMA mixture. The gradation index is defined as the absolute difference between the actual gradation and the maximum density line (FHWA 0.45 power gradation chart) using sieve sizes 3/8, #4, #8, #16, #30, and #50. The gradation index is used to refine the adjustment factors for rutting predictions (Equation I-23):

$$GI = \sum_{i=3/8}^{#50} |P_i - P_{i(0.45)}| \quad (I-23)$$

Where:

- GI = Gradation Index
- P_i = Percent passing sieve i , %
- $P_{i(0.45)}$ = Percent passing sieve i for the FHWA 0.45 maximum density line.

2. Determine the design air voids for each HMA mixture. For all HMA mixtures included in the validation process, a design air void level of 4 percent was assumed for all dense-graded mixtures.
3. Determine the saturation or optimum effective asphalt content by volume and weight for each HMA mixture. The saturation asphalt content is the value at which the density starts to significantly decrease and is dependent on the surface area and other surface characteristics of the aggregate. This mix property is unavailable for the HMA mixtures included within the validation study. Thus, the saturation asphalt content was set equal to the design asphalt content.
4. Make an adjustment to the k_{r1} parameter based on volumetric properties and gradation for each HMA layer by using Equation I-24.

$$k_{r1} = \text{Log} \left[1.5093 \times 10^{-3} (K_{r1}) (V_a)^{0.5213} (V_{be})^{1.0057} \right] - 3.4488 \quad (I-24)$$

Where:

- k_{r1} = Agency-specific calibration factor.
- K_{r1} = Intercept coefficient, refer to Figure I-35.
- V_a = Air voids after construction, %.
- V_{be} = Effective asphalt content by volume at construction (the in place value), %.

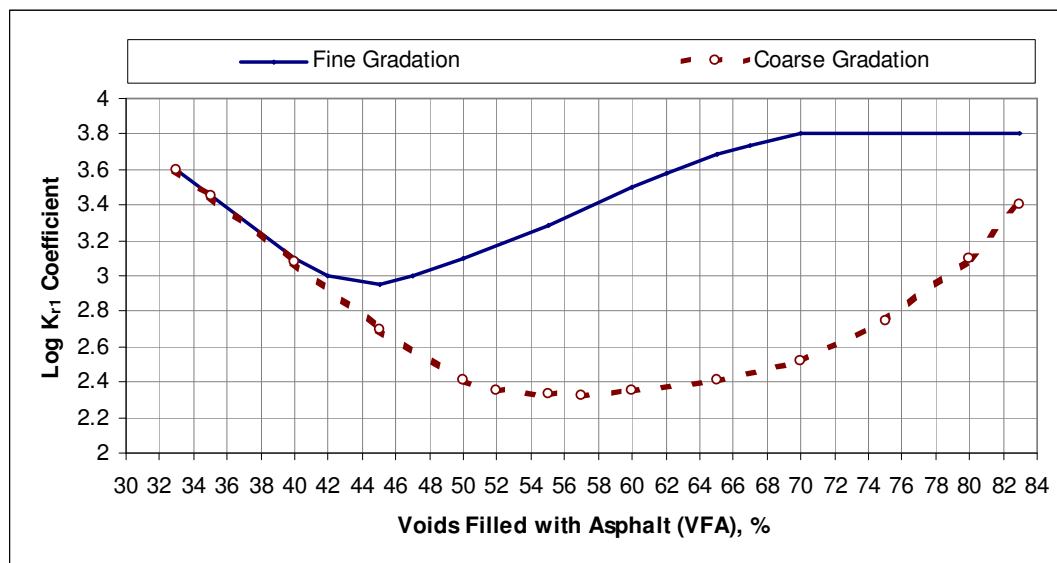


Figure I-35 Estimate of the K_{r1} intercept parameter from Voids Filled with Asphalt (VFA) and gradation.

NOTE: For maximum nominal size aggregates greater than 19mm, the #4 sieve size constitutes the break between the course and fine aggregate. For maximum size aggregates less than 19mm, the #8 sieve is the break point.

5. Make an adjustment to the k_{r2} parameter based on volumetric properties and gradation for each HMA layer by using Equation I-25.

$$k_{r2} = 1.5606 \left(\frac{V_a}{V_{a(\text{design})}} \right)^{0.25} \left(\frac{P_b}{P_{b(\text{opt})}} \right)^{1.25} (F_{\text{Index}})(C_{\text{Index}}) \quad (I-25)$$

Where:

- k_{r2} = Intercept coefficient.
 V_a = Air voids after construction, %.
 $V_{a(\text{design})}$ = Design air voids used to select the design asphalt content, %.
 P_b = Asphalt content by weight at construction (the in place value), %.
 $P_{b(\text{opt})}$ = Saturation or optimum asphalt content by weight, %.
 F_{Index} = Fine aggregate angularity index, refer to Table I-32.
 C_{Index} = Coarse aggregate angularity index, refer to Table I-33.

Table I-32 Fine Aggregate Angularity Index Used to Adjust Permanent Deformation Parameters, F_{Index}

Gradation – External to restricted zone	Fine Aggregate Angularity	
	< 45	> 45
Dense Grading – External to Restricted Zone	1.00	0.90
Dense Grading – Through Restricted Zone	1.05	1.0

Table I-33 Coarse Aggregate Angularity Index Used to Adjust Permanent Deformation Parameters, C_{Index}

Type of Gradation	Percent Crushed Material with Two Faces				
	0	25	50	75	100
Well Graded	1.1	1.05	1.0	1.0	0.9
Gap Graded	1.2	1.1	1.05	1.0	0.9

6. Make an adjustment to the k_{r3} parameter based on volumetric properties and gradation for each HMA layer by using Equation I-26.

$$k_{r3} = 0.4791(K_{r3}) \left(\frac{P_b}{P_{b(\text{opt})}} \right) \quad (I-26)$$

Where:

- K_{r3} = Slope coefficient; for fine-graded mixtures and coarse-graded aggregate blends with a $GI < 20$, $k_{r3} = 0.40$; for coarse-graded mixtures with a GI between 20 and 40, $k_{r3} = 0.70$; and for coarse-graded aggregate blends with a $GI > 40$, $k_{r3} = 0.80$.
 P_b = Asphalt content by weight at construction (in-place value), %.
 $P_{b(\text{opt})}$ = Saturation or optimum asphalt content by weight, %.

I-7.4.2 Comparison of Predicted to Measured Total Rut Depths

Figure I-36 compares the predicted to measured rut depths for all test sections located in Montana, while Figure I-37 compares the predicted to measured rut depth for those test sections located in adjacent States and Canadian provinces. As shown, the total rut depths predicted for the semi-rigid pavements, deep strength HMA pavements, conventional flexible pavements, and HMA overlays in comparison to the measured rut depths fall along the line of equality for all Montana sections. Figure I-38 shows the residual error for all sections as a function of the predicted total rut depths and suggests that the rut depth transfer functions have no bias.

An important observation in the data is that the Montana sections consistently have smaller rut depths, which was predicted by the MEPDG rut depth transfer functions. One potential reason for the lower rut depths in Montana is that these sections were found to have lower air voids at the time of construction. It is believed that the agency specific calibration coefficients determined for Montana are reasonable for both the HMA and unbound layers. The mixture adjustment procedure based on the volumetric properties seems to account for this bias between test sections built in Montana, as compared to those built in adjacent areas.

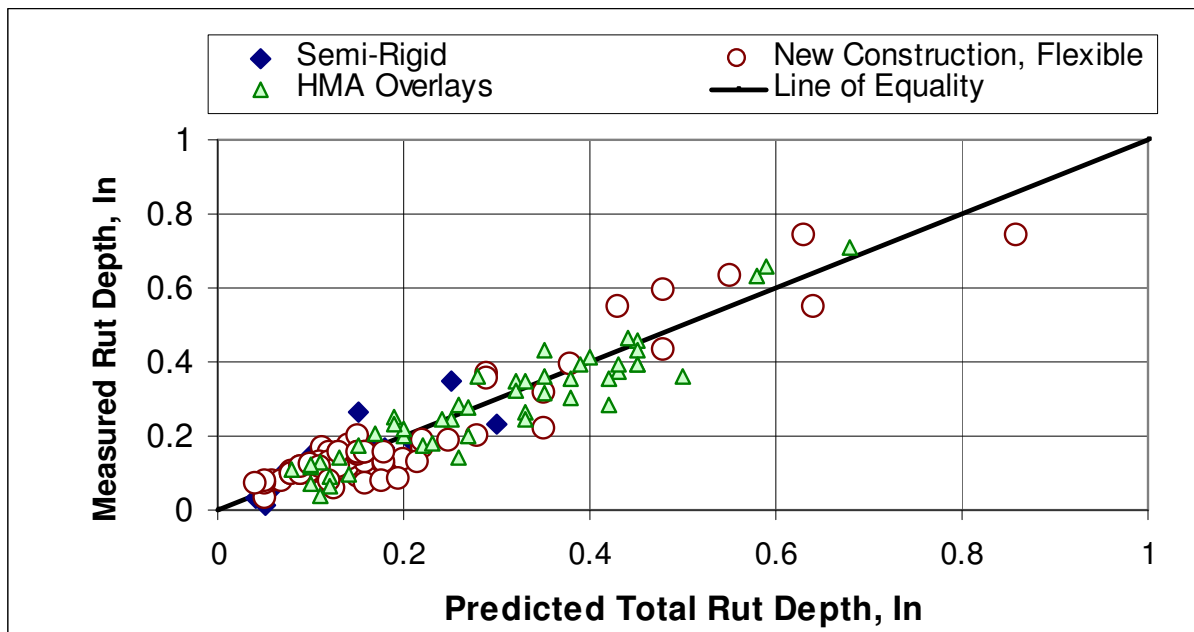


Figure I-36 Comparison of the predicted and measured total rut depths for the sites located in Montana.

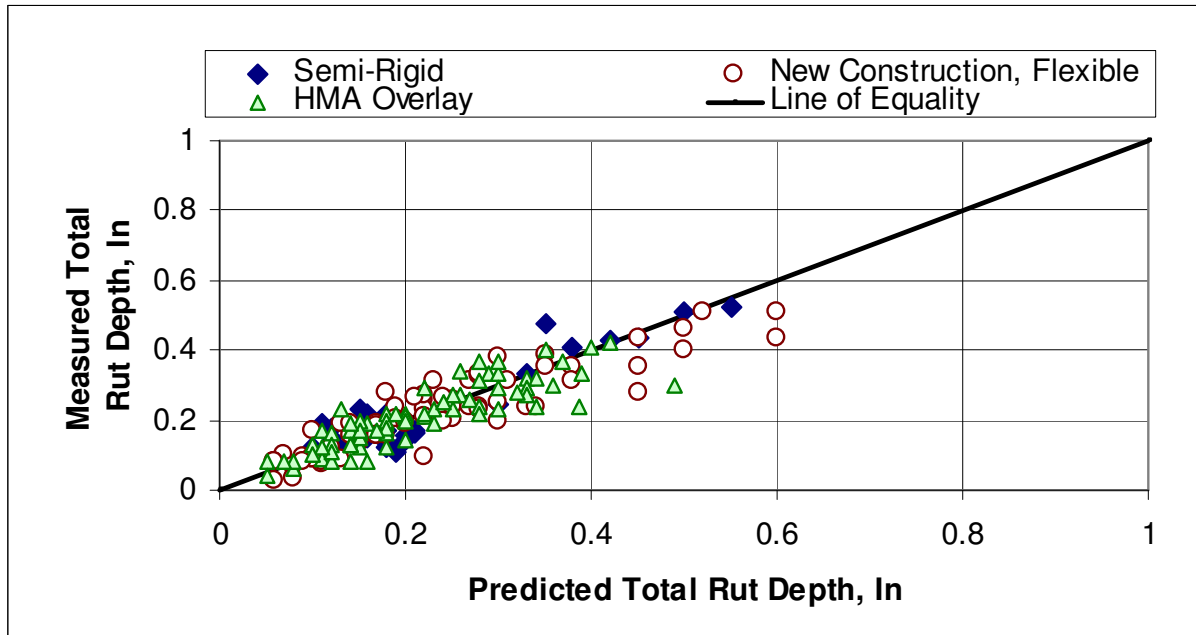


Figure I-37 Comparison of the predicted and measured total rut depths for the sites located in States and Canadian provinces adjacent to Montana.

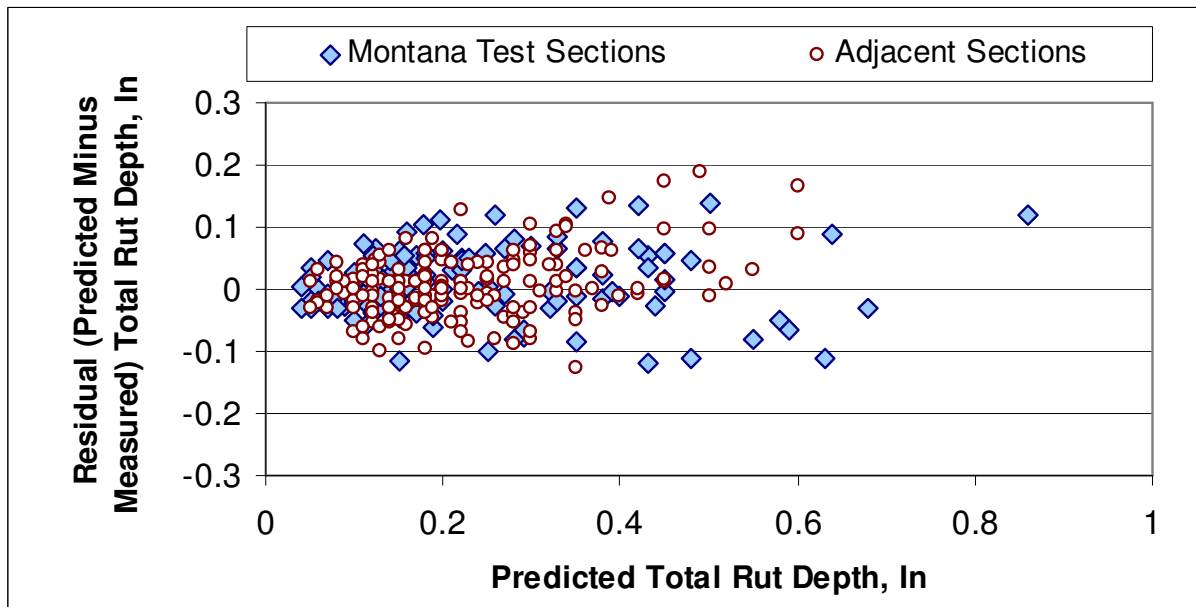


Figure I-38 Residual error (predicted minus measured total rut depths) as a function of the predicted rut depth for all sites combined.

Table I-34 lists the bias and other statistical information on the rut depth distress transfer function for the Montana sites and all sites combined. The Montana agency specific calibration coefficients for the rut depth transfer functions determined within this study are believed to be adequate and are recommended for use in design and forensic studies.

Table I-34 Summary of the Bias and Standard Error for the Rutting Prediction Model Using the Montana Calibration Factors for Unbound and HMA Rutting

Type of Pavement		No. of Points	Bias, in.	Standard Error, in.	RMSE, in.	S _e /S _y
Montana Sites	New Construction; Flexible Pavements	67	0.0069	0.0536	0.1098	0.342
	Semi-Rigid Pavements	18	-0.0103	0.0457	0.0789	0.662
	HMA Overlays of Flexible Pavements	50	0.0126	0.0520	0.0937	0.359
All Sites Combined	New Construction; Flexible Pavements	72	0.0108	0.0539	0.0988	0.418
	Semi-Rigid Pavements	32	-0.0023	0.0472	0.0833	0.384
	HMA Overlays of All Type Pavements	75	0.0058	0.0494	0.0941	0.4927

I-7.5 LOAD RELATED CRACKING, ALLIGATOR CRACKING & LONGITUDINAL CRACKING IN WHEEL PATHS

The MEPDG software predicts two types of load related cracking – bottom-up cracking defined as area fatigue cracking, and top-down cracking defined as longitudinal cracking in the wheel paths. The global calibration factors included in Version 0.9 of the MEPDG (*NCHRP 2006*) were initially used to predict both types of load related cracking for selected test sections in Montana. The following summarizes the findings from the use of the global calibration factors.

- The MEPDG over predicted the area or alligator cracks (bottom-up cracking) of new construction or in place pulverization of flexible pavements. Most of the test sections located in Montana have exhibited minimal alligator cracking along the LTPP test sections. For the non-LTPP test sections only one had appreciable alligator cracking.

Conversely, the MEPDG under predicted the area of alligator cracking for the HMA overlays of flexible pavements. These findings suggest that the global load related calibration coefficients for the area or alligator cracking prediction model need to be revised and could be pavement type dependent; HMA overlays versus new construction or reconstruction. However, changing the interface friction value increased the amount of fatigue cracks and significantly reduced the amount of bias. This issue will be discussed in greater detail in the following section of this chapter.

- The MEPDG over predicted the area of alligator cracks (bottom-up cracking) of new construction and HMA overlays for those test sections where some type of pavement preservation technique had been used. The C_2 coefficient of the fatigue cracking transfer function was adjusted to match the observed area of cracking. The magnitude of

the adjustment seemed to be related to the VFA, but there was insufficient data to make a precise determination of its magnitude.

- For the longitudinal cracking within wheel path prediction model, the residual errors are large, but no significant bias was found. A similar finding was reported within the original model calibration and from NCHRP Projects 9-30 (*NCHRP 2003*) and 1-40B (*Von Quintus et al. 2005b*).
- For the semi-rigid fatigue cracking transfer function, the MEPDG did not predict any cracking for the Montana sections, and none exhibited any fatigue cracking. This transfer function, however, was never calibrated under NCHRP Projects 1-37A (*ARA 2004a,b,c,d*) and 1-40D (*NCHRP 2006*). As a result, the MEPDG was used to predict the fatigue cracking of the semi-rigid pavements located in adjacent States, because over 50 percent of these sections have exhibited some minor levels of fatigue cracking. It predicted no fatigue cracking for these semi-rigid pavements, but a problem exists with the semi-rigid input module or screen. Any values entered into the program for the elastic modulus and the modulus of rupture of the CAM material always divert back to the default values that appear in the screen or window for this material. The default values are representative of a good quality lean Portland Cement Concrete (PCC) material. This input problem and calibration issue will be discussed in more detail within the next section of this chapter.

I-7.5.1 Calibration Refinement Process for Load Related Fatigue Cracking

The MEPDG assumes that the alligator and longitudinal cracking within the wheel paths are a result of the same cracking mechanism. The fatigue cracking mechanism for the semi-rigid pavements, however, is different and will be discussed separately under this section.

I-7.5.1.1 Fatigue Cracking of Conventional, Deep Strength, and Full-Depth Pavements, In Place Pulverization of Flexible Pavements, and HMA Overlays

The new construction and HMA overlay test sections with varying amounts of alligator cracking were used to determine Montana's agency specific calibration factors for calculating the number of allowable load applications for calculating incremental damage. These agency specific calibration factors were then assumed to be correct for the longitudinal cracking prediction model.

The mixture adjustment procedure recommended for use under NCHRP Project 1-40B (*Von Quintus et al. 2005b*) was used as a starting point to revise the coefficients and exponents of the load related fracture transfer functions. This procedure is summarized below and provided in detail in Volume III. Engineering judgment and previous experience from NCHRP Project 1-40B (*Von Quintus et al. 2005b*) and other studies was used to adjust the coefficient of the alligator cracking distress transfer functions.

1. Calculate the Voids Filled with Asphalt (VFA) for each dense graded HMA layer.
2. Determine the k_{f1} parameter based on VFA for the lower HMA layers, refer to Figure I-39. When multiple HMA layers have been placed, a weighed average value based on thickness is determined for the lower HMA layers. When more than two layers are placed, the k_{f1} and k_{f2} parameters should be calculated for the bottom two layers. This value is used to replace the global calibration factor included in the MEPDG software.

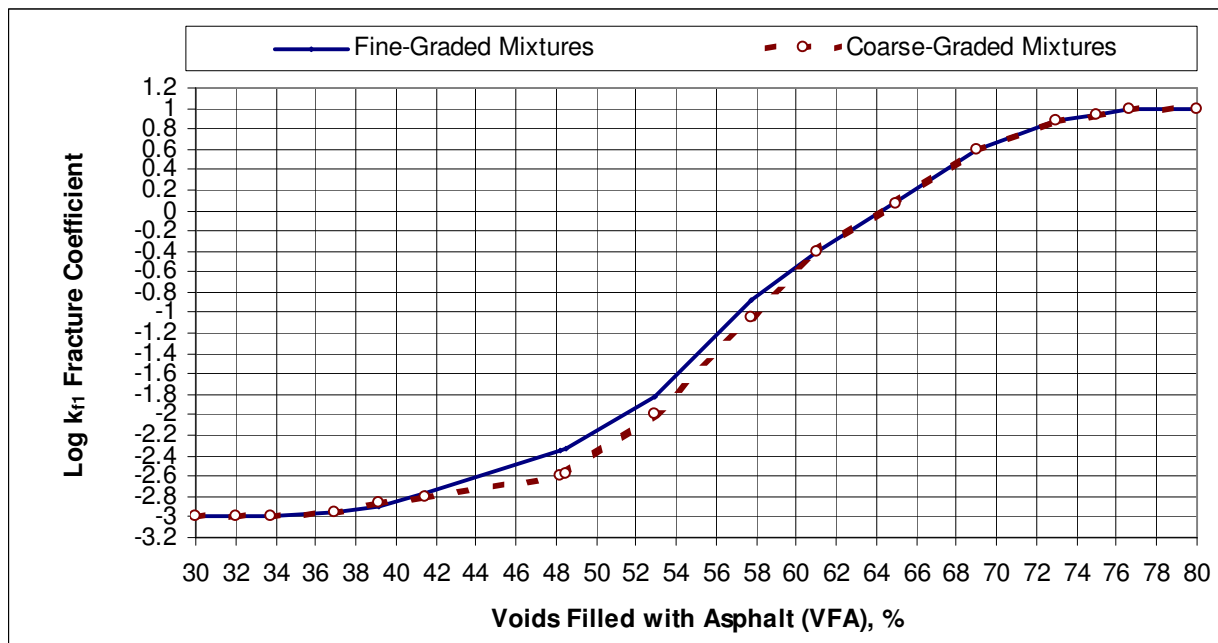


Figure I-39 Determination of the k_{f1} parameter from the VFA of the lower dense graded HMA layer.

3. Determine the k_{f3} parameter from the k_{f1} parameter for the lower HMA layer, refer to Figure I-40. This value is used to replace the global calibration factor included in the MEPDG software.
4. No adjustments are made to the k_{f3} parameter.
5. Determine the C_2 coefficient in the distress transfer function converting fatigue damage to area cracking based on VFA for the lower HMA layer, as shown in Figure I-41. This value is used to replace the global calibration factor included in the MEPDG software for flexible pavements and HMA overlays placed with and without the use of aggressive pavement preservation programs. For transferring the fatigue damage index into the length of longitudinal cracks, the C_2 parameter for top-down cracking was varied, but did not improve on the accuracy of the predictions. Thus, the global values were left unchanged.

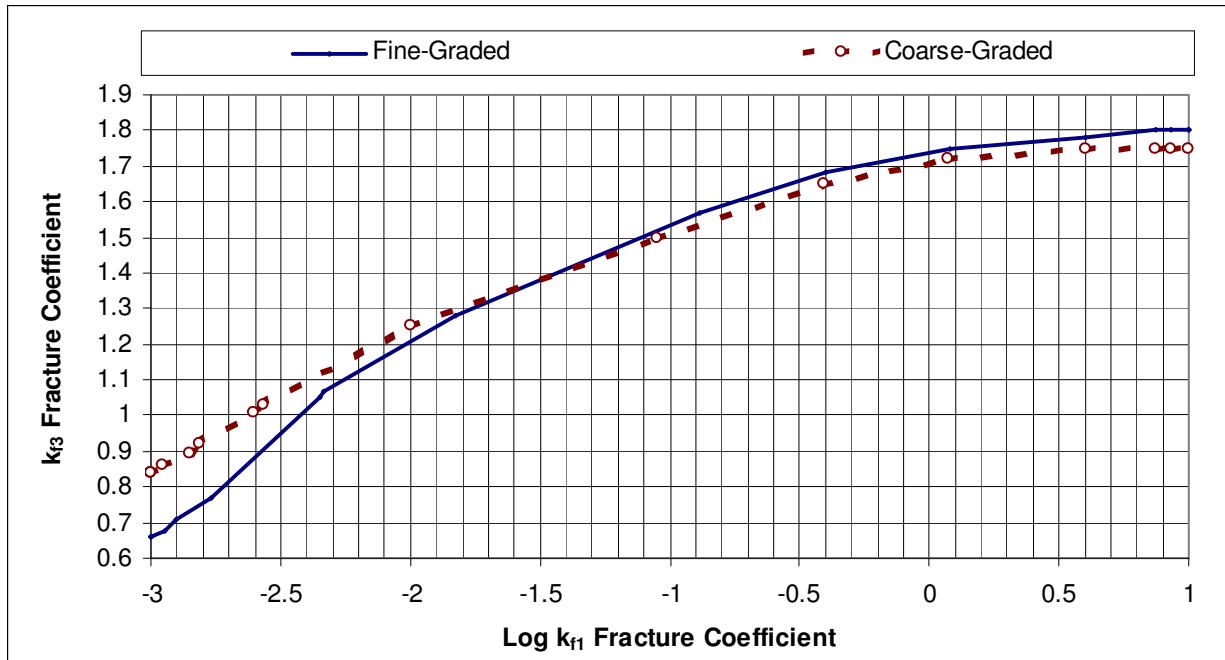


Figure I-40 Determination of the k_{f3} parameter from the k_{f1} parameter of the lower dense graded HMA layer.

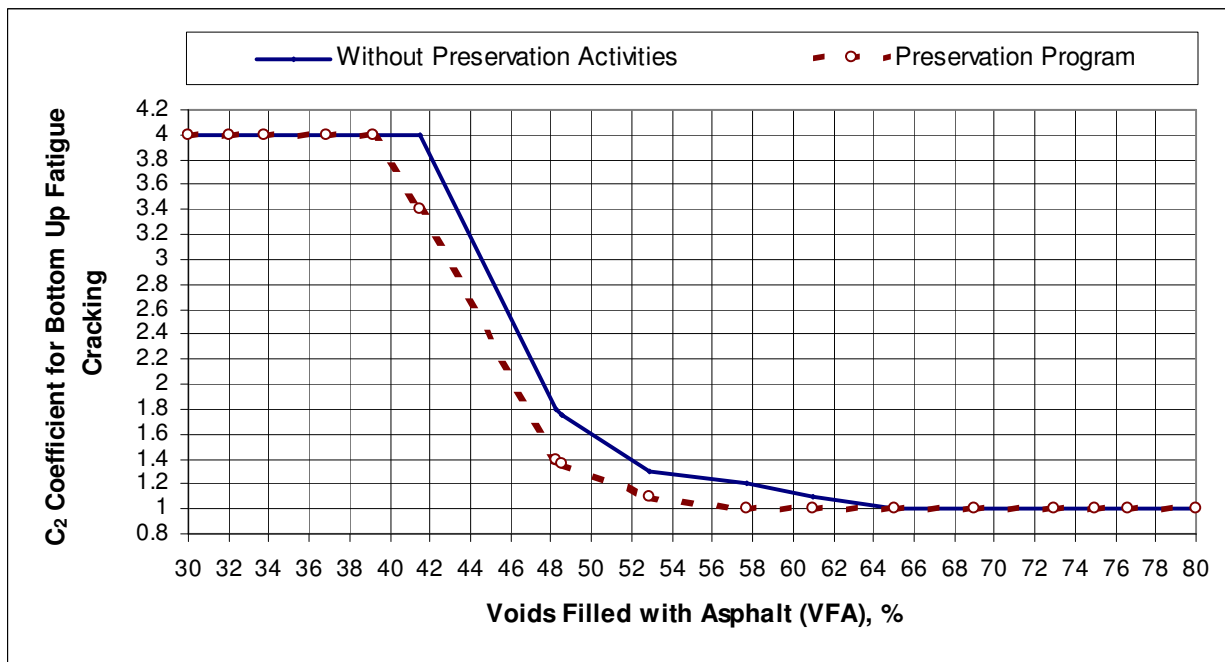


Figure I-41 Determination of the C_2 parameter from the VFA of the lower dense graded HMA layers.

6. If an asphalt treated open-graded drainage or Permeable Asphalt Treated Base (PATB) layer is present in the pavement structure, this layer should be treated as a good quality crushed stone base material. The high air voids in this layer will result in premature or accelerated fatigue cracking, even for thick HMA layers, which is inconsistent with previous experience and those test sections with PATB layers included in the LTPP SPS-1 experiment.

I-7.5.1.2 Fatigue Cracking of Semi-Rigid Pavements

As noted above, any values entered into the MEPDG software for the elastic modulus and modulus of rupture of the CAM material always divert back to the default values that appear in the screen or window for this material. These default values are representative of a good quality lean PCC material and result in no fatigue cracking predicted for any of the semi-rigid pavements used in the calibration refinement study for Montana.

As a result, the agency specific calibration factors for fatigue cracking of semi-rigid pavements (B_{c1} and B_{c2}) were varied until the amount of fatigue cracks predicted by the program eliminated the bias between the predicted and measured values. The following lists the agency specific calibration factors for the unbound layers and embankment soils that were determined from an iterative process to eliminate any bias between the measured and predicted values.

For High Strength CAM Mixtures (intact cores recovered with cement content greater than 6 percent; compressive strength generally greater than 1,000 psi):

$$B_{c1} = 0.85$$

$$B_{c2} = 1.10$$

For Moderate Strength CAM Mixtures (intact cores recovered with cement contents greater than 4 percent but less than 6 percent; compressive strength generally greater than 300 psi but less than 1,000 psi):

$$B_{c1} = 0.75$$

$$B_{c2} = 1.10$$

For Low Strength CAM Mixtures (intact cores cannot be recovered with cement content generally less than 4 percent; compressive strength generally less than 300 psi):

$$B_{c1} = 0.65$$

$$B_{c2} = 1.10$$

None of the semi-rigid pavement included within this calibration refinement study for Montana, however, exhibited fatigue cracking greater than 5 percent. As a result this prediction model is not considered robust and should be used with caution. This distress transfer function will need to be updated as these semi-rigid pavements begin to exhibit greater levels (areas) of fatigue cracking.

I-7.5.2 Comparison of Predicted to Measured Load Related Cracking

The MEPDG was used to predict the area of alligator cracking for all sections using the agency specific calibration factors discussed above. The predicted and measured amount of alligator cracks were found to compare reasonably well, with the exception of the alligator cracking

exhibited on the SPS-5 experiment. The MEPDG still significantly under predicted the area cracking. Based on a review of the construction reports for that project, there was some concern over the bond between the existing HMA surface and the HMA overlay. As a result, the interface friction between the overlay and existing surface was reduced to a value of 0, and the sections rerun. This change increased the area of alligator cracking and significantly reduced the bias.

Figure I-42 compares the predicted to measured alligator cracking for all test sections included in the study, with the exception of the semi-rigid pavements. As shown, the alligator cracking predicted for the full-depth, deep strength HMA, and conventional flexible pavements, and HMA overlays in comparison to the measured alligator cracks fall along the line of equality. Figure I-43 shows the residual error for all sections as a function of the predicted total rut depths and suggests that the fatigue cracking transfer function has no bias.

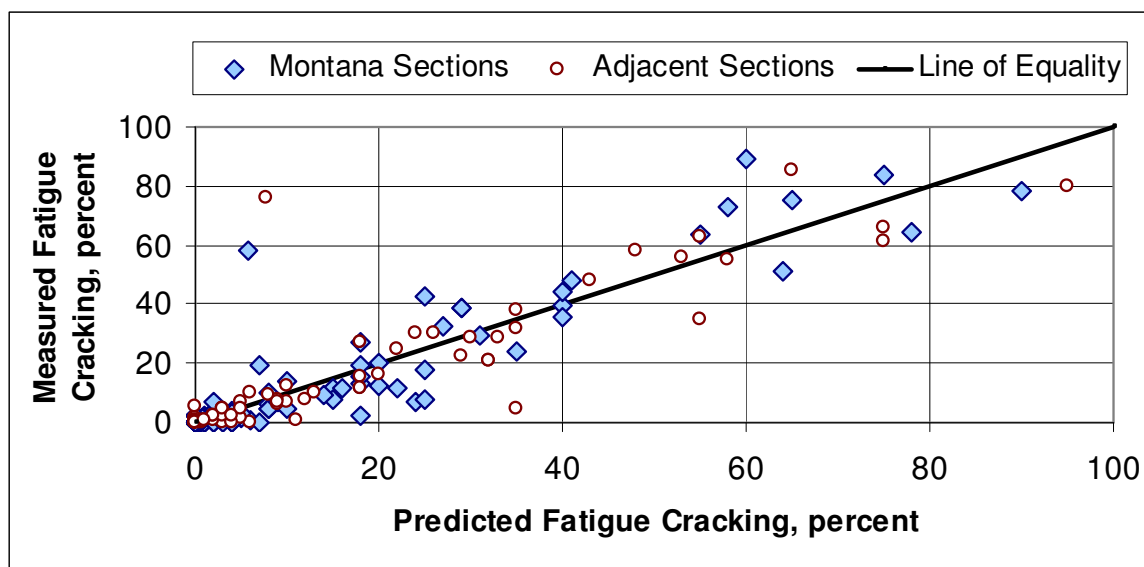


Figure I-42 Comparison of the predicted and measured alligator cracking for the sites, with the exception of the semi-rigid pavements.

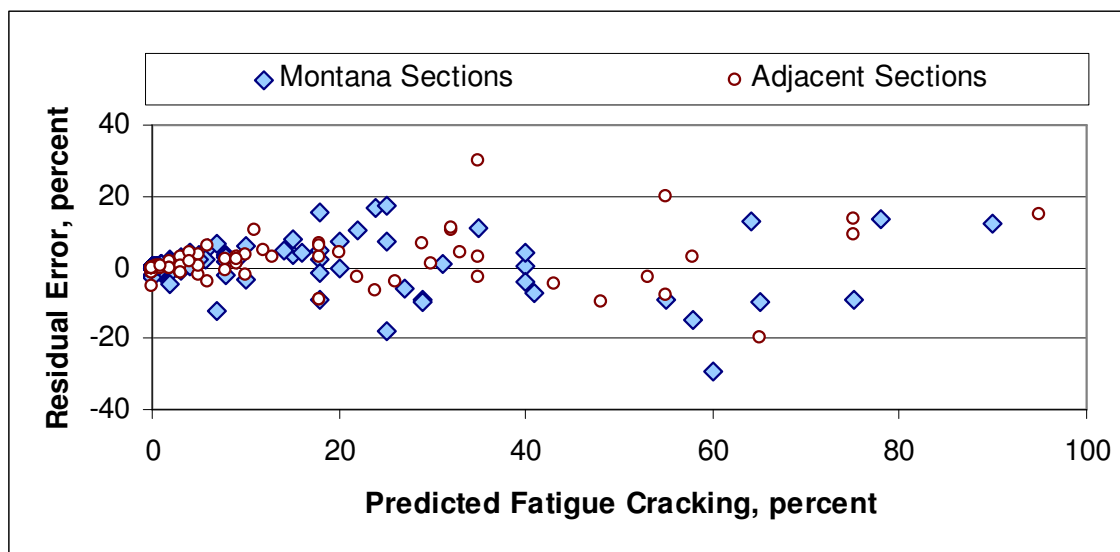


Figure I-43 Residual error (predicted minus measured total alligator cracking) as a function of the predicted alligator cracking with the exception of the semi-rigid pavements.

Predictions of top-down cracking were made using the global calibration factors included in the MEPDG, as derived from the NCHRP Project 1-40D (*NCHRP 2006*) updated calibration study. Figure I-44 shows a comparison of the predicted and measured longitudinal cracking. The difference between the measured and predicted values is significant, but could not be related to any site condition factor, or design feature of the pavements. Thus, the distress transfer function for longitudinal cracking within the wheel paths is not suggested for use in Montana in its present condition. If used, the original global calibration factors should be used in design.

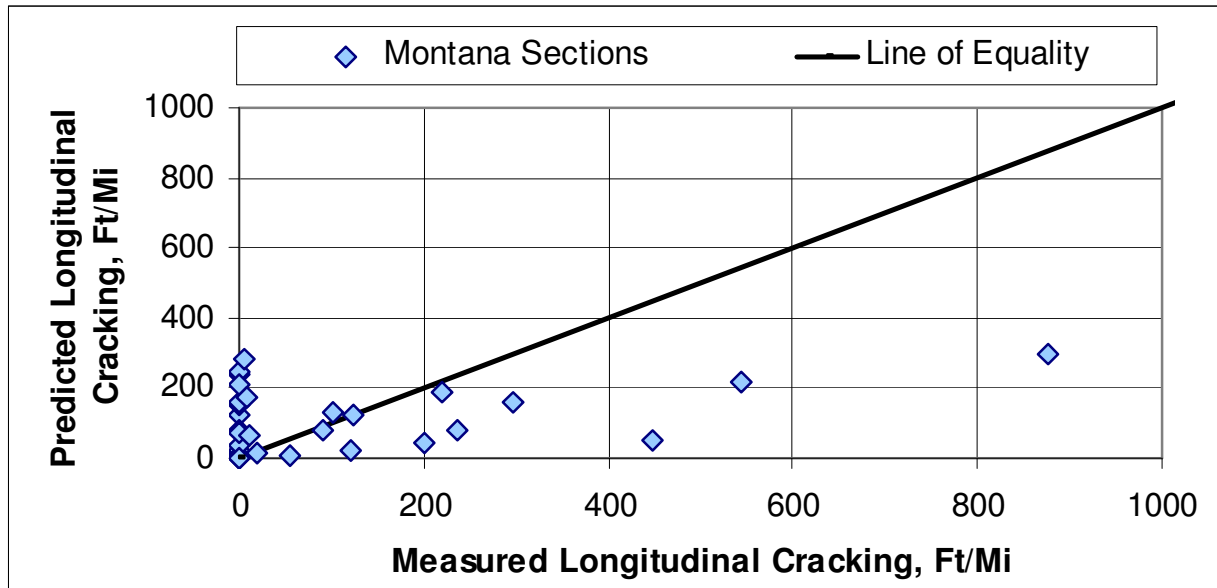


Figure I-44 Comparison of the predicted and measured longitudinal cracking for the Montana sites, excluding the semi-rigid pavements.

Figure I-45 compares the predicted to measured alligator cracking for the semi-rigid pavements using the agency specific calibration factors recommended for use in Montana. Figure I-46 shows the residual error for all semi-rigid pavement sections as a function of the predicted alligator cracking and suggests that the fatigue cracking transfer function has minimal bias, but a large error. The amount of alligator cracking is considered too small to complete a robust calibration and validation of this distress transfer function. This prediction model should be used with caution in future design studies until it can be verified with greater amounts of alligator cracking on a larger number of test sections, especially in Montana. The Montana semi-rigid pavements have exhibited no alligator cracking. Thus, it cannot be construed that this prediction model has been calibrated to the conditions and materials encountered in Montana.

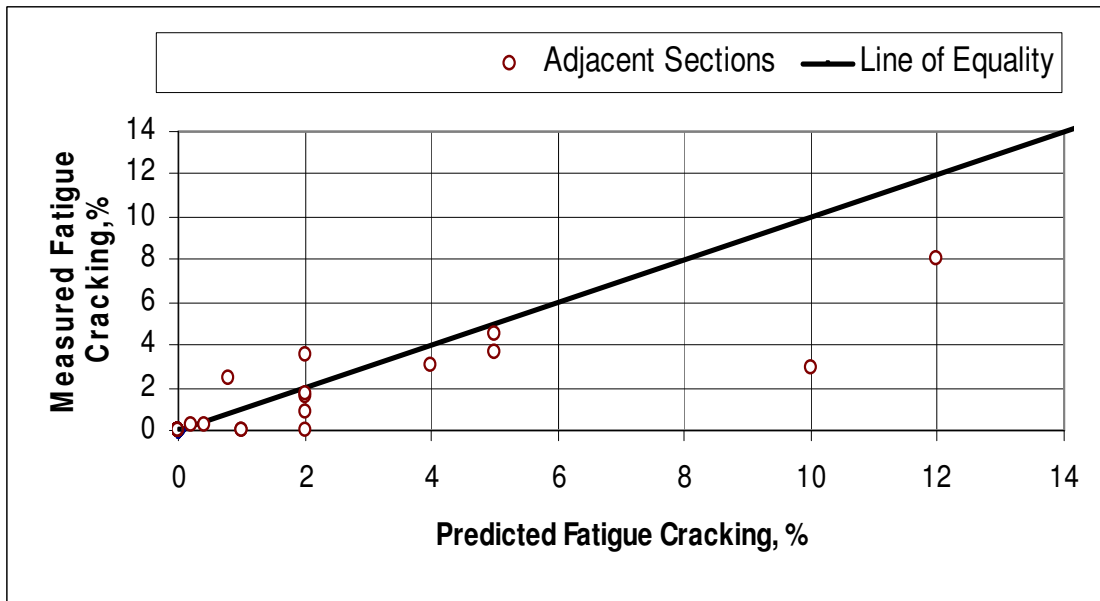


Figure I-45 Comparison of the predicted and measured alligator cracking for the semi-rigid pavement sites.

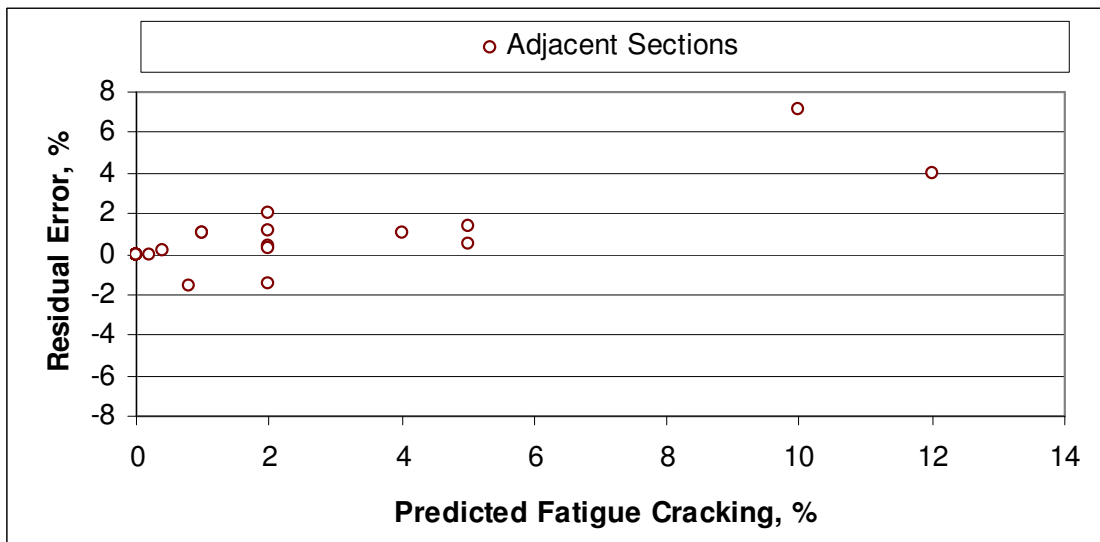


Figure I-46 Residual error (predicted minus measured total alligator cracking) as a function of the predicted alligator cracking.

Table I-35 lists the bias and other statistical information on the bottom-up or alligator cracking distress transfer function for the Montana sites and all sites combined. The Montana agency specific calibration coefficients for the fatigue cracking transfer functions determined within this study are believed to be adequate and are recommended for use in design and forensic studies. As noted above, the distress transfer function for semi-rigid pavements should be used with caution and the top-down or longitudinal cracking distress transfer function is not suggested for use.

Table I-35 Summary of the Bias and Standard Error for the Alligator Cracking Prediction Model Using the Montana Calibration Factors

Type of Pavement		No. of Points	Bias*	Standard Error*	RMSE*	S _e /S _y
Montana Sites	New Construction, Flexible Pavements	58	1.11	2.34	5.11	0.401
	Semi-Rigid Pavements	---	---	---	---	---
	HMA Overlays of Flexible Pavements	50	-0.02	8.17	14.30	0.318
All Sites Combined	New Construction, Flexible Pavements	76	0.15	2.45	4.67	0.315
	Semi-Rigid Pavements	51	0.51	1.51	2.86	0.532
	HMA Overlays of All Type Pavements	70	0.67	7.670	13.94	0.318

*Values are in percent of total lane area.

I-7.6 NON-LOAD RELATED TRANSVERSE CRACKING

The length of transverse cracks was predicted for each test section in Montana and in the adjacent States and Canadian provinces. The MEPDG generally over predicted the lengths of transverse cracks on the Montana sections and under predicted the lengths of the test sections located in adjacent areas to Montana. The global calibration coefficients included in Version 0.9 were used for the sections located outside of Montana, while the agency specific calibration coefficient was varied to eliminate any bias for the Montana sections. The Montana specific calibration coefficient for the Level 3 inputs is $B_{S3} = 0.25$. Figure I-47 shows a comparison of the predicted and measured transverse cracking. The Montana agency specific calibration coefficient for the length of transverse crack transfer function, determined within this study, is believed to be adequate, and is recommended for use in design and forensic studies.

I-7.7 HMA MIXTURE DISINTEGRATION

The indirect tensile strain at failure and IDT elastic modulus were used to evaluate the HMA mixtures resistance to disintegration type distresses (raveling and block cracking). Only one mixture tested did not meet the criteria established within Chapter I-3, and that was the HMA binder layer of the Vaughn Road Project. All other values exceeded the minimum requirements (2.0 mils per inch at 41 °F) and none of these sections have exhibited raveling and block

cracking. This observation is consistent with the lower air voids that were measured on many of the HMA mixtures placed in Montana.

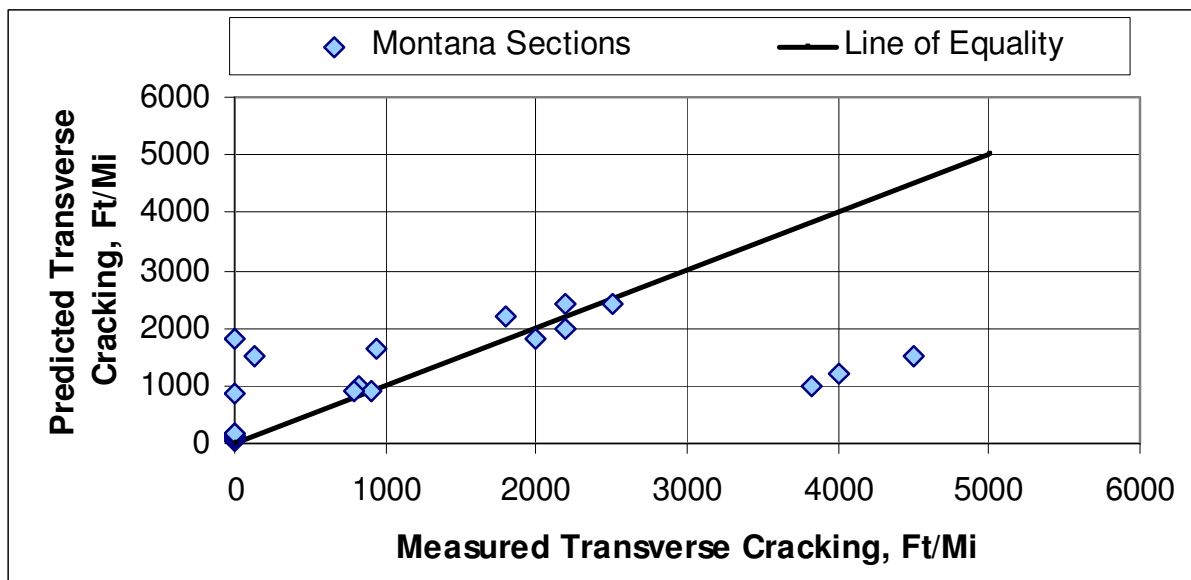


Figure I-47 Comparison of the predicted and measured transverse cracking for the Montana sites.

I-7.8 SMOOTHNESS

Smoothness was predicted for each test section in Montana and in the adjacent States and Canadian provinces using the global calibration factors included in Version 0.9. Obviously, the accuracy of these predictions to match the smoothness measurements are dependent on two conditions; the accuracy of the MEPDG to predict other load and non-load related distresses and estimating the initial IRI value after construction. For those sections without an initial IRI value, the mean value calculated for the sections with an IRI value was assumed for the other sections. Figure I-48 shows a comparison of the predicted and measured IRI values. In summary, the global calibration factors for the smoothness regression equation are believed to be adequate, and are recommended for use in design and forensic studies in Montana.

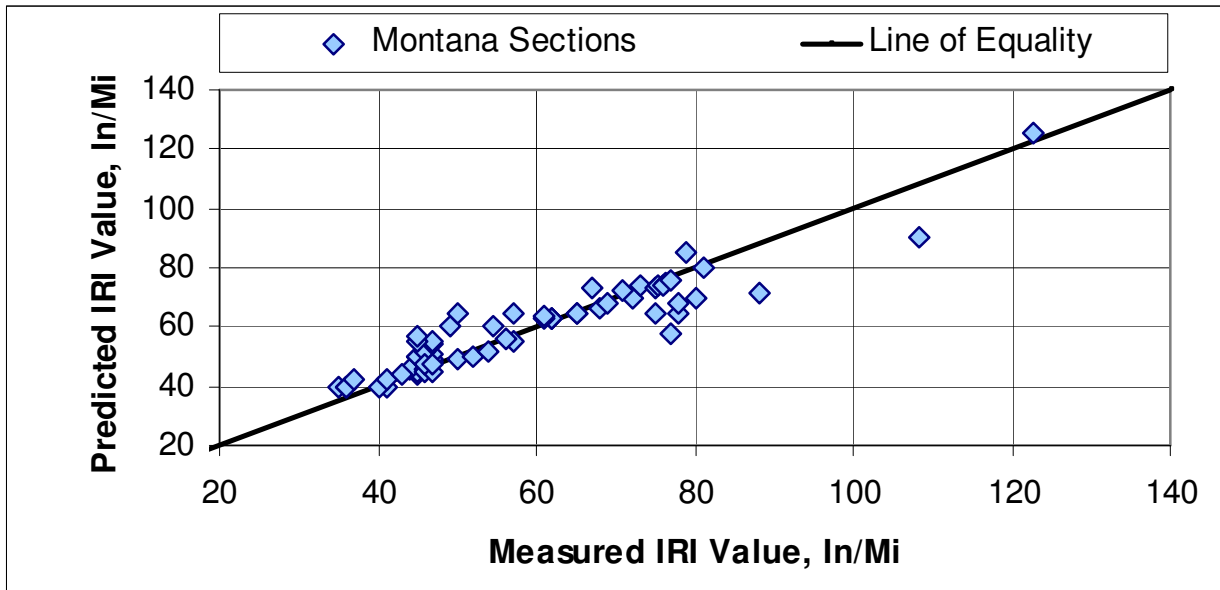


Figure I-48 Comparison of the predicted and measured IRI for the Montana test sections.

CHAPTER I-8 CONCLUSIONS AND RECOMMENDATIONS

I-8.1 FINDINGS AND CONCLUSIONS

A key finding from the comparison of distress is that the Montana sections for new construction are performing better with less distress. As an example, none of the Montana new construction test sections have exhibited any raveling, while over 30 percent of the test sections in the adjacent States have exhibited raveling. Although the test sections located in adjacent areas are slightly older, this would not account for the difference in performance. This finding questions the applicability of using the results from test sections in adjacent States for determining agency specific calibration factors for both cracking and rutting. Two factors that could explain this difference in performance, however, is that the air voids measured in the HMA mixtures of the Montana sections were less than those placed in adjacent areas, and the use of pavement preservation techniques placed shortly after construction of new HMA pavements or overlays.

The difference in air voids is believed to be important and the MEPDG appeared to account for this difference in terms of fatigue cracking and rutting. In other words, test sections with the higher air voids had more fatigue cracking and rutting – independent of whether they were placed in Montana or in adjacent States. The difference in air voids between the test sections did not explain the difference in transverse cracking predictions.

Different pavement preservation treatments were placed on many of the older test sections early in the life of the pavement structure. Where pavement preservation treatments had been placed early in the pavement's life cycle, the amount of cracking (transverse, longitudinal, and alligator) was less than for the test sections where a pavement preservation treatment had not been placed. This policy or pavement preservation strategy represents a confounding factor within the performance data and local calibration factors.

This systematic difference in air voids and the use of pavement preservation treatments of some test sections was considered in using the performance data for test sections in adjacent States for developing agency specific calibration factors for use in Montana. A summary of the significant findings and conclusions from the calibration refinement study are listed below, as they relate to the MEPDG predictive capability of pavement distress in Montana, which can assist decision makers in designing and managing their highway network.

I-8.1.1 Rut Depth Prediction Model

In summary, the MEPDG significantly over predicted the total rut depth, primarily because higher levels of rutting were predicted in the unbound layers and embankment soils. Most of the thicker test sections located in Montana, however, have exhibited only minimal rutting below the HMA layers based on the field investigations conducted as part of this project. Thus, a local adjustment factor for the unbound layers was determined to be 0.20.

The average rut depth measured on the test sections placed in Montana (0.29 in) is significantly less than the average rutting measured on the test sections in adjacent States (0.50 in). The MEPDG with the mixture specific adjustment factors accounted for this difference in rutting. Thus, this difference in rutting is believed to be more related to the HMA mixtures and lower air voids consistently measured on the Montana test sections, as noted above.

Mixture specific factors were used to modify or adjust the MEPDG global calibration factors. With these mixture adjustment factors, the HMA rut depth prediction model was found to be a reasonable estimate of the measured rut depths over a diverse range of conditions. The MEPDG rut depth prediction model accurately accounted for different climates, truck traffic, mixture volumetric properties, layer thicknesses, and mixtures. Thus, it is recommended that the MEPDG software with the local or mixture specific adjustment factors be used for designing HMA pavement layers to resist rutting and other surface distortions in Montana.

I-8.1.2 Fatigue Cracking Prediction Model for Flexible Pavements and HMA Overlays – Alligator Cracking or Bottom-Up Fatigue Cracking

The MEPDG fatigue cracking model was found to be a reasonable estimate of the measured magnitudes over a diverse range of mixtures and structures, using the mixture specific adjustment factors. The standard error for the area fatigue cracking prediction model was found to be relatively large but reasonable for this distress that exhibits high variability measurements. However, the amount of variation in the measured area fatigue cracking was found to be one of the error components that significantly increased the standard error for this prediction model. Thus, it is recommended that the bottom-up fatigue cracking (alligator or area cracking) model be used in Montana for pavement design.

I-8.1.3 Fatigue Cracking Prediction Model for Semi-Rigid Pavements

The semi-rigid pavements built in Montana are performing significantly better than those placed in adjacent States. For example, none of the Montana semi-rigid pavements have exhibited fatigue cracking, while about 55 percent of the sections located in adjacent States have exhibited some fatigue cracking. The amount of fatigue cracking for this pavement design strategy, however, is relatively low with an average area of 1.3 percent.

Two factors have a significant impact on the use of the MEPDG to design semi-rigid pavements in Montana. First, the fatigue cracking prediction model included in the MEPDG was never calibrated under NCHRP Projects 1-37A (*ARA 2004a,b,c,d*) or 1-40D (*NCHRP 2006*). Thus, the test sections located in adjacent States were used to determine the local calibration adjustment factors. Secondly, a programming error still exists in the MEPDG software Version 0.900 (*NCHRP 2006*) for the cement-treated layer of the semi-rigid pavements. As noted in previous chapters, the program does not retain any of the material inputs for the cement-treated layer. The user-defined inputs always divert back to the default values for that layer.

The MEPDG was used to predict the fatigue cracking of this pavement design strategy by varying the local calibration coefficients. These local calibration coefficients were found to be mixture quality dependent, as expected. Mean values are recommended for use in designing

semi-rigid pavement in Montana. However, it should be clearly understood that those local calibration coefficients are heavily based on the test sections that were built in adjacent States.

I-8.1.4 Fatigue Cracking Prediction Model – Longitudinal Cracking or Top-Down Fatigue Cracking

About 25 percent of the Montana semi-rigid pavements have exhibited longitudinal cracking, while 100 percent of the sections in adjacent States have exhibited this type of cracking. The average length of longitudinal cracking per project in Montana is 965 ft/mi, while the average length in the adjacent States is 1,576 ft/mi.

Longitudinal cracking in the wheel paths were calculated for the different test sections and found to be inaccurate for both the Montana test sections, as well as those built in adjacent States. The longitudinal cracking predicted for the test sections was found to be significantly greater for some test sections and significantly lower for others. In fact, significant lengths of longitudinal cracks were predicted for those sections that have yet to exhibit any of this type of cracking.

No consistent trend in the predictions could be identified to reduce the bias and standard error, and improve the accuracy of this prediction model. It is believed that there is a significant lack-of-fit modeling error for the occurrence of longitudinal cracks. Thus, the bias (residual error) was considered too large for use in structural design. The top-down fatigue cracking model is not recommended for use in making design decisions in Montana until it is further refined based on work completed under NCHRP Project 1-42 (*Christensen 2005*).

I-8.1.5 Transverse Cracking Prediction Model

The average length of transverse cracks measured on the Montana test sections (479 ft./mi.) was found to be significantly less than the average length measured on the test sections in the adjacent States (2,026 ft/mi). The average age of the Montana test sections is less than those in adjacent States, but the length of transverse cracks for the older test sections in Montana is still less than those in the adjacent States. This difference in transverse cracking is believed to be more related to the HMA mixtures (differences in air voids) and the use of pavement preservation treatments on some of the older sections.

The MEPDG transverse cracking prediction model was used to calculate the length of thermal cracks for all test sections. In general, the MEPDG over-predicted the length of transverse cracks for all test sections, even for those sections where the indirect tensile and creep compliance tests were performed on the recovered HMA mixtures. Laboratory test data were only available for the HMA mixtures recovered from the non-LTPP test sections established in Montana. As a result, the calibration refinement effort focused on the Level 3 inputs for the thermal cracking model.

A local calibration factor of 0.25 is suggested for use in predicting thermal cracking, and was based on the test sections located in Montana. The local calibration factor for thermal cracking was found to be agency dependent for the test sections located in adjacent States. Thus, only the Montana test sections were used in determining the local calibration factor for thermal cracking. The MEPDG prediction model with the local calibration factor was found to be

acceptable for predicting transverse cracks in HMA pavements and overlays in Montana. However, the standard error is relatively large, but similar to the standard error determined from the updated calibration work completed under NCHRP Project 1-40D (*NCHRP 2006*). Thus, the MEPDG and local adjustment factor are suggested for use in designing HMA mixtures to be resistant to thermal cracking in Montana.

I-8.1.6 Smoothness Prediction Models

The MEPDG prediction model for smoothness or increasing roughness is a result from a regression analysis of hundreds of test sections included in the LTPP program. This prediction model is not based on mechanistic principles so it can only be revised using regression-based procedures. In summary, there are too few test sections with significant or higher levels of distress located in Montana and in adjacent States to accurately revise this regression equation. Thus, the MEPDG regression prediction equations are recommended for use in Montana, because these equations were based on hundreds of test sections placed around the U.S. and were found to have reasonable error terms.

I-8.2 RECOMMENDATIONS FOR FUTURE CALIBRATION STUDIES

The MEPDG distress transfer functions have been validated for use in Montana. The area or alligator cracking (bottom-up cracking mechanism), HMA rut depth, transverse cracking, and smoothness prediction models are believed to be adequate for use in Montana. It is recommended that MDT move forward with using these distress prediction models in analyzing and designing flexible pavements and HMA overlays.

I-8.2.1 MEPDG Distress Prediction Models Requiring Future Updates

The following lists the recommendations for the future refinement and updated calibration studies of the distress prediction models included in the MEPDG for use in Montana.

I-8.2.1.1 Semi-Rigid Pavement Fatigue Cracking Model

Agency specific calibration factors were developed for the fatigue cracking of semi-rigid pavements and rutting in the unbound layers and embankment soils. However, few of the calibration test sections had any appreciable rutting below the HMA layers, and all of the semi-rigid pavements located in Montana have yet to exhibit levels of fatigue cracking considered high enough to trigger some type of rehabilitation activity. As a result, it is suggested that MDT conduct future calibration updates to confirm the agency specific calibration factors for using these prediction models in Montana; fatigue cracking of semi-rigid pavements and rutting in the unbound paving layers of the conventional HMA pavements. It is recommended that future calibration work to confirm the local calibration factors be postponed until the programming errors related to the material input screens have been fixed and Version 1.0 of the MEPDG is issued.

I-8.2.1.2 Rutting in the Unbound Layer Prediction Model

Agency specific calibration factors were developed for the unbound layers and embankment soils. However, few of the calibration test sections had rut depths below the HMA layers considered high enough to trigger rehabilitation. However, many of the test sections with thin HMA surface layers in Montana are relatively new. Rutting in the unbound layers of these test sections might increase with increasing truck traffic levels over time. As a result, it is suggested that MDT conduct future calibration updates to confirm the agency specific calibration factors for using the rut depth prediction models for the unbound layer in Montana.

I-8.2.1.3 Longitudinal Cracking Prediction Model – Surface Initiated Fatigue Cracks

The longitudinal cracking within the wheel paths (top-down cracking mechanism) was found to be inadequate. Significant lengths of longitudinal cracking were predicted for sections that have exhibited minimal longitudinal cracks, whereas no cracking was predicted for the sections with significant longitudinal cracking. Most of the calibration test sections with the higher lengths of longitudinal cracks were located in adjacent States and Canadian provinces. Therefore, no changes were made to the global calibration factors for the longitudinal cracking model. It is recommended that MDT postpone future updates to this prediction model until the distress mechanism included in the MEPDG has been revised or confirmed through NCHRP Project 1-42 (*Christensen 2005*).

I-8.2.2 Activities and Schedule for Future Calibration Updates

The remainder of this section of Chapter 8 focuses on the activities and schedule to conduct future calibration refinement updates for the fatigue cracking of semi-rigid pavements and rutting in the unbound paving layers and embankment soils.

Continue to collect traffic, distress, and profile (smoothness and rut depths) on the non-LTPP test sections. All data should be entered into the MDT MEPDG calibration database. Once the calibration refinement process has been planned or scheduled, any additional distress and performance data should be extracted from the LTPP database for those sections located in Montana and in adjacent States and Canadian provinces. These data should be entered into the MEPDG database.

MDT should continue to collect distress data on all non-LTPP test sections established for calibration refinement use in Montana. The condition surveys should be made annually to ensure that the time can be determined when cracking starts to occur.

The rut depths measured in 2005 at all of the sites were less than 0.20 in, with the exception of one test section – the Lavina West site. All of these sites are still considered smooth because little distress has occurred along these sections. Rut depths should be made every other year for the test sections that have been in place for more than 3 years. Profile measurements should be made every other year. It is important for calibration purposes that rut depth and profile measurements be taken every other year beginning three years after placement.

It is recommended that the deflection basin data be measured along each non-LTPP test section after the fatigue cracking exceeds about 5 percent on four of these semi-rigid sections.

A calibration update should be scheduled after greater than 5 percent fatigue cracking is observed on about half of the semi-rigid pavements located in Montana and established within the MDT MEPDG calibration database. However, the next calibration update should be completed after the MEPDG input screen for entering the material properties of the semi-rigid layers has been fixed and after the surface initiated fatigue cracking prediction model has been revised or confirmed.

In 2005, none of the 8 semi-rigid pavement test sections had exhibited any fatigue cracking, and only 4 of the 11 semi-rigid sections located in adjacent States had exhibited fatigue cracking in excess of 1 percent. Even all of those sections still had less than four percent fatigue cracking. Based on the performance of the LTPP semi-rigid sites located in adjacent States, the Montana semi-rigid sections are not expected to exhibit this amount of fatigue cracking until after five more years.

For those test sections with load related cracking, cores should be taken through the cracks to determine where the cracks initiated or confirm the direction of crack propagation. This field investigation should be completed prior to the next calibration update.

In addition, confirmation of the MEPDG prediction model and mixture adjustment factors should continue as the semi-rigid fatigue cracking prediction model and longitudinal cracking models are updated.

CHAPTER I-9 REFERENCES

- American Association of State Highway and Transportation Officials (AASHTO). (1986) *AASHTO Guide for Design of Pavement Structures*. Washington, DC.
- American Association of State Highway and Transportation Officials (AASHTO). (1993) *AASHTO Guide of Pavement Structures*. Washington, DC.
- American Association of State Highway and Transportation Officials (AASHTO). (2006a) *Standard Specifications for Transportation Materials and Methods of Sampling and Testing*. 26th Edition, Part 2A: Tests. Washington, DC.
- American Association of State Highway and Transportation Officials (AASHTO). (2006b) *Standard Specifications for Transportation Materials and Methods of Sampling and Testing*. 26th Edition, Part 2B: Tests. Washington, DC.
- Applied Research Associates, Inc. (ARA). ERES Consultants Division. (2004a) *Guide for Mechanistic-Empirical Design of New and Rehabilitated Pavement Structures: Part 1-Introduction and Part 2-Design Inputs*. Final Report. NCHRP Project 1-37A. National Cooperative Highway Research Program. Transportation Research Board. National Research Council. Washington, DC.
- Applied Research Associates, Inc. (ARA). ERES Consultants Division. (2004b) *Guide for Mechanistic-Empirical Design of New and Rehabilitated Pavement Structures: Part 3-Design Analysis and Part 4-Low Volume Roads*. Final Report, NCHRP Project 1-37A. National Cooperative Highway Research Program. Transportation Research Board. National Research Council. Washington, DC.
- Applied Research Associates, Inc. (ARA). ERES Consultants Division. (2004c) *Guide for Mechanistic-Empirical Design of New and Rehabilitated Pavement Structures: Appendices A to C*. Final Report. NCHRP Project 1-37A. National Cooperative Highway Research Program. Transportation Research Board. National Research Council. Washington, DC.
- Applied Research Associates, Inc. (ARA). ERES Consultants Division. (2004d) *Guide for Mechanistic-Empirical Design of New and Rehabilitated Pavement Structures: Appendix D – User’s Guide*. Final Report. NCHRP Project 1-37A. National Cooperative Highway Research Program. Transportation Research Board. National Research Council. Washington, DC.
- Christensen, D.W. (2005) *Top-Down Fatigue Cracking of Hot-Mix Asphalt Layers – Phase I*. NCHRP Project 1-42. Advanced Asphalt Technologies, LLC. National Cooperative Highway Research Program. Transportation Research Board. National Research Council. Washington, DC.
- Federal Highway Administration (FHWA). (2003) *Distress Identification Manual for Long Term Pavement Performance Program (Fourth Revised Edition)*. Publication No. FHWA-RD-03-031. Washington, DC.

- Larson, G. and Dempsey, B.J. (1997) *Enhanced Integrated Climatic Model (Version 2.0)*. Report No. DTFA MN/DOT 72114, University of Illinois at Urbana-Champaign, Urbana, IL.
- Lytton, R.L.; Uzan, J.; Fernando, E.G.; Roque, R.; Hiltunen, D.; Stoffels, S.M. (1993) *Development and Validation of Performance Prediction Models and Specifications for Asphalt Binders and Paving Mixes*. Report No. SHRP-A-357. Strategic Highway Research Program. National Research Council. Washington, DC.
- National Cooperative Highway Research Program (NCHRP). (2003) *Refining the Calibration and Validation of Hot Mix Asphalt Performance Models: An Experimental Plan and Database*. NCHRP Research Results Digest Number 284. NCHRP Project 9-30. Transportation Research Board. National Research Council. Washington, DC.
- National Cooperative Highway Research Program (NCHRP). (2006) *Changes to the Mechanistic-Empirical Pavement Design Guide Software Through Version 0.900*. NCHRP Research Results Digest 308. NCHRP Project 1-40D. Transportation Research Board. National Research Council. Washington, DC.
- National Cooperative Highway Research Program (NCHRP). (2007 Active) *Simple Performance Tester for Superpave Mix Design*. NCHRP Project 9-29. Advanced Asphalt Technologies. Transportation Research Board. National Research Council. Washington, DC.
- Strategic Highway Research Program (SHRP). (1990) *Specific Pavement Studies of Structural Factors for Flexible Pavements (SPS-1)*. National Research Council. Washington, DC.
- Strategic Highway Research Program (SHRP). (1993) *Distress Identification Manual for the Long Term Pavement Performance Project*. Report No. SHRP-P-338. National Research Council. Washington, DC.
- Von Quintus, H.L. and Killingsworth, B.M. (1997a) *Design Pamphlet for the Determination of Design Subgrade Modulus in Support of the 1993 AASHTO Guide for the Design of Pavement Structures*. Publication No. FHWA-RD-97-083. Federal Highway Administration. McLean, VA.
- Von Quintus, H.L. and Killingsworth, B.M. (1997b) *Design Pamphlet for the Determination of Layered Elastic Moduli in Support of the 1993 AASHTO Guide for the Design of Pavement Structures*. Publication No. FFWA-RD-97-077. Federal Highway Administration. McLean, VA.
- Von Quintus, H.L. and Killingsworth, B.M. (1998) *Analyses Relating to Pavement Material Characterizations and Their Effects on Pavement Performance*. Publication No. FHWA-RD-97-085. Federal Highway Administration. McLean, VA.
- Von Quintus, H.L. and Moulthrop, J.S. (2007a) *Performance Prediction Models: Volume II Reference Manual*. No. FHWA/MT-07-008/8158-2, Montana Department of Transportation, Research Programs, Helena, MT.
- Von Quintus, H.L. and Moulthrop, J.S. (2007b) *Performance Prediction Models: Volume III Field Guide – Calibration and User's Guide for the Mechanistic-Empirical Pavement Design*

Guide. No. FHWA/MT-07-008/8158-3. Montana Department of Transportation. Research Programs. Helena, MT.

Von Quintus, H.L. and Yau, A. (2001) *Evaluation of Resilient Modulus Test Data in the LTPP Database*. Publication Number FHWA/RD-01-158. Federal Highway Administration. Office of Infrastructure Research and Development. McLean, VA.

Von Quintus, H.L.; Andrei, D.; and Schwartz, C. (2005a) *Expand Population of M-E_DPM Database and Conduct Two Pre-Implementation Studies*. Final Report. NCHRP Project 9-30(001). Fugro Consultants LP and ARA Inc. ERES Consultants Division. National Cooperative Highway Research Program. Transportation Research Board. National Research Council. Washington, DC.

Von Quintus, H.L., Chetana, R. Stubstead, R., Minchin., R., Mawer, K. Nazarian, S., Prowell, B., Maghsoodloo, S. (2006 Active) "Nondestructive Testing Technology for Quality Control and Acceptance of Flexible Pavement Construction: Phase 2, Part A, Task 6." Interim Report. NCHRP Project 10-65. National Cooperative Highway Research Program. Transportation Research Board. National Research Council. Washington, DC.

Von Quintus, H.L.; Darter, M.I.; and Mallela, J. (2005b "Phase I – Local Calibration Adjustments for the HMA Distress Prediction Models in the M-E Pavement Design Guide Software." Interim Report. NCHRP Project 1-40B. National Cooperative Highway Research Program. Transportation Research Board. National Research Council. Washington, DC.

Von Quintus, H.L.; Scherocman, J.A.; Hughes, C.S.; Kennedy, T.W. (1991) *Asphalt-Aggregate Mixture Analysis System (AAMAS)*. NCHRP Project No. 338. National Cooperative Highway Research Program. Transportation Research Board. National Research Council. Washington, DC.

Witczak, M.W.; Kaloush, K.; Pellinen, T.; El-Basyouny, M.; and Von Quintus, H.L. (2002) *Simple Performance Test for Superpave Mix Design*. NCHRP Report No. 465. National Cooperative Highway Research Program. Transportation Research Board. National Research Council. National Academy Press. Washington, DC.

150 copies of this public document were produced at an estimated cost of \$2.58 each, for a total cost of \$386.92. This includes \$153.36 for postage and \$233.56 for printing.